



Superabsorbent Polymers in Concrete to Improve Durability

Project 18-02R

Final Report

Investigators

Dr. David A. Lange, University of Illinois, Urbana, IL

Dr. Kamal H. Khayat, Missouri S&T, Rolla, MO

Dr. Matthew D'Ambrosia, MJ2 Consulting, Bannockburn, IL

September 2021



TECHNICAL REPORT DOCUMENTATION PAGE

1. Report No. ISTHA 18-02R	2. Government Accession No. N/A	3. Recipient's Catalog No. N/A	
4. Title and Subtitle Superabsorbent Polymers in Concrete to Improve Durability		5. Report Date September 2021	
		6. Performing Organization Code N/A	
7. Author(s) David A. Lange Kamal Khayat Matthew D'Ambrosia Nima Farzadnia Yucun Gu Karthik Pattaje Jamie Clark Chuanyue Shen Ruofei Zuo		8. Performing Organization Report No. N/A	
9. Performing Organization Name and Address University of Illinois at Urbana-Champaign Department of Civil and Environmental Engineering 205 North Mathews Avenue, MC-250 Urbana, IL 61801		10. Work Unit No. (TRAIS) N/A	
		11. Contract or Grant No. DTFH61-01-C-00052	
12. Sponsoring Agency Name and Address Illinois State Toll Highway Authority 2700 Ogden Ave Downers Grove, IL 60515		13. Type of Report and Period Covered	
		14. Sponsoring Agency Code	
15. Supplementary Notes			
16. Abstract This research examined and documented the use of internal curing by superabsorbent polymer (SAP) to improve the durability of Tollway bridge decks. The project included laboratory studies to characterize material behavior and properties, and field testing to measure slab performance and observe behavior with full scale truck mixers.			
17. Key Words concrete, bridge structures, pavement, internal curing, superabsorbent polymer, shrinkage, durability, mix design		18. Distribution Statement No restrictions. This document is available to the public through the National Technical Information Service, Springfield, VA 22161.	
19. Security Classification (of this report) Unclassified	20. Security Classification (of this page) Unclassified	21. No of Pages 200	22. Price

Form DOT F 1700.7 (8-72) Reproduction of completed page authorized

ACKNOWLEDGMENT AND DISCLAIMER

This publication is based on the results of the Illinois State Toll Highway Authority Project entitled Superabsorbent Polymers in Concrete to Improve Durability. This study was funded by the Illinois State Toll Highway Authority. Acknowledgement is given to Mr. Dan Gancarz for leading Tollway oversight throughout the project. The authors acknowledge the cooperation of the following research assistants for their great help in conducting the experimental work: Robert Wiggins, Ariel Dubizh, Matthew Mota, Konrad Kepka, Jingjie Wei, Le Teng, Alfred Addai-Nimoh, Jiang Zhu, and Huanghuang Huang. The support of Mr. Jason Cox, Senior Research Specialist is especially acknowledged. The authors acknowledge the invaluable support from Ozinga for their facilities, materials and manpower for the field trials in November 2019 and in May 2021. Special thanks to S.T.A.T.E testing for their contribution in carrying out the testing during the field trials. The authors also acknowledge the contributions of the Technical Review Panel (TRP) members who met three times with the research team to review project direction and results.

The contents of this report reflect the view of the authors, who are responsible for the facts and the accuracy of the data presented herein. The contents do not necessarily reflect the official views or policies of the Illinois Center for Transportation or Illinois State Toll Highway Authority. This report does not constitute a standard, specification, or regulation.

EXECUTIVE SUMMARY

Proper curing of concrete is important to ensure satisfactory strength gain and durability. Internal curing by superabsorbent polymer (SAP) in concrete can control water in the microstructure, providing a timed release of water that leads to more complete hydration, denser microstructure, and lower shrinkage for high-performance concrete (HPC).

The comprehensive laboratory test program studied fresh and hardened properties of concrete made with SAP. Five commercially available SAP products with varying particle size and formulation were used in this study. SAP absorption behavior, optimum internal curing water content, extended mixing time were assessed. The SAP dosage was set so that the SAP would absorb a volume of water equal to the chemical shrinkage of the cement, an approach that has become commonly used by researchers. The study established strategies for addressing effects that SAP may have on fresh properties (e.g. adding superplasticizer to offset slight slump loss). The mechanical properties of hardened concrete with SAP were measured, including compressive strength, modulus of elasticity (MOE), and flexural strength. SAP generally had little effect on strength gain or frost durability, but the results showed that SAP led to lower shrinkage. The laboratory tests included comparison of internal curing using SAP with that of saturated lightweight aggregate. It was shown that the mixtures made with SAP have better mechanical and shrinkage properties than mixtures made with saturated lightweight aggregate.

Field trials were conducted in the project to demonstrate feasibility of truck mixing and to construct concrete slabs with HPC made with SAP. The field trials demonstrated that concrete with SAP could be produced using standard truck mixers if care was exercised to ensure good distribution when adding the SAP to the truck.

The project developed recommended revisions to ISTHA material specifications to allow contractors to use SAP for internal curing of concrete for Tollway projects.

CONTENTS

- ACKNOWLEDGMENT, DISCLAIMER, MANUFACTURERS' NAMES iii**
- EXECUTIVE SUMMARY..... iv**
- 1. INTRODUCTION AND LITERATURE REVIEW 15**
 - 1.1 Problem statement..... 15
 - 1.2 Research Background 18
 - 1.2.1 Superabsorbent Polymer Characteristics..... 18
 - 1.2.2 Effects of SAP on fresh and hardened properties of concrete 26
 - 1.3 Research objectives..... 33
 - 1.4 Research tasks 34
- 2. EXPERIMENTAL PROGRAM 36**
 - 2.1 Materials 36
 - 2.1.1 Superabsorbent polymers (SAPs)..... 36
 - 2.1.2 Chemical admixtures..... 38
 - 2.1.3 Cementitious materials and aggregate used at Missouri S&T 38
 - 2.1.4 Cementitious materials and aggregate used at UIUC 40
 - 2.2 Experimental program..... 41
 - 2.2.1 Task B: Laboratory testing of HPC with SAP and LWS 41
 - 2.3 Mixing and test methods..... 50
 - 2.3.1 Mixing procedure and curing 50
 - 2.3.2 Test methods..... 51
- 3. LABORATORY TESTING RESULTS AND DISCUSSION 60**
 - 3.1 Subtask B-1: Pre-test of SAP for internal curing of HPC 60
 - 3.2 Subtask B-2: Performance of HPC with optimized SAP 73
 - 3.2.1 B-2-1 Determine internal water content..... 73
 - 3.2.2 B-2-2 Determine acceptable mixing time 82

3.2.3 B-2-3 Investigate frost durability using SAP	90
3.3 Subtask B-3: Optimization of external curing regime.....	101
3.4 Subtask B-4: Comparison of HPC mixtures with LWS and SAP	104
4. FIELD TESTING RESULTS AND DICUSSION.....	113
4.1 Field test 1: Feasibility of HPC with SAP in the field.....	113
4.2 Field test 2: Field implementation of HPC with SAP	127
5. RECOMMENDED CHANGES TO TOLLWAY SPECIFICATIONS	147
6. SUMMARY AND CONCLUSIONS	149
REFERENCES.....	159
APPENDIX	173

LIST OF TABLES

Table 1-1. Example of field projects using internal curing	17
Table 2-1. Types of investigated SAP products	36
Table 2-2. Physical and chemical characteristics of cementitious materials and FA (S&T)	39
Table 2-3. Physical and chemical characteristics of cementitious materials and FA (UIUC)	40
Table 2-4. Mixture proportioning of investigated concrete	43
Table 2-5. Experimental program to evaluate HPC mixtures	43
Table 2-6. Mixture proportioning of investigated concrete in subtask B-2-1	44
Table 2-7. Mixture proportioning of investigated concrete in subtask B-2-2	45
Table 2-8. Mixture proportioning of investigated concrete in subtask B-2-3	45
Table 2-9. Parameters investigated in Subtask B-2	46
Table 2-10. Experimental program to evaluate bridge and pavement concrete mixtures	47
Table 2-11. Initial curing conditions for HPC mixtures	48
Table 2-12. Mixture proportioning of investigated concrete in subtask B-4	49
Table 2-13. Experimental program of subtask B-4	50
Table 3-1. Peak absorption and absorption times obtained in distilled water and infiltrated pore solutions made with and without chemical admixtures	63
Table 3-2. Fresh properties of HPC made with and without SAPs	66
Table 3-3. Yield stress and plastic viscosity of HPC made with and without SAPs	68
Table 3-4. Performance summary of HPC made with different SAPs	73
Table 3-5. Fresh properties of HPC made with different IC of SAPs	74

Table 3-6. Fresh properties of HPC made with WL PAM SAP and different retarder dosage ...	75
Table 3-7. Yield stress and plastic viscosity of HPC made with different IC of SAPs	76
Table 3-8. Electrical resistivity of HPC made with different IC of SAPs at 28-days of age.....	80
Table 3-9. Surface resistivity limits for chloride ion penetrability indication based on AASHTO TP 95-11	81
Table 3-10. Performance summary of HPC made with 50% and 100% IC of SAPs	82
Table 3-11. Fresh properties of HPC made with SAPs and different extended mixing time	83
Table 3-12. Yield stress and plastic viscosity of the HPC mixtures made with SAPs and different extended mixing time.....	85
Table 3-13. Electrical resistivity of HPC made with SAPs and different extended mixing time..	89
Table 3-14. Performance summary of HPC made with SAPs and different extended mixing time	90
Table 3-15. Fresh properties of the HPC mixtures made with and without AEA.....	91
Table 3-16. Yield stress and plastic viscosity of the HPC mixtures made with and without AEA92	
Table 3-17. Electrical resistivity of HPC made with SAPs and different extended mixing time..	97
Table 3-18 Hardened void analysis results for mixtures with and without AEA.....	100
Table 3-19. Performance summary of HPC made with and without SAPs and AEA	101
Table 3-20. Performance summary of HPC made with SAPs and different external curing period	104
Table 3-21. Fresh properties of HPC with SAP and LWS	105
Table 3-22. Hardened void analysis results for mixtures with SAP and LWS	111
Table 3-23. Performance summary of HPC made with SAPs and LWS	112

Table 4-1. Sample summary	114
Table 4-2. Summary of the HPC mixture design	115
Table 4-3. SAP dosages.....	116
Table 4-4. Summary of Fresh Properties	118
Table 4-5. Moist cured compressive strength.....	121
Table 4-6. 14 - day compressive strength (moist cured vs. air cured).....	122
Table 4-7. Hardened air void analysis results	125
Table 4-8. Summary of the HPC mixture design	136
Table 4-9. Fresh properties	137
Table 6-1. Performance summary of HPC made with different SAPs	150
Table 6-2. Performance summary of HPC made with 50% and 100% IC of SAPs	152
Table 6-3. Performance summary of HPC made with SAPs and different extended mixing time	153
Table 6-4. Performance summary of HPC made with and without SAPs and AEA	154
Table 6-5. Performance summary of HPC made with SAPs and different external curing period	156
Table 6-6. Performance summary of HPC made with SAPs and LWS	157

LIST OF FIGURES

Figure 1-1. Particle shape for SAP made by (a) solution polymerization or (b) inverse suspension polymerization; (c) left pore of SAP made by solution polymerization in hardened cement paste after drying (d) left pore of SAP made by inverse suspension polymerization in hardened cement paste after drying [63].....	21
Figure 1-2. Scheme for Co-polymerization.....	22
Figure 1-3. Chemical structure of typical crosslinkers used for superabsorbent.....	22
Figure 1-4. Change in swelling capacity with an increase in (a) Crosslinker concentration, (b) Degree of neutralization.	24
Figure 2-1. SEM images of different SAPs at a different relative humidity.....	37
Figure 2-2. Particle size distributions of SAPs.....	38
Figure 2-3. Particle size distribution of cementitious materials (μm) (S&T).....	39
Figure 2-4. Grain size distributions of fine and coarse aggregates (S&T).....	40
Figure 2-5. Grain size distributions of fine and coarse aggregates (UIUC).....	41
Figure 2-6. Surface settlement test	52
Figure 2-7. Test setup for compressive strength.....	52
Figure 2-8. Test setup for flexural strength measurement of beam specimens	53
Figure 2-9. Testing set-up of modulus of elasticity	54
Figure 2-10. Testing apparatus for surface resistivity (left) and bulk resistivity (right).....	54
Figure 2-11. Shrinkage measurement (a) drying shrinkage and (b) autogenous shrinkage	56
Figure 2-12. Restrained shrinkage measurement using ring test.....	56
Figure 2-13. Test setup for frost durability.....	57

Figure 2-14. NANO 2000T grinder-polisher machine setup	58
Figure 2-15. Example of the original scanned image (left) and the segmentation (right).....	59
Figure 3-1. Variations of absorption rate of SAPs in different filtrated solutions	63
Figure 3-2. Variations of desorption rate of the investigated SAPs with time.....	65
Figure 3-3. Compressive strength of HPC made with different SAPs	69
Figure 3-4. Autogenous shrinkage of the investigated HPC mixtures.....	70
Figure 3-5. Drying shrinkage of investigated mixtures (initial length determined at 1 day)	71
Figure 3-6. Drying shrinkage of investigated mixtures (initial length determined at 7 days that corresponds to beginning of drying)	72
Figure 3-7. Surface settlement of HPC made with different IC of SAPs.....	75
Figure 3-8. Compressive strength of HPC made with different IC of SAPs.....	77
Figure 3-9. Flexural strength (a) and MOE (b) of HPC made with different IC of SAPs at 28 days of age.....	78
Figure 3-10. Autogenous shrinkage of HPC made with different IC of SAPs.....	79
Figure 3-11. Drying shrinkage of HPC made with different IC of SAPs (initial length was recorded at 7 days of age after air drying).....	79
Figure 3-12. Surface settlement of HPC made with SAPs and different extended mixing time .	84
Figure 3-13. Compressive strength of HPC made with SAPs and different extended mixing time	86
Figure 3-14. Flexural strength (a) and MOE (b) of HPC made with SAPs and different extended mixing time at 28 days of age.....	86
Figure 3-15. Autogenous shrinkage of HPC made with SAPs and different extended mixing time	87

Figure 3-16. Drying shrinkage of HPC made with SAPs and different extended mixing time (Initial length was recorded at 7 days of age after air drying).....	88
Figure 3-17. Compressive strength of the HPC mixtures made with and without AEA.....	93
Figure 3-18. Flexural strength (a) and MOE (b) of the HPC mixtures made with and without AEA at 28 days of age	94
Figure 3-19. Autogenous shrinkage of the HPC mixtures made with and without AEA	95
Figure 3-20. Drying shrinkage of the HPC mixtures made with and without AEA (initial length was recorded at 7 days of age after air drying)	96
Figure 3-21. Relative dynamic modulus of HPC mixtures made with and without AEA.....	98
Figure 3-22. Durability factor of HPC mixtures made with and without AEA.....	98
Figure 3-23. Compressive strength of the HPC mixtures with different moist curing periods (1-d, 3-d, 7-d correspond to 1-d in mold and 0, 2, and 6 days in lime-saturated solution).....	102
Figure 3-24. Drying shrinkage of the HPC mixtures with different moist curing periods (1-d, 3-d, 7-d correspond to 1-d in mold and 0, 2, and 6 days in lime-saturated solution).....	103
Figure 3-25. Compressive strength of the HPC made with SAPs and LWS	106
Figure 3-26. Flexural strength of the HPC made with SAPs and LWS.....	106
Figure 3-27. Modulus of elasticity of the HPC made with SAPs and LWS	107
Figure 3-28. Autogenous shrinkage of HPC made with SAPs and LWS (initial length measured at 1 day).....	108
Figure 3-29. Drying shrinkage of HPC made with SAPs and LWS (initial length measured at 3 days).....	108
Figure 3-30. Restrained shrinkage over time (Ring test).....	109
Figure 3-31. Relative dynamic modulus of HPC mixtures made with SAPs and LWS.....	110

Figure 3-32. Durability factor of HPC mixes made with SAPs and LWS	110
Figure 4-1. Mixing procedure: (left) arrival of mixing truck containing the base HPC mixture, (middle) addition of SAP to back of mixing truck, (right) testing fresh properties and casting cylinders.	117
Figure 4-2. Addition of HydroMax.....	119
Figure 4-3. GCP applied technologies VERIFI® apparatus	120
Figure 4-4. BASF SAP stuck to fins of mixing truck	120
Figure 4-5. 28-day compressive strength	123
Figure 4-6. 14 - day compressive strength (moist vs. air curing).....	124
Figure 4-7. Schematic of the slab instrumentation	127
Figure 4-8. Strain gages (PMFL-60-2LJRTA).....	128
Figure 4-9. Strain gages mounted on positioning chair	129
Figure 4-10. Strain gage secured to positioning chair with zip tie	129
Figure 4-11. Strain gages and positioning chairs setup (photographed facing south)	130
Figure 4-12. LORD MicroStrain V-Link wireless node.....	131
Figure 4-13. Reference point for lift off gage measurements	132
Figure 4-14. Connection between reference point and lift off gage (LVDT)	133
Figure 4-15. Lift off gage (LVDT) installed on the slab	133
Figure 4-16. iButtons (temperature and relative humidity sensors).....	134
Figure 4-17. Installation of iButtons (L-R: removing plastic pipe after concrete hardened, placing iButton using magnetic stick, covering the space above iButton using the plastic pipe to form a seal).....	135

Figure 4-18. Dispersion issue seen during the BASF mixture pour.....	138
Figure 4-19. Compacting of HPC around the embedded strain gages.....	139
Figure 4-20. Finishing of the HPC slabs.....	139
Figure 4-21. Coating the top surface of the HPC slab with curing compound.....	140
Figure 4-22. Compressive strength	140
Figure 4-23. Wetness observed around the slabs.....	141
Figure 4-24. Ambient temperature near the HPC slabs	142
Figure 4-25. Ambient RH near the HPC slabs.....	142
Figure 4-26. Temperature within the HPC slabs	143
Figure 4-27. RH within the HPC slabs.....	143
Figure 4-28. Strain measurements of the BASF slabs with and without CC	144
Figure 4-29. Strain measurements of the PAM slabs with and without CC.....	145
Figure 4-30. Strain measurements of the control slabs with and without CC.....	145
Figure 4-31. Lift-off gage data of the HPC slabs	146

1. INTRODUCTION AND LITERATURE REVIEW

1.1 Problem statement

Concrete with a low water-to-cementitious materials ratio (w/cm) is known to create potentially severe internal stress that drives autogenous shrinkage. In Illinois, early-age shrinkage cracking of high-performance concrete (HPC) bridges and the pavement is a common problem. Cracking increases the risk of freeze-thaw damage and ingress of deleterious substances that can lead to structural deficiencies. In reinforced concrete bridge decks, cracking can lead to corrosion of the reinforcement and degradation of structural performance. Concrete with internal curing technology is of increasing interest due to its beneficial effect in reduction of shrinkage cracking, improving the durability, and enhancing the life cycle cost of bridges and pavements. Internal curing is especially suitable for HPC with low w/cm where it is anticipated that the mixing water is insufficient for full hydration of the cement. Internal curing is also suitable for concrete mixtures with silica fume that typically exhibit relatively high autogenous shrinkage. Internal curing can be accomplished by the use of the saturated lightweight aggregate (LWA) that carries water in the aggregate pores, and then releases the water as the cement paste demanded water for hydration reactions. Internal curing by LWA has gained wide acceptance as an effective way to reduce autogenous and drying shrinkage of HPC designated for bridge deck and pavement [1-4]. Better curing of concrete through the use of internal curing can reduce autogenous and drying shrinkage. This can reduce micro-cracking at the interfacial transition zone (ITZ) between the aggregate and the cement paste [5, 6]. Internal curing can also result in lower chloride diffusivity [7] and improved scaling resistance [8] of HPC.

Saturated LWA was previously the only material used as an internal curing agent. But there are some major problems connected with the use of LWA for internal water curing, including difficulties associated with the pre-wetting as well as controlling consistency and strength of concrete. These difficulties can be minimized with the use of superabsorbent polymer (SAP). Similar to LWA, SAP is a method to bring water into the microstructure and release the water in response to the demands of cement hydration when the internal relative humidity decreases. However, compared with LWA, SAP can be easier to incorporate into HPC, since it can absorb a large amount of liquid from the surroundings and retain it within their structure, thus can be used as a dry concrete admixture and takes up water during the mixing process [9-12]. Internal curing with SAP can provide control over the rheological properties of fresh concrete, purposeful

water absorption, and/or water release in either fresh or hardened concrete [13]. It can dramatically reduce the autogenous shrinkage of concretes made with relatively low w/cm [14]. The shrinkage reduction is very important in the first hours after the concrete setting time. It has been observed that the cracking of HPC was prevented by incorporating 1.56 kg/m³ SAP [14]. SAP can also benefit the freeze-thaw resistance of HPC [15, 16]. However, from a strength point of view, the addition of SAP to concrete has two opposite effects [11]: (1) SAP may reduce strength by creating voids or influencing hydration chemistry; (2) SAP may increase strength by providing internal water curing and enhancing the degree of hydration. Which of these two effects is dominant depends on the w/cm and the amount of SAP addition [17-19]. The trade-off between mechanical properties and autogenous shrinkage will need to be investigated with different concrete mixtures incorporating SAP.

To date, practical projects have examined the possibility of using LWA for internal curing of HPC bridge decks and pavement in the U.S. [1, 2, 20-30]. As summarized in Table 1-1, the use of LWA shows great potential in reducing shrinkage and cracking, increasing mechanical properties, and enhancing durability. However, there is a lack of cases applying SAP in practice in the U.S. Four applications using SAP for internal curing in other countries [31-34] are included in Table 1-1.

Table 1-1. Example of field projects using internal curing

Projects	Application	w/cm	External curing	Compared to HPC without internal curing			
				Compressive Strength*	Autogenous shrinkage**	Initial cracking**	Service life
Using SAP for internal curing							
Germany (2006) [31]	Thin walls	0.21	-	20% ↓	88% ↓	-	↑
China (2014) [32]	Railway bed slabs	0.37	-	10% ↑	60% ↓	No	↑
Belgium (2011) [33]	Bridge deck	0.30	-	19% ↓	100% ↓	No	↑
Denmark (2008) [34]	Wall panels	0.40	-	-	100% ↓	No	↑
Using LWA for internal curing							
Indiana DOT (2013) [21, 22]	Bridge deck	0.40	Not reported	10% ↑	80% ↓	No	300% ↑
Louisiana DOT (2016) [1]	Bridge deck	0.45	7-d wet burlap	30% ↑	-	Yes	↑
Illinois Tollway (2013) [23]	Bridge deck	0.35	Not reported	10% ↑	50% ↓	No	↑
Missouri DOT (2018) [20]	Bridge deck	0.40	3-d moist curing	20% ↑	40% ↓	-	↑
Ohio DOT (2007) [24]	Bridge deck	0.40	Moist curing until test	8% ↑	30% ↓	Yes	↑
Utah DOT (2013) [25]	Bridge deck	0.45	14-d wet burlap	13% ↓	-	Yes	15% ↓
New York State DOT (2012) [26]	Bridge deck	0.44	7 to 14-d moist curing	-	5% ↓	Yes	↑
Colorado DOT (2014) [2]	Bridge deck	0.42	3-d moist curing	10% ↑	30% ↓	Yes	60% ↑
Oregon DOT (2013) [27]	Bridge deck	0.40	14-d moist curing	30% ↑	25% ↓	No	↑
Florida DOT (2015) [28]	Bridge deck	0.40	Wet-burlap	10% ↓	-	No	↑
Missouri DOT (2018) [20]	Pavement	0.40	3-d moist curing	35% ↑	15% ↓	-	↑
North Texas Tollway (2013) [29]	Pavement	0.43	7-d wet burlap	10% ↑	50% ↓	Yes	100% ↑
Ohio DOT (2008) [30]	Pavement	0.40	Moist curing until test	6% ↑	100% ↓	No	↑
Florida DOT (2015) [26]	Pavement	0.40	Wet-burlap	5% ↓	-	No	↑

*LWA (coarse aggregate and fine aggregate) content determined according to ASTM C1761. SAP:

Superabsorbent polymers. w/cm: water-to-cementitious materials ratio. *Tested at 28 d. **Within 7 d.

1.2 Research Background

A thorough review of the available literature, specifications, research findings, and ongoing project documentation to determine the current state-of-the-practice for using internally cured concrete with SAP is summarized in this section.

1.2.1 Superabsorbent Polymer Characteristics

Superabsorbent polymer, also known as hydrogels, is a type of polymer that can absorb and retain extremely large amounts of a liquid relative to its mass, according to the definition of IUPAC. The synthesis of the first water-absorbent polymer goes back to 1938 when acrylic acid (AA) and divinylbenzene were thermally polymerized in an aqueous medium [1, 35]. In the late 1950s, the first generation of hydrogels was introduced. These hydrogels were mainly based on hydroxyalkyl methacrylate and related monomers with swelling capacity up to 40-50%. They were used in developing contact lenses which have made a revolution in ophthalmology [2, 36]. In the early 1960s, the United States Department of Agriculture (USDA) developed a resin based on the grafting of acrylonitrile polymer onto the backbone of starch molecules (i.e., starch-grafting) to improve water conservation in soils. It has water absorption of up to 400g/g. Commercial production of SAP began in Japan in 1978 for use in the hygiene industry [3, 37]. Further developments lead to SAP materials being employed in baby diapers in Germany and France in 1980 [38, 39]. Nowadays, the application of SAP in the field of agriculture works as miniature water storage reservoirs especially for the small and marginal farmers living under arid and semi-arid regions to optimize water use efficiency and the yield of cash crops. The use of SAP in cement-based materials from the 2000s in which Jensen and Hansen firstly used SAP for cement-based materials to reduce autogenous shrinkage [40, 41]. Nowadays, there are a lots of research about SAP used in cement-base materials, aimed at reducing shrinkage [42, 43], controlling workability [10], enhancing the resistance of freezing [44], and enhancing the ability of self-sealing or self-healing [45-47].

Types of SAP

SAPs are classified majorly based on the presence or absence of electrical charge, type of monomeric unit, and source [48-50].

I. Based on presence or absence of electrical charge located in the cross-linked chains [49, 50]:

- a) Non-ionic (poly acrylamide (AA))
- b) Ionic (including anionic and cationic)
- c) Amphoteric electrolyte (ampholytic) containing both acidic and basic groups
- d) Zwitterionic (polybetaines) containing both anionic and cationic groups in each structural repeating unit.

For example, the majority of commercial SAP hydrogels are anionic.

II. SAPs are again classified based on the type of monomeric unit used in their chemical structure, thus the most conventional SAPs are held in one of the following categories [48]:

- a) Cross-linked polyacrylates and polyacrylamides
- b) Hydrolyzed cellulose-polyacrylonitrile (PAN) or starch-PAN graft copolymers
- c) Cross-linked copolymers of maleic anhydride

III. According to sources, SAPs are often divided into two main classes [49]:

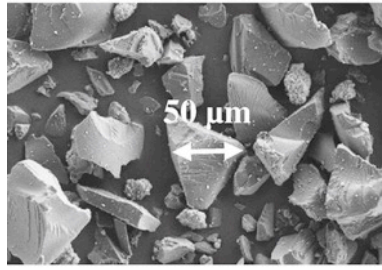
- a. Synthetic (petrochemical-based, e.g., poly(acrylate)-based copolymers)
- b. Natural (e.g., polysaccharide and polypeptide based).

For the SAP used in cement-based materials, mainly including the synthetic SAP, such as cross-linked acrylic acid and its salt [51-53] and cross-linked co-poly acrylic acid (or its salt)-acrylamide [41, 51-55]. As yet, there is no has become a public with non-ionic polymers as admixtures, such as cross-linked poly acrylamide, in cement-based materials. There is also some reference used biopolymer for cement-based materials such as alginate biopolymers [56] and carrageenan-based superabsorbent biopolymers [57]. Some novel SAP is also used for cement-based materials. A type of spherical SAP particles composed of an organic core (poly (acrylic acid) crosslinked with ethylene glycol dimethacrylate) and an inorganic shell (SiO₂ or CaO-SiO₂ inorganic shell) compatible with the cement technology were successfully fabricated [58]. Some novel pH-responsive superabsorbent polymers: methylenebisacrylamide-based and amine-based [49, 59] are also used for cement-based materials. Besides, a new type of cross-linked poly (2-acrylamido-2-methyl propane sulfonic acid) was investigated. It has a higher

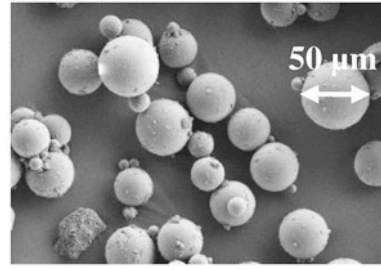
swelling capacity than carboxylic-based superabsorbent because of higher ionic strength, they also have high levels of swelling in saline solutions, they have higher gel strength, and the interaction between sulfonic groups and cement is stronger [60].

Preparation of SAP

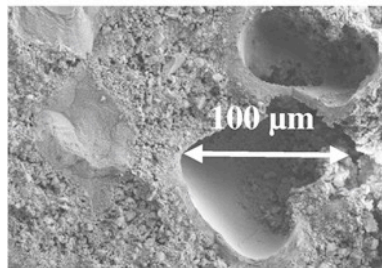
SAPs are prepared by free-radical initiated polymerization of partially neutralized acrylic acid and/or other comonomers e.g., methacrylic acid, along with a suitable cross-linker. In the polymerization process, the significant factors in these processes are the monomer and the cross-linker concentrations, the initiator type and concentrations, polymerization modifiers, the relative reactivity of the monomers, the basic polymerization kinetics, and the reaction temperature. There are three types of methods for polymerization of SAP: bulk polymerization [61], solution polymerization, and inverse suspension polymerization [62]. Bulk polymerization is the simplest technique that involves only monomer and monomer-soluble initiators. A high rate of polymerization and degree of polymerization occurs because of the high concentration of monomer. The advantage of bulk polymerization is that it produces high purity polymer. However, the viscosity of the reaction increases markedly with the conversion which generates the heat during polymerization. These problems can be avoided by controlling the reaction at low conversions and carrying it out in a solution (known as solution polymerization). In solution polymerization reactions, the ionic or neutral monomers are mixed with the multifunctional cross-linking agent. The polymerization is initiated thermally, by UV-irradiation, or by a redox initiator system. The presence of solvent serving as a heat sink is the major advantage of the solution polymerization over the bulk polymerization. The prepared SAPs need to be washed with distilled water to remove the unreacted monomers, oligomers, cross-linking agent, the initiator, the soluble and extractable polymer, and other impurities. This technique is associated with the difficulty associated with drying and grinding of superabsorbent gel into smaller particles, and the particle of SAP is irregular, as shown in Figures 1-1 (a) and (c). In inverse suspension polymerization, the monomer solution is dispersed in the non-solvent, such as hexane or cyclohexane, forming fine monomer droplets, which are stabilized by the addition of a stabilizer [63]. This polymerization method results in spherical SAP particles with a size range of 1 μm to 1 mm, as shown in Figures 1-1 (b) and 1-1 (d). The polymerization is initiated by radicals from the thermal decomposition of an initiator. The newly formed micro-particles are then washed to remove unreacted monomers, cross-linking agent, and initiator. The technique has gained importance because it allows easy removal of water and isolation of the product.



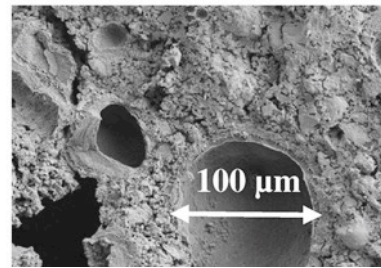
(a)



(b)



(c)



(d)

Figure 1-1. Particle shape for SAP made by (a) solution polymerization or (b) inverse suspension polymerization; (c) left pore of SAP made by solution polymerization in hardened cement paste after drying (d) left pore of SAP made by inverse suspension polymerization in hardened cement paste after drying [63]

Crosslinking, forming a chemical bridge between polymer chains is a very important step for the polymerization of SAP. The chains are cross-linked during polymerization by including a bifunctional monomer, a compound with two independent, polymerizable alkene functionalities. As shown in Figure 1-2, one end of the crosslinking agent acts as a monomer in the polymerization of one chain, while the other end of the crosslinking agent acts as a monomer in the polymerization of another chain. As a result, the two chains are linked together.

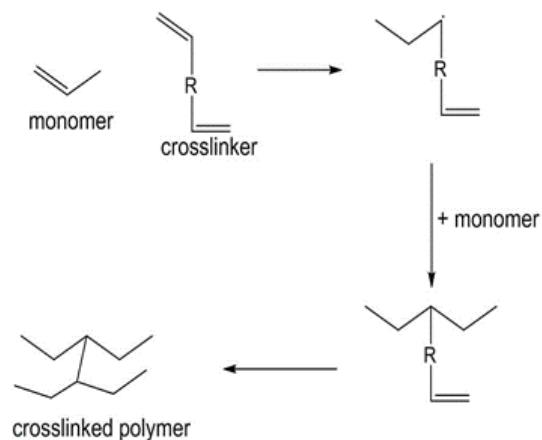


Figure 1-2. Scheme for Co-polymerization

Relatively small amounts of crosslinkers play a major role in modifying the properties of superabsorbent polymers. In addition to modifying the swelling and mechanical properties, the crosslinker affects the amount of soluble polymer formed during the polymerization. Typical crosslinkers used are N, N'-methylene bisacrylamide, di- & tri-acrylate esters e.g., 1,1,1-trimethylol-propane triacrylate or ethylene glycol diacrylate, as shown in Figure 1-3. The tendency of a cross-linker to be attached to the growing polymer chain depends on its relative reactivity ratio with acrylic acid or sodium acrylate, etc. The choice of the cross-linker depends on the method used for polymerization.

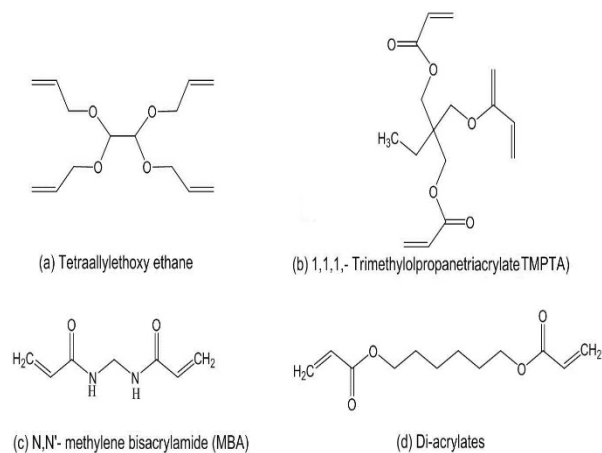


Figure 1-3. Chemical structure of typical crosslinkers used for superabsorbent

Absorption and desorption properties of SAP in solution

The main properties of SAP include absorption kinetics, such as the highest absorption capacity (maximum equilibrium swelling) in solution, highest absorbency under load (AUL), and absorption rate [37, 64]. The absorption capacity of SAP is calculated from the increase in the mass of the polymer sample and is typically reported as a ratio of the grams of fluid absorbed per gm of dry polymer. For SAP used in cement-based materials, absorption values in the filtrated solution or artificial pore solution are usually characterized [65, 66]. On the other hand, the use of SAP in items of application, such as personal hygiene, makes it necessary for it to hold the absorbed fluid even under the action of applied pressure. This property is known as the absorption under load. Diapers must absorb liquids under compressive loads of the order of 2.0 kPa, higher absorbency under load is desirable. This is a composite property of superabsorbent polymers, incorporating aspects of swelling capacities while under compressive stress, gel rigidity, and flow of liquid through a collection of particles. At the same time, for the SAP used in the cement-based materials, the mixing procedure would cause some pressure to SAP, which may affect the absorption of SAP. However, there is no relevant research for the AUL of SAP in cement-based materials. Polymers with higher elastic modulus resist the compression better than those with lower modulus and therefore have higher absorbency under load. At last, the rate of absorption of a liquid by a polymer depends on the maximum amount of liquid that can be absorbed as it provides the driving force for the swelling process. Lower crosslink density provides for larger maximum swelling capacity and thus increased driving force. Other factors affecting the absorption rate are the particle size and the particle size distribution in the sample, the density of the polymer, and the specific surface area of the particles. Small particle size and a high surface-to-volume ratio of the particles are necessary to increase the overall absorption rate.

The soluble fraction is that part of the polymer particle that is not attached directly to the network. The amount of soluble polymer is increased at lower crosslink density and at lower crosslinker efficiency (which occurs at the high conversion of monomer) and depends on the relative reactivities of the cross-linker and the acrylic acid. The uncross-linked chains do not contribute to the modulus of the sample but can be solvated and contribute to swelling if they are retained in the gel phase. The presence of soluble polymer in the gel lowers the chemical potential of the water in the gel, thereby increasing the difference in the chemical potential of water between the phases, which is the driving force for swelling. Because of an increased

driving force for swelling, the swelling rate can be increased by the presence of soluble polymer in the gel. However, once extracted from the gel, the soluble polymer can depress the swelling of the sample by reducing the chemical potential of water in the external liquid phase

Absorption and desorption properties of SAP in cement-based materials

Among these properties of SAP, the key properties of superabsorbent polymers are the absorption and desorption behavior of SAP which is related to swelling capacity or the elastic modulus of the swollen cross-linked gel. The absorption of a liquid by a polymer depends both on the nature of the liquid and the polymer. From the nature of the polymer, the swelling capacity depends on the number of ionic units in the polymer and the cross-link density. The absorption capacity of SAPs depends on several factors: (1) the polymer elasticity—a high cross-linking degree results in a stiffer and more brittle material which can take up less water than materials showing a lower crosslinking degree. However, cross-linking is essential to preserve the structural integrity of an SAP; (2) the polymer affinity for the solvent—hydrophilic functionalities including carboxylic acid (–COOH) and carboxylate (–COO–) moieties attract and hold water; (3) the osmotic pressure due to ion concentrations—if the aqueous solution consists of a small number of ions and the polymer bears ionic groups, water will penetrate the SAP due to osmosis, while the polymer elasticity still affects the extent of absorption. The swelling capacity or absorption also increases with an increase in the degree of neutralization of carboxylic acid groups, as shown in Figure 1-4.

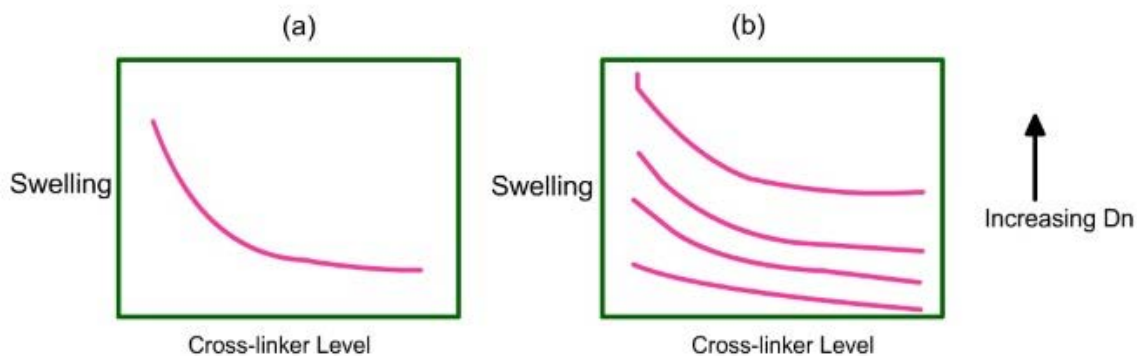


Figure 1-4. Change in swelling capacity with an increase in (a) Crosslinker concentration, (b) Degree of neutralization.

When the drying SAP contacts with water, SAP/water interactions (the external water molecules are attached by hydrophilic groups of SAP) give rise to osmotic pressure $\Delta\pi(\text{mix})$, which leads to

water flow into SAP. This osmotic pressure also leads to the expansion of SAP when it contacts the pore solution in cement-based materials [65]. Besides, the deprotonated acrylic-based polymers following the neighboring chains are charged and results in strong electrostatic repulsion. An expansive pressure term begins to contribute to the thermodynamic equilibrium $\Delta\pi(\text{ion})$. At the same time, a counteracting elastic force $\Delta\pi(\text{elastic})$ due to the cross-linking of SAP arises and limits the expansion. The ions in the solution change the inner- and intramolecular interaction of the poly-electrolyte due to shielding of charge ($\Delta\pi(\text{bath})$) on the polymer chain. As the ion concentration of the solution increases, the water absorption lowers concurrently because of polyelectrolyte shielding which generally reduces the osmotic pressure [67, 68]. Thus, an osmotic pressure $\Delta\pi$, as expressed by Eq. 1-1 [68], caused by the four different types of osmotic pressure forced the water into SAP to occupy the “phantom space” (fully expanded SAP space) of the SAP. That is to say, the hydrated polymer chains require more space than the non-hydrated ones in the dry state. Consequently, the absorption of SAP leads to expansion [10]. With the increase of absorption, the internal ionic concentration decreases, and the osmotic pressure difference tends toward equilibrium. However, in the cement-base materials, in addition to parameters depending on the SAP structure, the ionic strength of the aqueous solution is of special importance for the swelling of the SAP. The ionic concentration of the pore solution would change over time with the hydration of cement. The ions in the pore solution change the inner- and intramolecular interaction of the poly-electrolyte due to shielding of charge ($\Delta\pi(\text{bath})$) on the polymer chain. As the ion concentration of the solution increases, the water absorption lowers currently because of polyelectrolyte shielding which generally reduces the osmotic pressure [67, 68].

$$\Delta\pi = \Delta\pi(\text{mix}) + \Delta\pi(\text{elastic}) + \Delta\pi(\text{ion}) + \Delta\pi(\text{bath}) \quad (1-1)$$

The absorbency of SAP decreases with an increase in concentration and ionic strength of the solution due to a reduction in osmotic pressure. Moreover, the research [52] shows that the absorption of SAP is not only dependent on the concentration or ionic strength of the solution. Bivalent cations (such as Ca^{2+}) or trivalent cations (such as Al^{3+}) in the solution cause a much greater decrease in the swelling of SAP because of their bind with carboxylate groups in the acrylate chains, forming additional cross-links that inhibits swelling further. This term $\Delta\pi(\text{bath})$ further reduces the osmotic pressure and may even be so intense as to lead to a hydrogel collapse (contraction). On the other hand, the effect of anion type and valency on swelling behavior of SAP is relatively small [69]

1.2.2 Effects of SAP on fresh and hardened properties of concrete

Effect of SAP on fresh properties

High-performance concretes are made with significantly low water to cement ratios. This low amount of water would lead to autogenous shrinkage and crack propagation which reduces the durability of the concretes. Therefore, applying the internal curing method by using some materials such as SAPs would provide an optimal water supply, and improve the fresh concrete properties. At present, only a few results are available in the literature regarding the influence of SAP on concrete rheology [70-72]. If dry/under-saturated SAP is added to the matrix, SAP particles may absorb water from the matrix and decrease the internal water content or actual water to the cementitious material ratio (w/cm). It was reported that the addition of SAP (125-25 μ m) is equivalent to removing water from the system based on the particle size and dosage applied [11]. Jensen and Hansen concluded that the addition of 0.4% of a type of SAP would reduce the free w/c up to 0.06. This reduction can lead to the increase of yield stress and plastic viscosity up to 25% for concrete with a water to cement ratio of 0.4 [70]. For empirical methods such as the slump test, a decrease in the slump flow spreading [73] and an increase in flow time occurred of mortars [74]. Based on this, SAP was also used as a rheology modifying agent to regulate the rheological properties of concrete, such as shotcrete [10]. The fluidity of cement-based materials can be guaranteed with the appropriate size and content of SAP to be consistent with that of the control specimen [75]. The additional water amount can be used to provide the required water by SAP so that SAP will not adversely affect the surrounding matrix [70]. As a result, the rheological properties of fresh concrete are governed by water absorption and/or water release in fresh concrete as a function of size and dosage of SAP based on w/cm of concrete. It is reported that with the increase of particle size of SAP, the absorption of SAP increased and more time was required to reach a stable state [10]. It means that the larger SAP particle size would affect the rheology of UHPC greater in comparison to smaller particles. Mechtcherine et al. [76] studied the effect of SAP on the fresh properties of a self-compacting fiber-reinforced high-performance concrete. They compared the slump and V-funnel flow time of the control mixtures with corresponding mixtures including 0.4% SAP. They raised the water to cement ratio of the mixtures with SAP up to 0.05%. The results indicated that extra water increases the slump flow maximum 13%, while the V-funnel flow time can be increased. Monning [77] explored the effect of time on the slump flow of mortars containing varied contents of different SAPs. The slump time was recorded after additional 2 or 5 minutes mixing time

intervals. The results showed that when full saturation of the SAPs is attained, workability progression of the SAP included mixture is similar to the control mortar. It was also concluded that the effect of SAPs on the workability progression of the concrete due to the SAPs absorption period or the time that they hold water could be different. However, the extent of effect on the rheological properties of the mortar could not be derived from this research. Dudziak and Mechtcherine [78] researched to reduce the cracking potential of Ultra-High Performance Concrete (UHPC) using SAP. Three types of mixtures were prepared. One fine-grained steel fiber reinforced, the other one fiber-free including coarse aggregate, and finally five mixtures containing 0.3% to 0.4% of SAP were studied. Additional water to cement ratio of 0.04 to 0.07 was used. The average slump flow of the internally cured mixtures grew by about 2.2% compared to the reference mixtures. Dudziak and Mechtcherine [79] reported that the absorption of mixing water by SAPs causes a workability reduction in concrete containing SAP. The lower water to cement ratio affects more the strength of the concrete, especially at the early ages. They showed, even additional water cannot compensate for the water uptake by the SAP. They calculated the swelling capacity of SAP in artificial pore-fluid in their work and did not consider the real swelling capacity of the fresh mortar. They added 0.3–0.6 m% SAP by weight of cement to evaluate their effect. Snoeck et al. [75] studied the effect of high amounts of SAPs and additional water on the workability, microstructure and strength of a mortar with w/c of 0.5. They concluded that the small size and high absorption capacity of a type of studied SAP which is a copolymer of acrylamide and sodium acrylate with particle size of $100.0 \pm 21.5 \mu\text{m}$ ($n = 50$) would have a negative effect on the workability if it is used more than 1 m%. Sikora and Klemm [80] investigated the effect of three different SAPs on the cement hydration process. They concluded that the influence of SAPs on workability depends on their water absorption and compatibility with the hydration process. They reported that, although a type of SAP can have high water absorption capacity, the water absorption/desorption process may be delayed depending on the cement type.

Effect of SAP on mechanical properties

The effects of SAP on the mechanical properties of cement-based materials are not consistent. On one hand, SAP was added in HPC with additional water to ensure good workability, and the additional water can increase the number of capillary pores in the cementitious matrix after hardening. Besides, when SAPs release water, they can leave a large number of voids in the

hardened cementitious matrix. On the other hand, the IC effect of SAPs can increase the hydration of cement and improve the microstructure of cement-based materials.

Piérard et al. indicated that the compressive strength was 7% and 13% less than that of the control concrete (effective w/c = 0.35) at a curing age of 28 days for SAP contents of 0.3% and 0.6%, respectively. Esteves et al. showed that the compressive strength of SAP-modified mortar was 15–20% lower than that of the mortar without adding SAP under the curing condition of 95% RH. However, the compressive strength of mortar modified with SAP was only 5% less than that without SAP at 30% RH. Results of Justs et al. indicated that the compressive strength of UHPC with SAP contents of 0.206 wt% and 0.313 wt% decreased by 16% and 33% with respect to that of control UHPC at 2 days of age, and this difference was reduced to 9% and 19% at 28 days. Similar trends were also observed for the flexural strength and elastic modulus in this study. On the contrary, Mignon et al. indicated that there was no significant difference in flexural strength of mortar with w/c of 0.5 made with or without SAP. Bentz et al. also pointed out that the compressive strength of SAP-modified mortar was 73 MPa at 28 days, which was 1.2 times higher than that of reference mortar, with 0.35 w/c.

In general, the effects of SAP on the mechanical properties of cement-based materials depend on the specific mixture proportions, curing conditions, and testing age. The amount of additional water and the voids SAP leaves after water release are two factors that negatively affect the mechanical properties of cement-based materials. However, the IC effect of SAP can compensate for the strength loss and even can improve the mechanical properties.

Effect of SAP on Dimensional Stability

Plastic shrinkage

Shrinkage may also occur during the first hours after casting while the cement-based materials are still plastic and when it shows no significant strength development [81]. The cause of this plastic shrinkage is the (rapid) evaporation of water near the surface leading to high capillary pressures as water menisci begin to develop in between the solid particles [82]. This causes capillary tension among the solid particles and thus settlement and shrinkage. At some point, the water menisci disappear and air will flow in between the particles. If the specimen deformation is restrained, it may crack. By introducing internal curing utilizing the stored mixing water in the SAPs, the plastic shrinkage can be partially mitigated, next to the mitigation of

autogenous shrinkage during setting of the cement paste. Dudziak and Mechtchrine have studied the plastic shrinkage behavior of fresh cement paste until hardening [83]. The test was carried out in an extreme ambient environment (constant high temperature, simulated wind), the water-cement ratio of the control group was 0.3, and SAP (0.6% cement quality) and additional water were added in the experimental group ($w_e/c=0.087$). Dudziak and Mechtchrine found that the capillary pressure and the plastic deformations were reduced in the SAP mixtures, but the settlement deformation increased compared to reference sample. The plastic shrinkage cracking of concrete specimens was investigated by Olivier et al. [84]. It was indicated that the plastic shrinkage of mixes containing SAP reduced in comparison to the mix without SAP. Besides, by low field Nuclear Magnetic Resonance (NMR) test, Snoeck et al. [85] found that smaller particle size of SAP ($100.0 \pm 21.5 \mu\text{m}$) is better than larger SAP ($476.6 \pm 52.9 \mu\text{m}$) to mitigate plastic shrinkage by providing its stored water towards the cementitious matrix ($w/c=0.3$) during harsh drying conditions when a cement paste is hardening. In the interior of the samples, hydration occurs in sealed conditions. Near the drying surface, the free water is consumed first, followed by a gradual release of the stored water in SAP A, thus effectively mitigating plastic shrinkage.

Chemical shrinkage

Chemical shrinkage depends on the hydration degree of cement [86] and the degree of reaction of SCMs [87]. Usually, the chemical shrinkage is the same as the autogenous shrinkage before the initial setting. Chemical shrinkage was first investigated as a measurement of the degree of chemical reaction that had occurred in a hydrating cement paste [88]

As internal curing water releases, the later hydration degree of cement increases [89, 90], and chemical shrinkage increases. Therefore, it is concluded that the value of internal curing water is lower than the practical water amount for internal curing. Besides, the addition of SCMs to high-performance cement-based materials could affect the chemical shrinkage [91], and this also affects the efficiency of internal curing.

Autogenous shrinkage

By adding SAP, the development rate of early autogenous shrinkage of cement-based materials can be reduced, and the appearance of cracking can be delayed. When uses SAP for internal

curing of high performance cement-based materials, the dosage [41, 54, 55, 92], type [54, 55], particle size [41, 92], and pretreatment [93] of SAP, and water to cementitious ratio (w/cm) [42, 94] of cement-based matrix play a significant role on the efficiency of internal curing. Absorbed water in SAP acts as a reservoir of free water and has made these polymers promising materials to use with cementitious materials in concrete for reducing the autogenous shrinkage via internal curing [95-97]. Igarashi and Watanabe [94] found that the addition of SAP (0.35% by mass of cement, $(w/c)_{IC}=0.045$) can drastically reduce autogenous shrinkage for a cement mixture with a low W/C of 0.25. When the dosage of SAP is doubled, autogenous shrinkage was completely prevented. However, autogenous shrinkage cannot be prevented completely when a higher W/C of 0.33 was used, even when a very high amount of SAP was incorporated into the paste. The effectiveness of SAP on mitigating autogenous shrinkage is related to the particle size of the SAP. SAP with a larger particle size has a large water absorption [92], and a good effect on mitigating autogenous shrinkage [98]. However, when the w/c of internal curing ($(W/C)_{IC}$) introduced from the SAP is too large, it would increase the total w , which has a negative effect on concrete performance (workability, strength, etc.). It is recommended that the $(w/c)_{IC}$ should be controlled in a proper range, which means that the particle size and dosage of SAP should be considered. In another study conducted by Liu et al. [99], the shrinkage of ultra-high strength concrete with very low w/cm (0.18) was evaluated. It was found that the inclusion of SAP at different dosages changed the autogenous shrinkage values, remarkably. It was reported that the autogenous shrinkage reduced by 27.6% and 41.2% by including 0.3% and 0.6% of SAP, respectively. To overcome the high autogenous shrinkage of reactive powder concrete, the impact of supplementary cementitious materials and internal curing utilizing SAP were studied [100, 101]. It was reported that the autogenous shrinkage of the mixture with SAP could be reduced to half of the reference mix. Although, this reduction can be attributed to the internal curing which maintained the internal relative humidity at a higher level, so that the self-desiccation of the reactive powder concrete was strongly limited, which resulted in limiting the autogenous shrinkage.

Although SAP is promising for use in concrete [10], the internal curing may be influenced by the addition of SCMs in high-performance cement-based materials [102]. The addition of SAP (0.70% by mass of cement) could not completely prevent autogenous shrinkage of cement paste incorporation of SF [94]. Snoeck et al. [101] showed that the size of SAP A (with a mean diameter of 100 μm) is preferable in restraining autogenous shrinkage compared to the size of SAP B (with a mean diameter of 477 μm) when the cement paste contains different mineral

admixtures (fly ash and slag). At the same time, due to the pozzolanic effect, the autogenous shrinkage rate could increase quickly in the later period of hydration (28d). As a result, the SAP dosage should be increased to mitigate the effect of pozzolanic activity of SCMs that would contribute to enhancing long-term cement hydration.

Drying shrinkage

For a given effective w/cm, the addition of SAP increases drying shrinkage of high-performance cement-based materials [103, 104]. However, the drying shrinkage decreased with the increase of dosage of SAP under the condition of the same total w/cm [41, 104]. This is in agreement with the results reported by Assmann [105] and Kong et al [106]. Moennig and Reinhardt [107] found that SAP could reduce drying shrinkage. There are some controversies about drying shrinkage, and it may depend on the w/cm of the cement matrix. In contrast, Liu et al. [99] reported that the inclusion of 0.3% and 0.6% SAP would increase the drying shrinkage by 2.7% and 10.9%, respectively. On causes for the increase of drying shrinkage, Assmann [108] suggested that the absorbed water of SAP had higher mobility, and could evaporate more easily than the water in capillary pores. However, the drying stress caused by extra water is low, and the drying shrinkage is not big. Ma, et al. proposed that it may be because that the surface of the mortar could easily lose water, which caused humidity difference between the surface and inside of the concrete, thereby increasing by drying shrinkage [104]. Moreover, Kong et al [109] analyzed the influence of SAP in systems of larger water-to-cement ratio and found that for a water-to-cement ratio of 0.7, SAP had little influence on drying shrinkage of mortar, and under a water-to-cement ratio of 0.5-0.6, SAP could obviously decrease shrinkage. Overall, SAP increases the drying shrinkage, but decrease of the autogenous shrinkage contributes to the decrease of the total shrinkage (i.e., the autogenous and drying shrinkage). If the environment is particularly dry, the water in the SAP particles evaporates quickly, and cracking also happens.

Effect of SAP on Durability

Chloride ion permeability

Limited studies investigated the effect of SAP on corrosion and chloride migration compared to LWA. Hasholt and Jensen [61] studied the chloride mitigating properties of SAP in concrete. The authors concluded that if the addition of SAP increased the gel-space ratio, it would reduce

the chloride transport in concrete. It was found that if SAP was used without additional water, the reduction in w/c increased the gel-space ratio and improved chloride ingress resistance. Beushausen and Alexander [110] investigated the effect of SAP on Cl penetration of different binary cement mortars with w/cm of 0.45 and 0.55. Their results showed that the SAP was found to have a negligible effect on chloride penetration with a w/cm of 0.45, whereas the performance of the SF mortars showed a noteworthy improvement with increasing SAP content with a w/cm of 0.55. Farzanian et al. [111] investigated the different types and sizes of SAP on the electrical resistivity of cement pastes without additional water. They concluded that the electrical resistivity of cement pastes with slow desorbing SAPs appeared to be increased by pore structure densification. They reported that the hydrated products surrounded the SAPs particles and hindered the release of water from SAPs. Jin et al. [112] investigated the chloride penetration of concrete made with SAP exposed to the marine environment. Their results indicated that the SAP in the ocean-atmosphere zone can help to improve the chloride penetration resistance of concrete. However, excessive SAP dosage led to large voids and defects, which provided more space for the growth of corrosion products.

Carbonation resistance

The carbonation resistance of concrete containing SAP has been investigated in a few studies [113, 114]. Beushausen et al. [114] studied carbonation resistance of concrete with SAP at the age of 28 days. Samples were exposed to a carbonation chamber for 6 weeks, and the depth of carbonation was measured using phenolphthalein solution. The results confirmed the constructive effect of SAP in reducing carbonation depth. It was reported that the addition of SAP with the content of 0.4% can be considered as the optimum amount in durability improvement. Ma et al. [113] used SAPs with different sizes and reported that the SAP with a larger diameter (840 μm mean diameter) gave lower carbonation depth compared to SAP with a smaller diameter (125 μm mean diameter).

Freezing and thawing resistance

The mechanism that SAP can contribute to the frost durability is based on the air voids and pores that remain after the release of IC water from the SAP microstructure upon drying [12, 115]. The dried SAP can act as an air-entrained agent and improve the resistivity of concrete against freeze-thaw cycling [116]. Riyazi et al. [117] evaluated the potential benefits of SAP as a

mechanism for air-entraining. To reach this aim, the different contents of SAPs were included in cement mortars with w/cm of 0.48 in dry and pre-saturated conditions and were compared with concrete containing conventional air-entraining agents (AEA). Image analysis and high-resolution flatbed scanning techniques were used to evaluate the quality of the air void system during freeze-thaw cycling. The results showed that SAP was able to make a sufficient and satisfactory air void system in comparison to the AEA [117]. RILEM Technical Committee 225 [15] reported that the impact of SAP addition was ranged from negligible to significantly positive on mass loss of concrete samples after exposure to freeze-thaw cycles. Accordingly, concrete samples were prepared with w/c of 0.45 and 0.50. SAP, AEA, and deicing salt were added to compare with samples without any additive. A wide range of accelerated test methods was used to qualify the concrete resistance against freeze-thaw cycling. Furthermore, they found that finer SAP and application of SAP without additional water had better performance in freeze-thaw cycling. The relative dynamic modulus was reduced to below 60% in 83 and 116 freeze-thaw cycles for the mixture made with larger SAP and finer SAP, respectively. A similar phenomenon was also observed in a study by Kim et al. [118]. They used acrylic acid polymers with two sizes of 38 to 50 μm and 38 to 100 μm , and one type of copolymer of acrylic acid and acrylamide with the size of 600 to 1200 μm . They concluded that the larger SAP with the size of 600 to 1200 μm created a larger pore than the entrapped air, adversely affecting freeze-thaw resistance.

1.3 Research objectives

The main objective of this research is to examine and document the use of internal curing by SAP to improve the durability of Tollway bridge structures. The use of SAP can facilitate the production of internally cured HPC by a simple method before batching and reduce the cost-to-performance ratio compared with the HPC prepared with LWS. The specific objectives of the proposed research project are as follows:

- Investigate different types, particle size, water addition, absorption kinetics, and mixing time of SAP on the performance of HPC.
- Compare the effectiveness of SAP and LWS in controlling cracking and improving the durability of HPC designated for Tollway bridge structures.

- Evaluate the coupled effect of SAP content and initial moist curing regime on the performance of HPC, including shrinkage, mechanical properties, and durability.
- Determine the feasibility of using SAP in lieu of pre-saturated LWS for internally cured HPC.
- Determine the optimized HPC mixtures for bridge applications made with SAP.
- Monitor shrinkage deformation of large-scale slabs made with HPC internal cured with SAP.

1.4 Research tasks

The work plan included the following research tasks:

Task A: Literature review

The purpose of this task is to conduct a thorough review of the available literature, specifications, research findings, and ongoing project documentation to determine the current state-of-the-practice for using internally cured concrete with SAP,

Task B: Laboratory testing of HPC with SAP and LWA

A comprehensive laboratory research program included tests of SAP properties and absorption behavior. Characterization of absorption behavior is needed to calculate dosage of SAP to carry water equivalent to chemical shrinkage experienced by the cement during hydration. The SAP particle size was also measured. The mixtures will be tested for shrinkage (autogenous and drying shrinkage) and mechanical properties (compressive strength at 1 and 28 d) in addition to workability and rheology. Frost durability of HPC with SAP was also assessed. Curing conditions were also evaluated. The laboratory study included comparison of SAP with Lightweight Aggregate as a means of achieving internal curing.

Task C: Field implementation of HPC with SAP

A field testing program was undertaken to validate the performance of mixtures under actual field conditions and demonstrate the effectiveness of internal curing to control cracking and enhance durability and service life of bridge structures and pavement. Various measuring

techniques will use embedded strain gauge, lift-off displacement sensors, thermocouples, and humidity sensors to monitor the variations of deformation, temperature, and humidity of the concrete elements.

Task D: Specifications for SAP and concrete with SAP

The project developed practical guidance for constructing Tollway bridge structures with concrete with SAP. Recommendations for qualification procedures and specifications.

Task E: Final report

This final report documents all activities performed as part of this effort, including recommendations for future Tollway actions needed to ensure high quality concrete materials when using SAP for internal curing.

2. EXPERIMENTAL PROGRAM

2.1 Materials

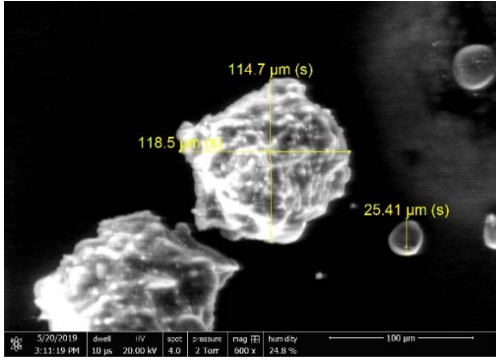
The laboratory work of this project was collaboratively conducted by Missouri S&T and UIUC. Both labs used the same types of SAPs and chemical admixtures from the same suppliers., but different locally provided cementitious materials and aggregates. The characteristics of cementitious materials and aggregates used by Missouri S&T and UIUC were presented in sections 2.1.3 and 2.1.4, respectively.

2.1.1 Superabsorbent polymers (SAPs)

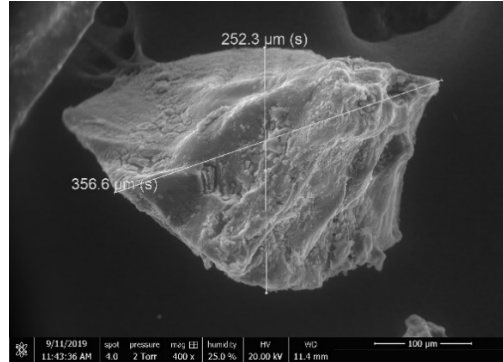
Table 2-1 lists the five types of SAPs that were characterized in Task B-1 of the project. Different types and sizes of commercial SAPs were used for internal curing in this study. These SAPs including Hydromax, Waste Lock 770, Waste Lock PAM/Type S, Waste Lock crushed PAM are abbreviated in this report as Hydro., WL-700, WL-PAM, and WL-CP, respectively. Figure 2-1 shows scanning electron microscope (SEM) images of four SAP types including the Hydro., WL 770, WL PAM, and BASF. The images were obtained under a different relative humidity of 16% and 25%. The particle size distributions of the SAPs are presented in Figure 2-2. The results represent averages of two tests conducted for each SAP. The WL CP SAP was obtained by crushing the WL PAM SAP into the finer size ranging from 0 to 63 μm .

Table 2-1. Types of investigated SAP products

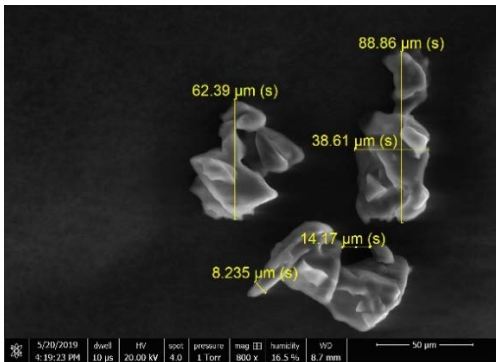
Type	Name
Powdered SAP	BASF SAP
	Hydromax
	M2Polymer Waste Lock 770 (Sodium neutralized acrylic homo polymer)
	M2Polymer Waste Lock PAM/Type S (Potassium neutralized acrylic acrylamide co polymer)
	M2Polymer Waste Lock crushed PAM (Potassium neutralized acrylic acrylamide co polymer)



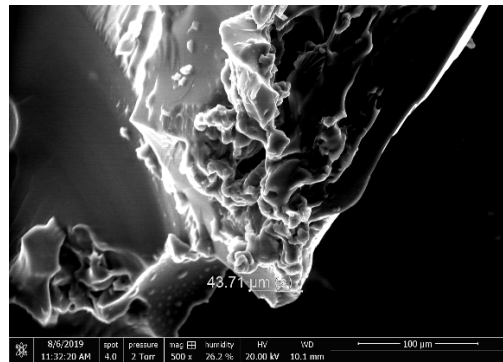
(a) Hydromax at 25% relative humidity



(b) WL-770 at 25% relative humidity



(c) BASF at 16% relative humidity



(d) WL PAM at 25% relative humidity

Figure 2-1. SEM images of different SAPs at a different relative humidity

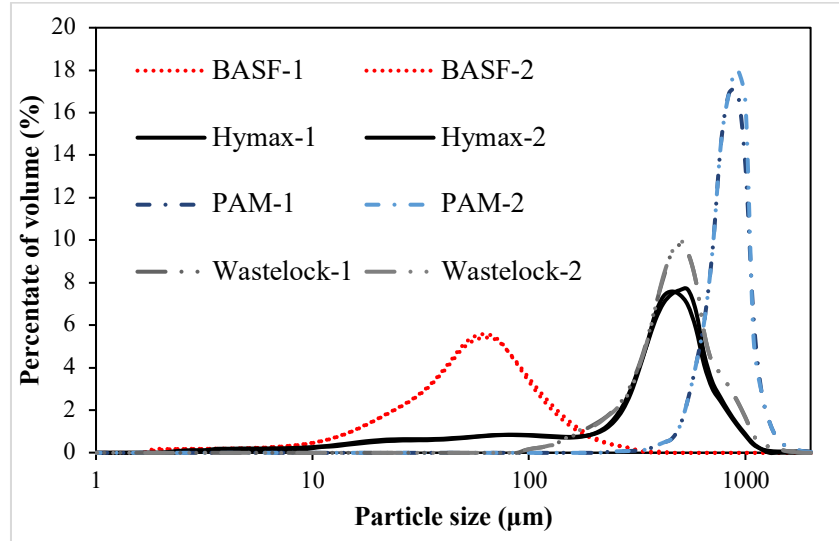


Figure 2-2. Particle size distributions of SAPs

2.1.2 Chemical admixtures

A polycarboxylate-based high-range water reducer (HRWR), Sika-ViscoCrete-2100, and a synthetic resin type air-entraining agent (AEA), Sika-AEA-14, were used to maintain flowability and air content within the target ranges. A set retarder (SikaTard-440) made with sucrose, gluconates, phosphates, and liginosulphonates was used to control the hydration of cementitious materials. The chemical admixtures used in this study comply with ASTM C494 [119].

2.1.3 Cementitious materials and aggregate used at Missouri S&T

A Type I/II ordinary Portland cement (OPC), complying with ASTM C150 [120], a Class C fly ash (FA) per ASTM C618 [121], and a ground-granulated blast-furnace slag (slag) per ASTM C989 [122] were used. Figure 2-3 shows the particle size distribution of the cement and FA. Table 2-2 presents the physical and chemical properties of the cementitious materials including the Blaine finesse of the binder materials.

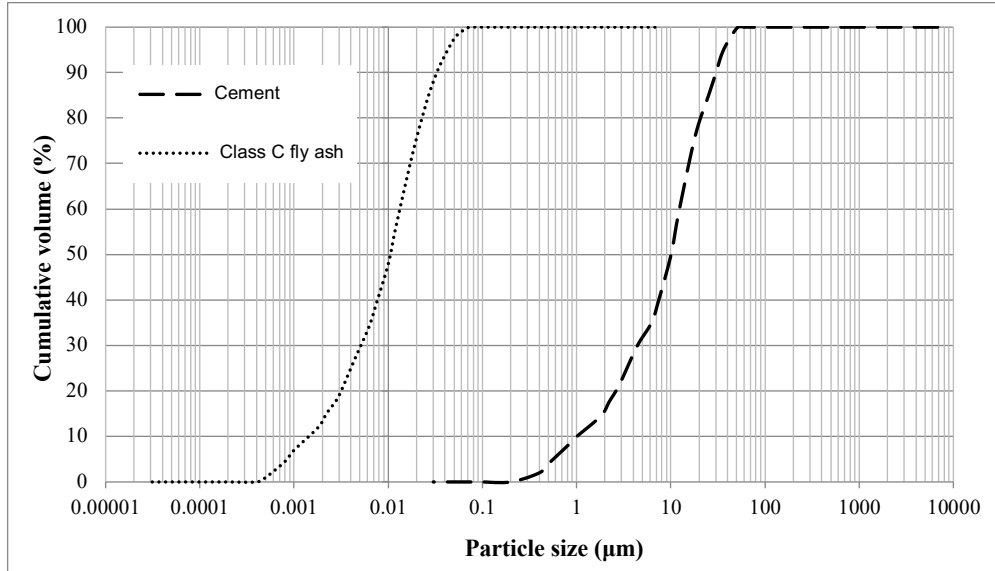


Figure 2-3. Particle size distribution of cementitious materials (µm) (S&T)

Table 2-2. Physical and chemical characteristics of cementitious materials and FA (S&T)

Binder	SiO ₂ (%)	Al ₂ O ₃ (%)	Fe ₂ O ₃ (%)	Ca O (%)	MgO (%)	SO ₃ (%)	Na ₂ O eq., %	CaCO ₃ (%)	Blaine surface area, m ² /kg	Specific Gravity	LOI, %
OPC	19.0	3.9	3.5	68.3	1.7	2.4	0.6	3.3	390	3.14	1.5
FA	40.4	19.8	6.3	24.4	3.5	1.0	1.3	-	490	2.71	-
Slag	36.2	7.7	0.7	44.2	7.6	1.7	0.52	-	530	2.86	-

A continuously graded natural sand was procured from Capital Sullivan Quarry in Missouri. The sand has a fineness modulus of 2.6, a specific gravity of 2.57, and a surface saturated dry (SSD) water absorption value of 0.36. A crushed limestone aggregate procured from the Capital Sullivan Quarry in Missouri was used. The coarse aggregate has a nominal maximum aggregate size of 1 in., a specific gravity of 2.72, and SSD water absorption of 1%. The grain size distribution of the fine and coarse aggregates is shown in Figure 2-4.

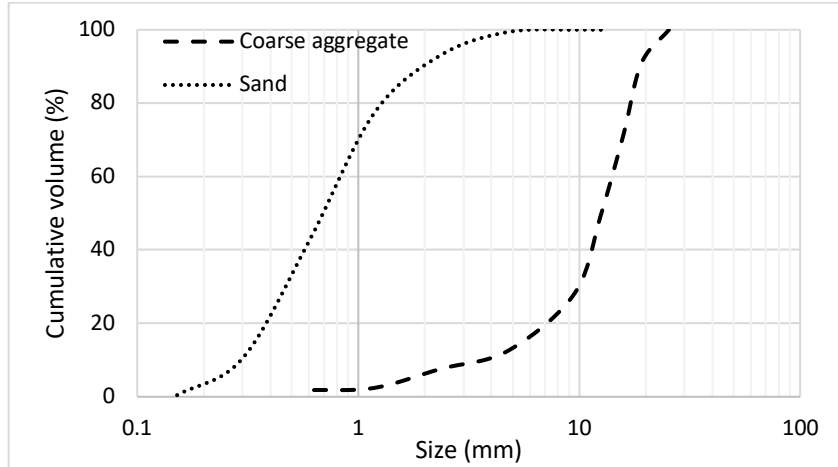


Figure 2-4. Grain size distributions of fine and coarse aggregates (S&T)

2.1.4 Cementitious materials and aggregate used at UIUC

A Type I/II ordinary Portland cement (OPC), complying with ASTM C150 [120], a Class C fly ash (FA) per ASTM C618 [121], and a ground-granulated blast-furnace slag (slag) per ASTM C989 [122] were used. Table 2-3 presents the physical and chemical properties of the cementitious materials including the Blaine finesse of the binder materials.

Table 2-3. Physical and chemical characteristics of cementitious materials and FA (UIUC)

Binder	SiO ₂ (%)	Al ₂ O ₃ (%)	Fe ₂ O ₃ (%)	CaO (%)	MgO (%)	SO ₃ (%)	Na ₂ O eq., (%)	CaCO ₃ (%)	Blaine surface area, m ² /kg	Specific Gravity	LOI, %
OPC	19.9	4.9	3.0	62.3	3.3	4.0	0.14	1.0	381	3.14	0.8
FA	36.2	17.6	5.4	27.2	6.1	1.9	2.0	-	-	2.75	0.5
Slag	36.2	7.7	0.7	44.2	7.6	1.7	0.52	-	530	2.86	-

Continuously graded natural sand and crushed limestone aggregate from Vulcan materials company in Kankakee, Illinois was used. The sand has a fineness modulus of 3.05, a specific

gravity of 2.57, and a surface saturated dry (SSD) water absorption value of 1.67%. The coarse aggregate has a nominal maximum aggregate size of 1 in., a specific gravity of 2.72, and SSD water absorption of 2.82%. The grain size distribution of the fine and coarse aggregates is shown in Figure 2-5. Lightweight sand from Haydite fines with a specific gravity of 1.35 and a 72 hours absorption of 22.2% was used.

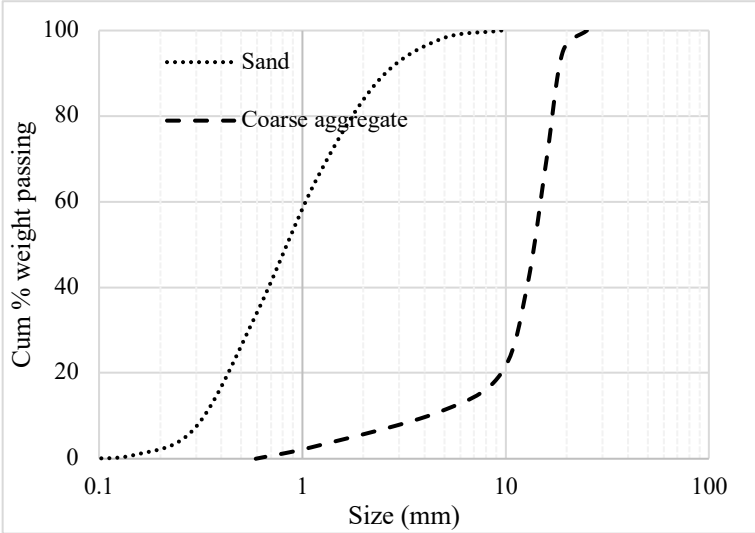


Figure 2-5. Grain size distributions of fine and coarse aggregates (UIUC)

2.2 Experimental program

2.2.1 Task B: Laboratory testing of HPC with SAP and LWS

The feasibility of using SAP in HPC mixtures was investigated in this section. This step focused on the effects of SAP types, different contents of IC water (i.e., SAP content), extended mixing time, and external curing period on workability, mechanical properties, viscoelastic properties, and durability of HPC mixtures made with SAPs designated for bridge structures. Task B includes four tasks, i.e., Subtask B-1: Pre-test of SAP for internal curing of HPC; Subtask B-2: Performance of HPC with optimized SAP; Subtask B-3: Optimization of external curing regimes; Subtask B-4: Comparison of HPC mixtures with LWS and SAP.

Task B-1: Pre-test of SAP for internal curing of HPC

This subtask was the preliminary study on high-performance concrete (HPC) prepared with five types of SAP used for internal curing. Five commercial SAPs were investigated to select two candidate materials for internal curing of HPC. The choice of SAP was finalized at the end of this task. The selected SAPs should be chemically stable and able to swell in the high alkaline saline solution similar to that of the pore solution in cement paste.

The mixture proportions of the investigated HPC mixtures are reported in Table 2-4. The w/cm was set to 0.37. The HPC was prepared with a ternary binder made with 35% slag and 13% FA replacement, by mass of the binder. The HRWR and AEA dosage rates were adjusted to maintain an initial slump of 5 to 8 in. and air content of 5% to 8%, respectively, in compliance with Illinois Tollway specifications. The specifications also stipulate that the minimum slump and air content after 55 min should be 3 in. and 4%, respectively.

In this study, the required mass of the SAP to compensate for chemical shrinkage was calculated per ASTM C1761/C1761M [123], as follows:

$$M_{sap} = \frac{C_f \times CS \times \alpha_{max}}{S W_{sap}} \quad (1)$$

where C_f is the content of the binder (lb/yd^3); CS is the chemical shrinkage of the binder at 100 % hydration rate; α_{max} is the maximum potential degree of hydration of the binder (0.91 in this study); S is the absorption rate of SAP in filtrated pore solution (52% OPC + 13% FA + 35% Slag), and W_{sap} is desorption rate of the SAP upon equilibrium at a relative humidity of 94% expressed as a fraction of oven-dry mass.

Table 2-4. Mixture proportioning of investigated concrete

Mixture	Materials (pcy)							Admixtures (fl oz/yd ³)		
	Cement	Slag	FA	Sand	CA	Water	SAP	HRWR	AEA	Retarder
Reference	310	210	80	1241	1810	222	0	15	6.5	12
Hydromax							2.73	22		
WL PAM							1.52	22		
WL 770							1.37	19.5		
BASF							1.13	28		
WL CP							1.85	34		

Table 2-5 lists the experimental program for evaluating HPC mixtures made with different SAP types in this task. The water absorption of SAP in the solution was measured using the tea bag method. of samples with SAP was conducted by two methods using a) unrestrained lineal prisms; b) sealed corrugated samples.

Table 2-5. Experimental program to evaluate HPC mixtures

Concrete property	Test
Absorption	Absorption and desorption of internal curing materials
Workability	Unit weight (ASTM C 138), air vol. (ASTM C 173), slump, up to 55 min
Rheology	Co-axial rheometer
Stability	Bleeding (ASTM C 232), Surface settlement
Mechanical properties	Compressive strength (ASTM C 39), 7, 14, 28, 56 days
Volume change	Autogenous shrinkage (ASTM C 1698), drying shrinkage (ASTM C 157)
Microstructure	SEM

Task B-2: Performance of HPC with optimized SAP

In this subtask, the optimum internal water content (SAP content), the acceptable extended mixing time, and the frost durability of HPC using SAPs were investigated to attain the proper working procedure for internal curing using SAPs in HPC. The optimum SAP content should ensure the proper internal curing for compensation of chemical shrinkage and the extended mixing time should ensure the homogeneous dispersion of SAPs. The performance of HPC in terms of workability, viscoelastic properties, mechanical properties, transport properties were evaluated to determine the optimum SAP content and extended mixing time in HPC. Then, the frost durability of HPC made with the optimum SAP content and proper extended mixing time was investigated. This subtask was divided into three phases, namely, B-2-1 Determine internal water content; B-2-2 Determine acceptable mixing time, and B-2-3 Investigate frost durability using SAP. The mixture proportioning of these three phases is listed in Table 2-6 to 2-8.

Table 2-6. Mixture proportioning of investigated concrete in subtask B-2-1

Mixture	Materials (pcy)							Admixtures (fl oz/yd ³)		
	Cement	Slag	FA	Sand	CA	Water	SAP	HRWR	AEA	Retarder
Reference	310	210	80	1241	1810	222	0	15	6.5	12
P-50-M3*							0.76	22		
P-100-M3							1.52	24		
B-50-M3							0.56	22		
B-100-M3							1.13	26		

*P- and B- denote WL PAM and BASF SAPs, respectively; 50- and 100- denote 50% and 100% of IC; M3 denotes 3-min extended mixing time

Table 2-7. Mixture proportioning of investigated concrete in subtask B-2-2

Mixture	Materials (pcy)							Admixtures (fl oz/yd ³)		
	Cement	Slag	FA	Sand	CA	Water	SAP	HRWR	AEA	Retarder
Reference	310	210	80	1241	1810	222	0	15	6.5	12
P-100-M3*								24		
P-100-M5							1.52	28		
P-100-M7								34		
B-100-M3								26		
B-100-M5							1.13	26		
B-100-M7								28		

*P- and B- denote WL PAM and BASF SAPs, respectively; 100- denotes 100% of IC; M3, M5, M7 denote 3-min, 5min and 7 min extended mixing time, respectively

Table 2-8. Mixture proportioning of investigated concrete in subtask B-2-3

Mixture	Materials (pcy)							Admixtures (fl oz/yd ³)		
	Cement	Slag	FA	Sand	CA	Water	SAP	HRWR	AEA	Retarder
Reference	310	210	80	1241	1810	222	0	15	6.5	12
Ref-without AEA								22	0	
P-100-M3							1.52	24	6.5	
P-100-without AEA								26	0	
B-100-M3							1.13	26	6.5	
B-100-without AEA								26	0	

Two SAP types selected from Subtask B-1 were employed. Three levels of water content corresponding to 0, 50%, 100% of the theoretical internal curing water to compensate for chemical shrinkage was investigated. The HPC was subjected to 6 days of external moist curing (1 d in mold + 6 din water). The testing parameters are elaborated in Table 2-9. In total, 5 HPC mixtures were tested. At the end of this step, the SAP content, and the associated level of internal curing were recommended for concrete pavement and Tollway structures.

Table 2-9. Parameters investigated in Subtask B-2

Objective	No. of HPC	Parameters	Ranges
Determine internal water content	5	Internal curing water with SAP content	0, 50%, 100% of the theoretical internal curing water
Determine optimum time to hydrate SAP	7	Extended mixing time after water addition	3 min, 5 min, 7 min
Investigate frost durability of using SAP	6	Air entrainment methods	Two SAP and one air-entraining admixture

The time of mixing was extended by 3, 5, and 7 minutes to evaluate the efficiency of hydration of SAP and its impact on workability and other key properties of the HPC, as elaborated in Table 2-10. The detailed testing parameters are elaborated in Table 2-9. HPC mixtures for typically used for bridge decks were prepared. At the end of this step, the optimum time duration of mixing was determined.

Frost durability of HPC with two selected SAP candidates was studied in B-2-3. Air entrainment with conventional air-entraining admixtures often encounters technical difficulties, such as coalescence of air bubbles in fresh concrete, loss of air during consolidation or pumping, and chemical incompatibility with high-range water reducer. Therefore, such a void system can be unstable. The effect of the two selected SAP types on freeze-thaw resistance of HPC was determined and compared with that of HPC with proper air entrainment. HPC mixtures either with or without SAP or with or without air-entraining admixture.

Table 2-10. Experimental program to evaluate bridge and pavement concrete mixtures

Concrete property	B-2-1	B-2-2	B-2-3	Test
Workability	*	*	*	Unit weight (ASTM C 138), air vol. (ASTM C 173), slump, up to 55 min
Rheology	*	*	*	Co-axial rheometer or ICAR rheometer
Stability	*	*	*	Surface settlement
Mechanical properties	*	*	*	Compressive strength (ASTM C 39), 1, 7, 28, 56 days
	*	*	*	Modulus of elasticity (ASTM C 469), 28 days
	*	*	*	Flexural strength (ASTM C 78), 28 days
Volume change	*	*	*	Autogenous shrinkage (ASTM C 1698), drying shrinkage (ASTM C 157)
Durability			*	Frost durability (ASTM C 666, Proce. A)
			*	Air-void parameters (ASTM C 457)
	*	*	*	Bulk electrical conductivity (ASTM C 1760), 28 days

Task B-3: Optimization of external curing regimes

Three HPC mixtures made with two selected SAPs with the optimum content (100% IC) from Task B-1 were investigated under three curing regimes. The curing regimes are elaborated in Table 2-11. The drying shrinkage within 28 days and compressive strength at 7, 14, 28, 56 days were tested in this task.

Table 2-11. Initial curing conditions for HPC mixtures

Moist curing duration	Detail
Air curing	1 day in mold, then air drying at 23 °C
Moist curing for 3 days	1 day in mold, then 2 days moist curing, then air drying at 23 °C
Moist curing for 7 days	1 day in mold, then 6 days moist curing, then air drying at 23 °C

Task B-4: Comparison of HPC mixtures with LWS and SAP

Two HPC mixtures made with the selected SAPs from the previous subtasks and one HPC mixture with lightweight sand (LWS) were investigated in this subtask. The mixture proportioning used in this subtask is listed in Table 2-12. The performance of the HPC in terms of workability, mechanical properties, viscoelastic properties, and durability were evaluated. Detailed testing parameters are listed in

Table 2-13. All specimens were air cured in this subtask to study the behavior under the least water curing conditions, where internal curing can help the most.

Table 2-12. Mixture proportioning of investigated concrete in subtask B-4

MIX ID	Materials (pcy)								Admixtures (fl. oz./yd ³)		
	Cement	Slag	FA	Sand	LWS	CA	Water	SAP	SP	AEA	Ret.
Reference	310	210	80	1250	-	1810	222	-	30	3	12
WL-PAM								1.51	48	2.1	12
BASF								1.12	45	2.1	12
LWS				959	188			-	30	3	12

Table 2-13. Experimental program of subtask B-4

Concrete property	Test
Workability	Unit weight (ASTM C 138), air vol. (ASTM C 173), slump, up to 55 min.
Mechanical properties	Compressive strength (ASTM C 39) 3, 7, 14, 28 days
	Modulus of elasticity (ASTM C 469), 28 day
	Flexural strength (ASTM C 78), 28 day
Volume change	Autogenous shrinkage (ASTM C 1698), drying shrinkage (ASTM C 157)
	Ring test (ASTM C 1581)
Durability	Frost durability (ASTM C 666, Proce. A)
	Air-void parameters (ASTM C 457)

2.3 Mixing and test methods

2.3.1 Mixing procedure and curing

The batching and mixing procedure were as follows: coarse aggregate and sand were mixed in a drum mixer at S&T and in a pan mixer at UIUC with half of the mixing water with the AEA diluted in water for 1 minute. The cement, FA, and slag were then added with a quarter of the mixing water and set retarder that were mixed for 30 s, followed with another quarter of the mixing water and HRWR. The concrete was then mixed for 90 s. The slump, air content, and unit weight were then measured within 5 minutes. The concrete mixed again for 2 min, followed by the introduction of the SAP, and mixing for 3 min. A funnel was used to add the SAP during mixing to ensure proper dispersion of the SAP material. The HRWR was also added to maintain the targeted fluidity given the

impact of the SAP on the absorption of some of the mixing water. The slump, air content, and unit weight were then measured at the end of the second mixing stage. The slump and air content were measured roughly at 2 min and 15 min for reference and mixtures made with SAP, respectively, after water came in contact with cementitious materials and marked as the initial slump and air content. The second and third slump measurement was also conducted 20 min and 40 min after the initial slump measurement. During the two 20-min intervals, the concrete was at rest for 4 min and agitated with a high rotational velocity in the mixer for 1 min at every 5 minutes. The second air content measurement was conducted 40 min after the initial air content measurement.

Concrete specimens were cast soon after testing. The specimens were demolded after one day. In Task B-1 and B-2, the specimens were then cured in lime-saturated water for 6 days at a temperature of 73 ± 3 °F followed by air drying at the ambient temperature of 73 ± 5 °F until the time of testing. In Task B-3, three different external curing were selected for the specimens after demolded, including 1) cured in lime-saturated water for 6 days at a temperature of 73 ± 3 °F followed by air drying at the ambient temperature of 73 ± 5 °F; 2) cured in lime-saturated water for 2 days at a temperature of 73 ± 3 °F followed by air drying at the ambient temperature of 73 ± 5 °F, and 3) cured air drying at the ambient temperature of 73 ± 5 °F.

2.3.2 Test methods

Fresh properties

The workability tests, including slump, unit weight, air content and surface settlement were evaluated. The unit weight and air content of the mixtures were measured according to ASTM C138 [124] and ASTM C231 [125] respectively. The slump was measured according to ASTM C143 [126]. The stability of the mixtures was measured using a surface settlement test that is shown in Figure 2-6. The yield stress and plastic viscosity of the mixtures were measured using the ConTec 5 rheometer. The fresh concrete was pre-sheared at 0.5 rps for 30 seconds. Then the rotational speed was reduced from 0.4 to 0.025 rps in 10 steps. For each step, 25 points were collected. The flow curves were evaluated to ensure equilibrium, and the highest two data points were eliminated. The Bingham model was used to calculate the yield stress and plastic viscosity based on eight data points with a maximum rotational velocity of 0.4 rps.



Figure 2-6. Surface settlement test

Mechanical properties

The compressive strength of concrete was determined at 7, 14, 28, and 56 days using 4×8 in. cylindrical samples in compliance with ASTM C39 [127]. The cylinders were capped using a high-strength Sulphur capping compound, per ASTM C 617 [128]. The loading rate was controlled to secure compressive stress of 35 ± 7 psi/sec. Figure 2-7 shows the compressive strength test setup.



Figure 2-7. Test setup for compressive strength

The flexural strength testing was conducted on prismatic samples measuring 3×3×16 in. with a span length of 12 in. according to ASTM C1609 [129]. The loading rate was maintained at

displacement control of 0.0035 in./min until the failure of beam samples. Figure 2-8 shows the test set-up for this test.

The flexural strength was calculated as follows:

$$F = PL/bd^2 \tag{2}$$

where F is the strength (psi); P is the load (lbf), L is the span (in.), b is the average width of the sample (in.), and d is the average depth of the sample (in.).

The residual strength was calculated using the above equation and the residual loads at deflections of L/600 and L/150.



Figure 2-8. Test setup for flexural strength measurement of beam specimens

The modulus of elasticity was tested using 4x8 in. cylinder samples according to ASTM C469 [130]. The specimens were loaded at three cycles. The testing procedure was set as the moving head travels at a rate of about 0.05 in./min. The load rate was maintained to secure compressive stress within the range of 35 psi/s. The specimen was loaded until the applied load is 40% of the average ultimate load of the companion specimens. Figure 2-9 shows the test set-up for this test. The modulus of elasticity was calculated as follows:

$$E = (S_2 - S_1) / (\epsilon_2 - 0.000050) \tag{3}$$

where E = modulus of elasticity, S₂ = stress corresponding to 40% of ultimate load, S₁ = stress corresponding to a longitudinal strain, ε₁, of 50 millionths, and ε₂ = longitudinal strain produced by stress S₂.



Figure 2-9. Testing set-up of modulus of elasticity

Transport properties

The electrical resistivity measurement was used to classify concrete based on the corrosion rate. The electrical resistivity was determined on saw-cut cylindrical samples at the age of 28 days. The measurement of electrical resistivity was determined using two different methods: as shown in Figure 2-10 using the direct two-electrode method ASTM 1760 [131] and the four-point Wenner probe method (AASHTO TP 95-11), corresponding to bulk electrical conductivity and surface resistivity, respectively.



Figure 2-10. Testing apparatus for surface resistivity (left) and bulk resistivity (right)

Viscoelastic properties

Drying shrinkage ASTM C157 [132] was determined on prismatic samples measuring 3×3×11.25 in. using a digital type extensometer. After demolding, the specimens were placed in lime-saturated water for an hour, and the 1st reading was then taken. The specimens were cured in lime-saturated water for 6 days. The length at the end of the curing period was used as the initial length to calculate shrinkage. The samples were air-dried in an environmental control room (50% ± 4% relative humidity and 73 ± 3 °F temperature). The length change was determined at 4, 7, 14, 21, and 28 days of drying.

Autogenous shrinkage was evaluated per ASTM C1698 [133]. The samples were cast in standard corrugated plastic tubes for autogenous shrinkage measurement of each mixture. The tubes for the autogenous shrinkage testing were 16.5 in. in length. The diameter of the tubes was 1.2 in. at the ridge and 1.0 in. at the groove. Shrinkage measurements were performed starting at around 18 hours after the water came in contact with the cementitious materials (the final setting was assigned as the zero time), and after 6 and 12 h after the final setting time, and then daily for the first week and on weekly basis until the age of 28 days. Figure 2-11 shows the drying shrinkage and autogenous measurement test setups.

Induced tensile stress was evaluated using restrained shrinkage per ASTM C1581 [134]. The samples were cast around an instrumented steel ring with outer diameter of 13 in. and wall thickness of 0.5 in. Concrete forming tubes of inner diameter 16" were used to form the concrete rings. The rings were 6 in. high. The shrinkage of the concrete causes a compressive strain in the steel ring. Cracking of the concrete leads to a sudden decrease in this strain. Two concrete rings were cast for each concrete mixture and stored in an environmentally controlled room at 73.5 ± 3 °F temperature and relative humidity of 50 ± 4 %. Figure 2-12 shows the ring test setup.



Figure 2-11. Shrinkage measurement (a) drying shrinkage and (b) autogenous shrinkage



Figure 2-12. Restrained shrinkage measurement using ring test

Frost durability

The resistance of concrete to freezing and thawing was determined per ASTM C666 [135], procedure A. Saturated prisms of dimension 3×4×16 in. were subjected to cycles of freezing and thawing between 0 ± 3 °F and 40 ± 3 °F and are shown in Figure 2-13 . The relative dynamic modulus of elasticity of each prism was determined at the beginning of the cycles and then periodically at intervals not exceeding 36 cycles. It was calculated as follows:

$$P_C = \left(\frac{n_1^2}{n^2} \right) \times 100 \quad (4)$$

where P_c is the relative dynamic modulus of elasticity, after c cycles of freezing and thawing (%), n is the fundamental transverse frequency at 0 cycles of freezing and thawing, and n_1 is the fundamental transverse frequency after c cycles of freezing and thawing.

The test was carried out till the relative dynamic modulus of elasticity reached 60% of the initial value or 300 cycles whichever occurred first. The durability factor was calculated based on the obtained results using the following formula:

$$DF = \frac{PN}{M} \tag{5}$$

where DF is durability factor (%), P is relative dynamic modulus of elasticity at N cycles (%), N is the number of cycles at which P reaches the specified minimum value at which the cycles are stopped, and M is the specified number of cycles at which the cycles are stopped.



Figure 2-13. Test setup for frost durability

Hardened void analysis

Concrete cylinders (4 × 8 in.) were cut into two circular disks of approximately 1 in. thickness. The disks were cut about 2 in. away from the ends of the cylinder. The specimens from the laboratory testing were polished by grinding the specimen against abrasive papers with grits of

60, 120, 180, 400, 800, and 1000 using NANO 2000T grinder-polisher by PACE Technologies as seen in Figure 2-14. The specimens from field trial 1 were prepared using diamond discs with grits of 80, 180, 360, 800, and 1200 on a lapping wheel ASW-1800.



Figure 2-14. NANO 2000T grinder-polisher machine setup

The polishing protocol was in accordance with ASTM C457/C457M-12 [136]. The specimens after polishing were dried in air until completely dry. Polished surfaces of dried specimens were then prepared for scanning following an advanced technique developed by Lange research lab [137]. Orange florescent chalk power was used to fill the voids on the surface, and extra powder were removed from the surface using a sharp razor blade at low angle. The void filled specimens were scanned using a flatbed scanner at a resolution of 4800 dpi, and a 2 in. × 2 in. center section of each scanned image was selected for air void analysis. Based on deep learning method [138], the three major components of concrete, i.e. aggregate, paste, and voids, were segmented from the scanned images. The air void parameters were then obtained from further processing the segmentation results. Figure 2-15 shows a pair of original scanned image and its segmentation as an example.

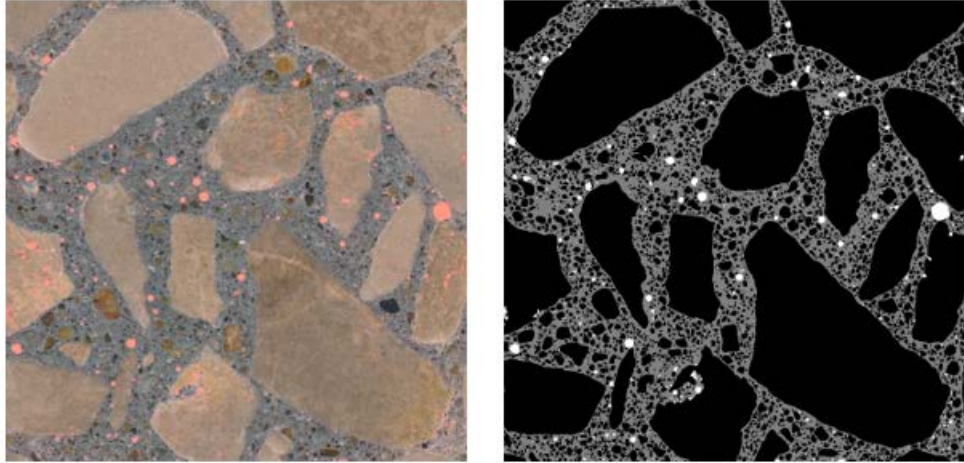


Figure 2-15. Example of the original scanned image (left) and the segmentation (right)

3. LABORATORY TESTING RESULTS AND DISCUSSION

This section reports the results and discusses the effect of different SAP types, contents of internal curing water by varying the SAP content, mixing time, and duration of the external curing regime on the performance of internally cured HPC. The targeted properties include workability, mechanical properties, viscoelastic properties, and durability of HPC mixtures designed for Illinois Tollway bridge decks.

3.1 Subtask B-1: Pre-test of SAP for internal curing of HPC

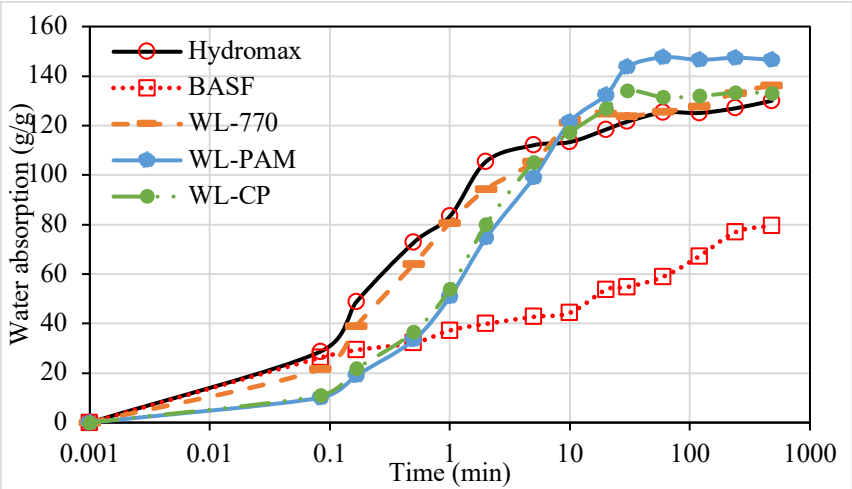
This subtask focuses on characterizing five commercially available superabsorbent polymers (SAPs) to select candidate materials for internal curing of HPC. The choice of SAP was finalized at the end of Task B-1. The selected SAP was chemically stable and able to swell in the high alkaline saline solution similar to that of the pore solution in cement paste.

Absorption and desorption kinetics of SAPs

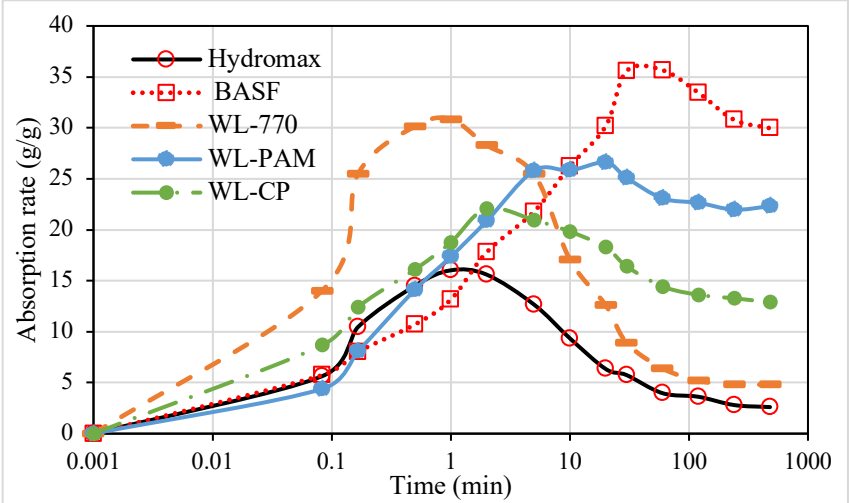
Figure 3-1 shows the absorption rate (g/g) over 8 h of SAP in distilled water and filtrated pore solutions made with 52% cement + 35% Slag + 13% FA, both with and without various chemical admixtures. The results from Figure 3-1(a) and (b) show that the absorption rate of all the SAPs in distilled water was significantly higher than those in the filtrated pore solution. The absorption rate of the BASF and WL PAM SAPs gradually increased to peak values of 35.7 and 25.8 g/g, respectively, in filtrated pore solution made without any chemical admixtures, and then slightly decreased and remained stable after 2 and 8 h, respectively. The absorption rate of the Hydromax and WL 770 SAPs increased rapidly to peak values then decreased sharply to low absorption rates of 2.6 and 4.8g/g, respectively.

Furthermore, it can be observed that the addition of a set retarder to the filtrated pore solution significantly delayed the peak of maximum absorption rate of the Hydro. and WL 770 SAPs. The maximum absorption rate of the Hydro. and WL 770 SAPs were reached after approximately 1 min when a set retarder was not used in the solution, as shown in Figure 3-1(b), while the maximum absorption rate for the Hydro. and WL 770 SAPs were reached after 2 and 10 min, respectively, as shown in Figure 3-1(e). It can also be observed that the use of a set retarder did not have a significant effect on the maximum absorption rate of the SAPs. The absorption rate of SAPs in the filtrated pore solution with the 0.25%HRWR+0.15%Retarder +0.08%AEA

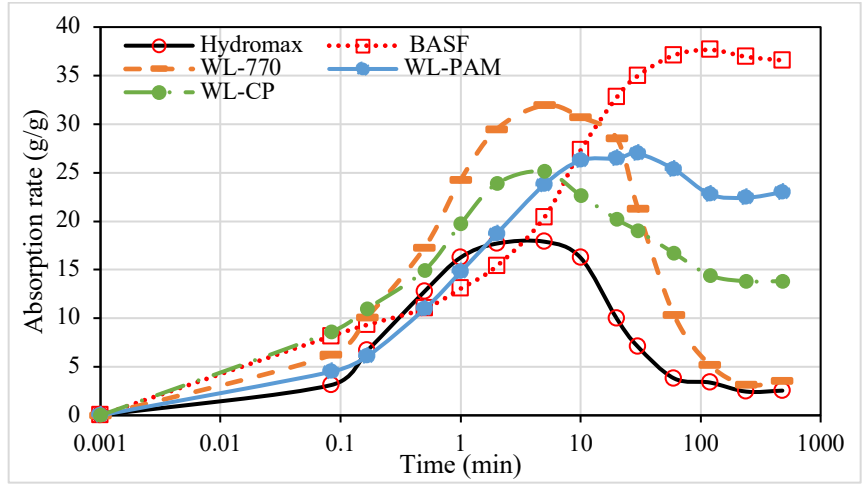
followed a similar pattern with those in the filtrated solution made with 0.15%Retarder. The maximum absorption rates obtained with the different SAPs are listed in Table 3-1. In general, the addition of chemical admixtures did not have a significant effect on the maximum absorption rate of the SAP but delayed the peak of maximum absorption rate for the Hydro. and WL-770 SAPs.



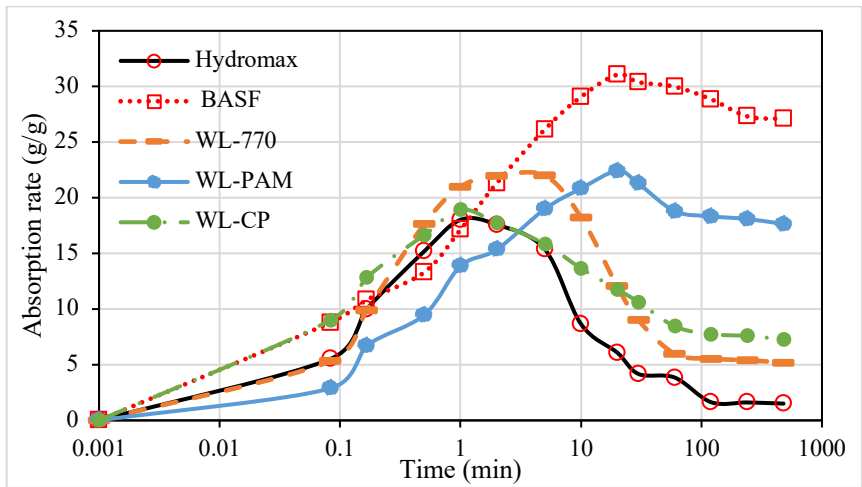
(a) Distilled water



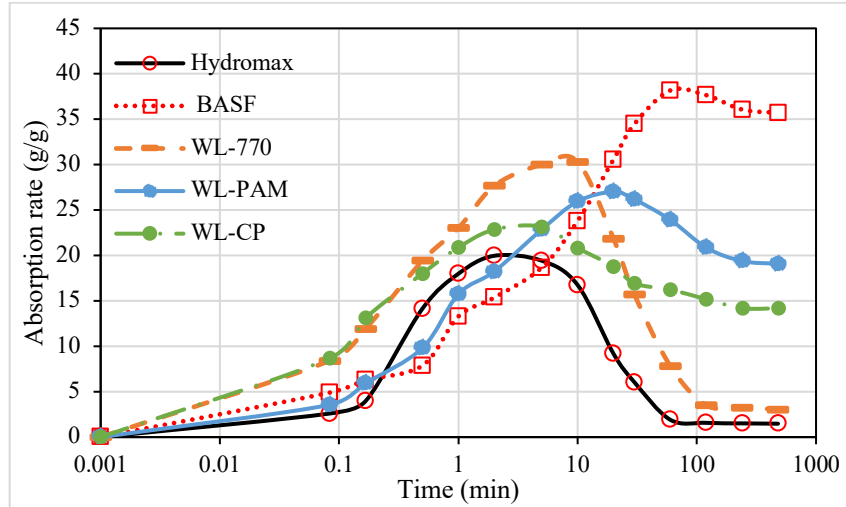
(b) 52%OPC+13%FA+35%slag



(c) 52%OPC+13%FA+35%slag with 0.25%HRWR+0.15%Retarder+0.08%AEA



(d) 52%OPC+13%FA+35%slag with 0.25%SP



(e) OPC+13%FA+35%slag with 0.15%Retarder

Figure 3-1. Variations of absorption rate of SAPs in different filtrated solutions

Table 3-1. Peak absorption and absorption times obtained in distilled water and filtrated pore solutions made with and without chemical admixtures

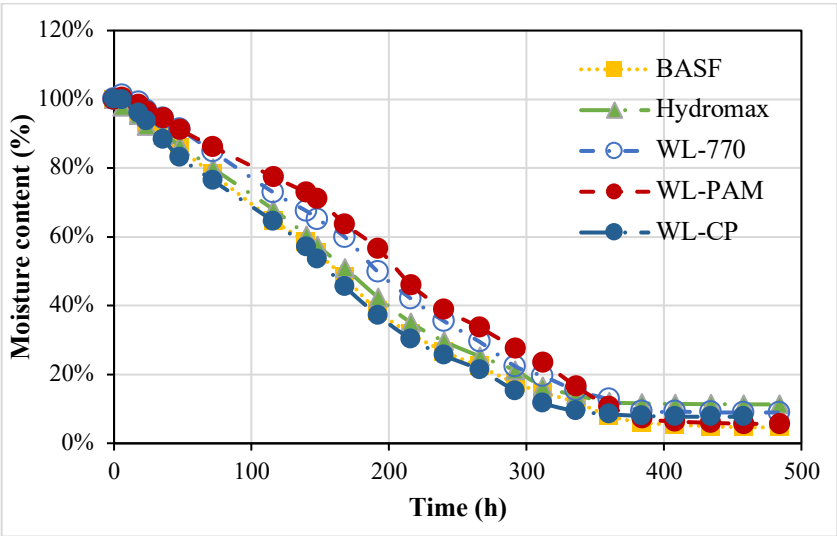
		Hydro.	BASF	WL PAM	WL CP	WL 770
Filtrated pore solution	Peak absorption (g/g)	16.0	35.7	25.8	22.1	30.8
	Peak absorption time (min)	1	60	10	2	1
	Absorption at 5 min (g/g)	12.7	21.8	25.8	20.1	25.5
Filtrated pore solution with 0.25%SP+0.15%Retarder+0.08%AEA	Peak absorption (g/g)	17.9	37.7	27.0	25.1	32
	Peak absorption time (min)	5	120	30	5	5
	Absorption at 5 min (g/g)	17.9	20.4	23.8	25.1	32.0
Filtrated pore solution with 0.25%SP	Peak absorption (g/g)	18.0	31.0	22.4	18.9	22.0
	Peak absorption time (min)	1	20	20	1	5
	Absorption at 5 min (g/g)	15.4	26.1	19.0	15.9	22.0
Filtrated pore solution with 0.15%Retarder	Peak absorption (g/g)	19.9	38.2	26.2	23.2	30.3
	Peak absorption time (min)	2	60	30	5	10
	Absorption at 5 min (g/g)	19.4	18.7	22.9	23.2	30.0

Figure 3-2 shows the desorption rate (%) of the investigated SAPs saturated with 2.5 ml distilled water and filtrated pore solutions (52% cement + 35% Slag + 13% FA) prepared with and

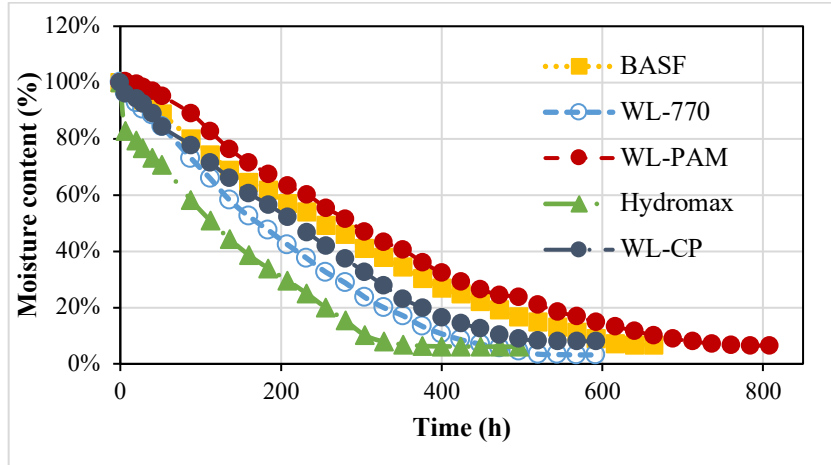
without chemical admixtures. The desorption rate (%) of SAPs saturated filtrated pore solutions was recorded until the mass of saturated SAPs reaches a spread of 0.01g per day.

The desorption of the SAPs saturated with distilled water was faster than those saturated with filtrated pore solution. The desorption of the WL PAM SAP was the slowest in both distilled water and filtrated pore solution made without any chemical admixture. The final desorption rate of the Hydro. and WL-770 SAPs were 5% and 6% lower in distilled water than in filtrated pore solution made without chemical admixtures. However, the final desorption rate of the other SAPs differed within 2% in distilled water or infiltrated pore solution without chemical admixtures.

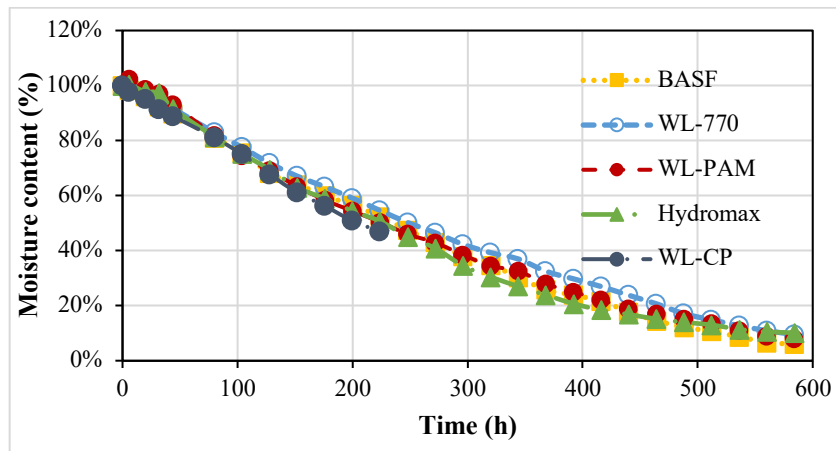
Based on Figure 3-2(b) to (c), the chemical admixtures significantly delayed the desorption of Hydro., WL-770 in filtrated pore solution, whereas no obvious effect on desorption of WL-PAM, WL-CP, and BASF SAPs was found. The chemical admixtures also reduced the final desorption rate of Hydro. and WL-770 SAPs by 4% and 6%.



(a) saturated SAPs in 2.5 ml distilled water



(b) saturated SAPs with 2.5 ml filtrated pore solution made without chemical admixtures



(c) saturated SAPs with 2.5 ml filtrated pore solution made with 0.25%HRWR+0.15%Retarder+0.08%AEA

Figure 3-2. Variations of desorption rate of the investigated SAPs with time

Fresh properties

Table 3-2 summarizes the fresh properties of the investigated HPC mixtures, including the initial slump, air content, and unit weight. The SP demand was adjusted to maintain an initial slump within the target value of 8 inches. Illinois Tollway stipulates that slump loss should be limited to 2 in. per 20 minutes. The initial slump and air content measurement were conducted 2 min and

12 min after the cement and water contact for the reference and the other mixtures made with SAP, respectively.

The initial slump values after the addition of SAP were approximately 8 to 8.5 in., which were similar to the values before SAP addition. The addition of SAP resulted in a significant increase in SP dosage ranging from 4.5 to 19 fl oz/yd³, with the highest value observed with the WL-CP SAP. The total SP content for the mixtures made with SAPs ranged from 19.5 to 34 fl oz/yd³ compared to 15 fl oz /yd³ for the reference mixture. Compared to the reference mixture, the use of the WL CP SAP and BASF SAPs increased the SP content by 126% and 75%, respectively, while the use of other SAPs increased the SP content by 30% to 47%. The main reason for the higher increase in SP content of the WL CP SAP and BASF SAPs is due to their smaller particle sizes.

Table 3-2. Fresh properties of HPC made with and without SAPs

Mixture	Slump (in.)			Air volume (%)		Unit weight (lb/ft ³)	SP content (fl oz/yd ³)		
	Initial*	20 min	40 min	Initial*	40 min		Before SAP addition	After SAP addition	Total
Reference	8.1	7.5	6.8	5.0	6.8	144.4	15	-	15.0
Hydro.	8.7	8.4	8.2	5.1	5.3	150.4	15	7.0	22.0
WL PAM	8.0	4.5	1.3	5.1	5.8	146.7	15	7.0	22.0
WL 770	8.3	8.2	8.0	5.8	6.4	142.2	15	4.5	19.5
BASF	8.4	6.6	4.8	6.1	6.6	145.9	15	11.5	26.0
WL-CP	8.5	7.6	6.9	5.4	6.1	145.6	15	19.0	34.0

The slump loss of the mixtures made with the Hydro., WL 770, and WL CP SAPs was less than 1 in. after 20 min, which meets the requirement of the Illinois Tollway. However, the use of the BASF and WL PAM SAPs resulted in greater slump loss over time, with values of approximately

1.8 and 3 in. per 20 minutes, respectively. The greater slump loss of the HPC made with the BASF or WL PAM SAP can be attributed to their absorption kinetics that exhibited continued absorption up to 50 minutes. The finer particle size of the BASF SAP required an increase in SP demand, which can also contribute to slump retention. On the other hand, the larger size of the WL PAM SAP that contributed to lower SP demand caused higher slump loss over time (up to 3 in. per 20 minutes). The HPC mixtures prepared with the various SAPs had initial air contents of approximately 5.1% to 6%. The air content increased slightly from 5.3% to 6.6% at 40 min of age.

Rheology

Table 3-3 summarizes the yield stress and plastic viscosity of HPC made with and without SAPs. The rheology test was conducted at approximately 5 min and 15 min of age (about 3 min after starting the initial slump measurement) for reference and other mixtures made with SAPs. The results showed that the addition of WL PAM, BASF, WL CP, and WL 770 SAPs significantly increased the yield stress and plastic viscosity, while Hydro. slightly increased the yield stress and plastic viscosity. The yield stress and plastic viscosity were 76 Pa and 79 Pa·s for reference, respectively. The effect of WL PAM SAP on increasing the yield stress and plastic viscosity was maximum, where 390% and 127% increase in the yield stress and plastic viscosity were recorded, respectively. On the other hand, the addition of Hydro. SAP only increased the yield stress by 50%. The effect of SAPs on yield stress and plastic viscosity varied from their absorption and desorption kinetic. Specifically, higher absorption within 5 min of WL PAM, BASF, WL CP, and WL 770 SAPs resulted in a significant increase in the yield stress, whereas the limited effect was observed due to the fast desorption after 2 min for Hydro. SAP.

Table 3-3. Yield stress and plastic viscosity of HPC made with and without SAPs

Mixture	Yield stress (Pa)	Plastic viscosity (Pa·s)
Reference	76	79
Hydro.	114	82
WL PAM	372	178
WL 770	213	86
BASF	330	142
WL CP	338	154

Compressive strength

Figure 3-3 shows the compressive strengths at 7, 14, 28, and 56 days of the HPC reference mixture and the mixtures made with the investigated SAPs. The 7- and 14-day compressive strengths were higher than 4000 psi, which is required by the Illinois Tollway. The results showed that the addition of SAP improved compressive strength in most cases, whereas the compressive strength of the HPC mixtures made with the WL 770 SAP was slightly lower than the reference mixture. However, the compressive strength was not impaired by the addition of SAPs. For example, the 28- and 56-day compressive strengths of the mixture made with WL 770 SAP were only 6% and 9% lower than the reference mixture, respectively. But the compressive strengths of the other mixtures were increased by up to 20% compared to the reference mixture. The 7-, 14-, 28- and 56-day compressive strengths of the mixtures made with the BASF SAP were 20%, 7%, 16%, and 13% higher than the reference mixture, respectively.

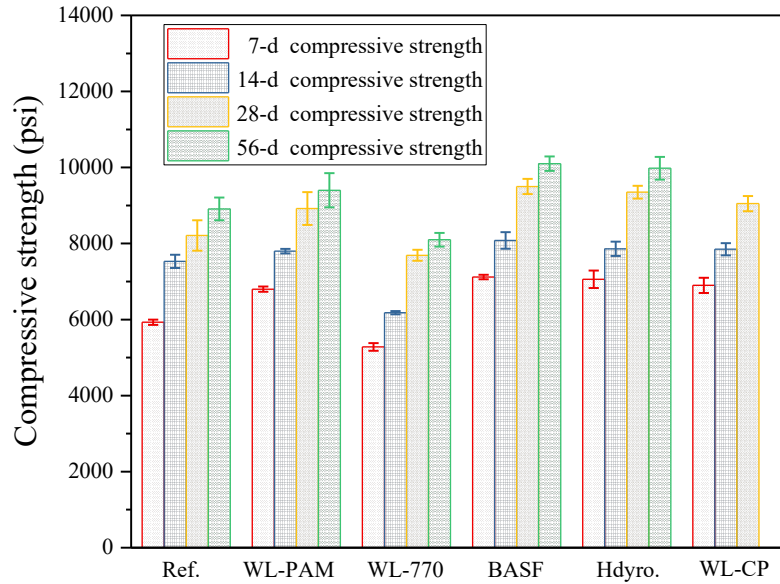


Figure 3-3. Compressive strength of HPC made with different SAPs

Viscoelastic properties

Figure 3-4 shows the variation of autogenous shrinkage for 28 days of the investigated mixtures. The HPC mixtures containing SAP exhibited lower autogenous shrinkage compared to that of the reference mixture. The 28-day autogenous shrinkage was 515 μ strain for the reference. The effect of WL PAM SAP on reducing autogenous shrinkage was maximum where 41% reduction of shrinkage was recorded at 28 days. The HPC mixtures made with WL 770, WL CP, and BASF SAPs had significantly lower autogenous shrinkage at 28 days with values of 385, 380, and 370 μ strain, respectively. The results showed that the effect of the Hydro. SAP on reducing autogenous shrinkage was low compared to the other investigated SAPs. The 28-day autogenous shrinkage was 12% lower than the reference mixture.

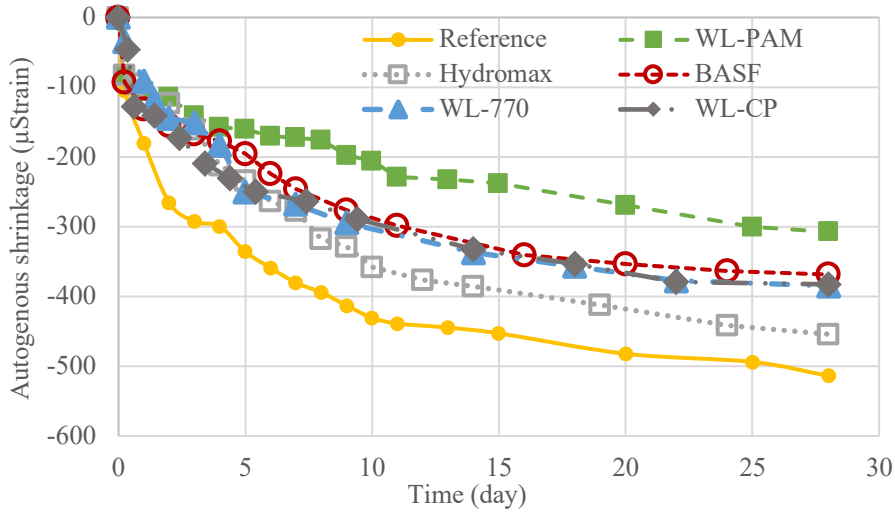


Figure 3-4. Autogenous shrinkage of the investigated HPC mixtures

Figure 3-5 shows the variations of length change of the investigated mixtures made with and without SAP measured after 7 days of water curing and 21 days of air-drying ($50\% \pm 4\%$ relative humidity and 73 ± 3 °F). Shrinkage results are relative to the initial values determined after demolding at 1 day and immersion for 1 hour in lime-saturated water. The 28-day shrinkage of the reference mixture was 155 μ strain. It can be observed that mixtures made with the WL PAM and BASF SAPs had a lower shrinkage compared to the reference mixture. The 28-day shrinkage of the mixture made with the WL PAM and BASF SAPs were 75% and 35% lower than the reference mixture, respectively. But the mixtures made with the Hydro. and WL-CP SAPs had 170 and 160 μ strain greater shrinkage, respectively, at 28 day compared to the reference mixture.

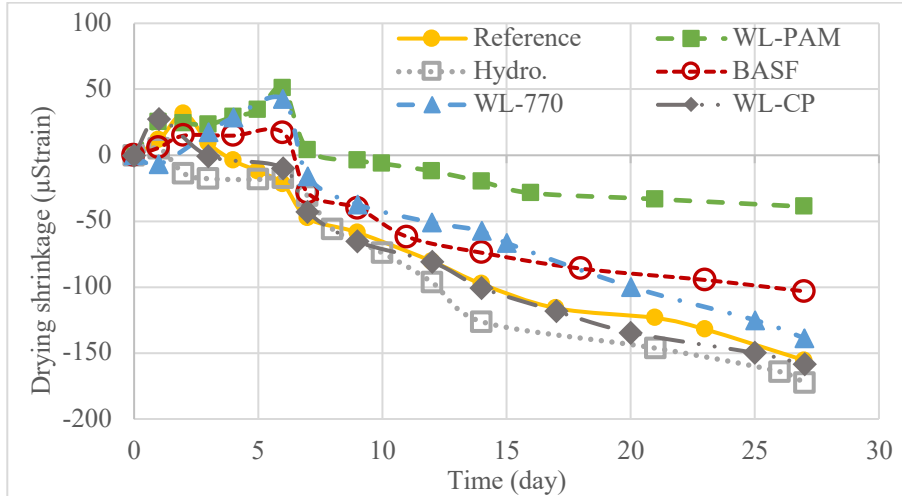


Figure 3-5. Drying shrinkage of investigated mixtures (initial length determined at 1 day)

Figure 3-6 shows the variations in drying shrinkage of the mixtures made with and without SAP with the initial length determined after 7 days of age, which corresponds to the beginning of drying. The 21-day drying shrinkage of the reference mixture was 135 μ strain. It can be observed that the effect of the WL PAM SAP was best in mitigating drying shrinkage. The 21-day drying shrinkage of the mixture made with the WL PAM SAP was 90 μ strain, which is 33% lower than that obtained with the reference mixture. The BASF SAP also had exhibited a slight effect on mitigating drying shrinkage where the 21-day drying shrinkage was 120 μ strain, which is essentially the same as the reference mixture. On the contrary, the 21-day drying shrinkage of the mixture made with WL 770 SAP was 25% higher than that of the reference mixture, which may be due to the porosity of the SAP. It is important to note that all the shrinkage values were less than 0.030% (300 μ strain) after 21 days of drying (initial length determined at 7 days), which is the upper limit permitted by the Illinois Tollway.

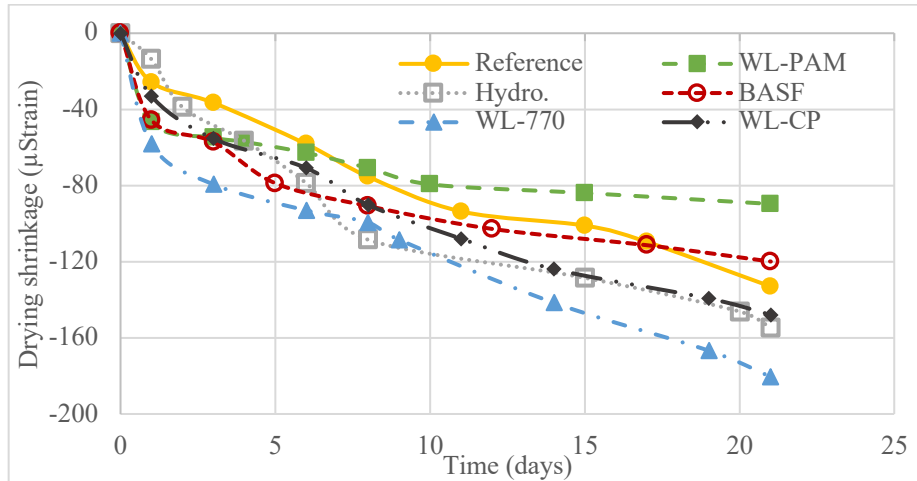


Figure 3-6. Drying shrinkage of investigated mixtures (initial length determined at 7 days that corresponds to beginning of drying)

Major findings of Subtask B-1

Table 3-4 lists the performance summary of HPC made with different SAPs in Subtask B-1. The results from the shrinkage test confirmed that the WL PAM product was the most effective SAP in inhibiting autogenous and drying shrinkage. Also, it contributed significantly to compressive strength development at the investigated ages. The BASF is another candidate SAP that showed acceptable performance in compressive strength and viscoelastic properties due to their high absorption capacity. However, the incorporation of both SAPs increased the required SP content by 45% to 75% to maintain the initial slump.

Table 3-4. Performance summary of HPC made with different SAPs

Mixture	SP dosage (%)	28-day compressive strength (%)	56-day compressive strength (%)	28-day autogenous shrinkage (%)	21-day drying shrinkage (%)
Reference	100	100	100	100	100
WL-PAM	145	109	105	59	60
WL-770	130	96	91	73	125
Hydromax	145	114	112	88	115
BASF	175	116	113	72	80
WL-CP	226	110	108	74	111

3.2 Subtask B-2: Performance of HPC with optimized SAP

The effect of the amount of internal curing water (different SAP contents) and different extended mixing time on key fresh and hardened properties of HPC are discussed in this section. Besides, the effect of SAP, AEA, and SAP+AEA on frost durability was also compared. Based on the results from workability, viscoelastic properties, mechanical properties, transport properties, the optimum SAP content, and extended mixing time are selected for the next tasks.

3.2.1 B-2-1 Determine internal water content

Fresh properties

Table 3-5 summarizes the fresh properties of the investigated HPC mixtures made with 0%, 50%, and 100% IC of WL PAM and BASF SAPs. The fresh properties included the initial slump, air content, and unit weight. Results showed that the total SP content was increased with the increase of SAP content to maintain an initial slump within the target value of 8 inches. For

instance, the use of the 50% and 100% IC of BASF SAP increased the SP content by 47% and 73%, respectively, as compared to the reference mixture.

Table 3-5. Fresh properties of HPC made with different IC of SAPs

Mixture	Slump (in.)			Air volume (%)		Unit weight (lb/ft ³)	SP content (fl oz/yd ³)		
	Initial*	20 min	40 min	Initial*	40 min		Before SAP addition	After SAP addition	Total
Reference	8.5	7.8	7.0	5.6	6.4	145.4	15	-	15
P-50-M3	8.6	6.8	5.2	5.4	6.2	145.5	15	7	22
P-100-M3	8.6	5.8	2.6	5.1	5.6	146.1	15	9	24
B-50-M3	8.7	7.9	7.2	5.3	5.8	144.8	15	7	22
B-100-M3	8.6	7.2	6.3	5.2	5.5	145.7	15	11	26

*Initial slump and air content measurement was conducted 2 min and 12 min after the cement and water contact for the reference concrete and the other mixtures made with SAP, respectively.

The results showed that the slump loss of HPC was increased with the addition of SAP content. For instance, approximately 3 in. and 6 in. of slump loss in 40 min was recorded for 50% and 100% IC of WL PAM SAP, respectively. The HPC mixtures prepared with the various SAPs contents had initial air contents of approximately 5.1% to 5.6%. The air content increased slightly from 5.5% to 6.4% at 40 min of age.

To increase the slump retainment for the mixture made with WL PAM SAP, 50% and 100% more retarder were added. Table 3-6 summarizes the fresh properties of HPC made with WL PAM SAP and different retarder dosage. Results showed that the slump loss per 20 minutes can be reduced to 2.5 and 1.9 inches with 50% and 100% more retarder.

Table 3-6. Fresh properties of HPC made with WL PAM SAP and different retarder dosage

Mixture	Slump (in.)			Air volume (%)		Unit weight (lb/ft ³)	Retarder (fl oz/yd ³)
	Initial*	20 min	40 min	Initial*	40 min		
P-100-1	8.6	5.8	2.6	5.1	5.6	145.5	12
P-100-2	8.8	6.3	4.0	5.3	5.8	145.7	18
P-100-3	8.7	6.8	5.0	5.2	6.1	144.9	24

Figure 3-7 shows the surface settlement of HPC made with 50% and 100% IC of WL PAM and BASF SAPs. Results showed that the addition of WL PAM SAP significantly reduced the total surface settlement, while BASF SAP slightly decreased the total surface settlement. The total surface settlement was 0.13% for reference. The total surface settlement was reduced to 0.02% after 100% IC of WL PAM SAP was introduced.

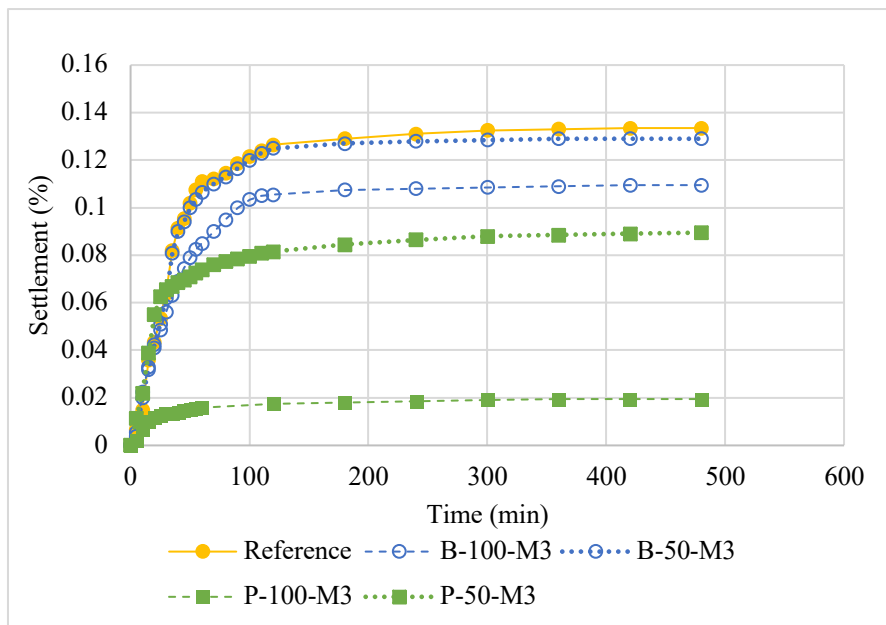


Figure 3-7. Surface settlement of HPC made with different IC of SAPs

Rheology

Table 3-7 summarizes the yield stress and plastic viscosity of the HPC mixtures made without and with different IC of WL PAM and BASF SAPs. Results showed that the yield stress and plastic viscosity of HPC were increased with SAP content. Compared to the reference mixture, the yield stress of mixtures made with 50% and 100% IC of WL PAM SAP was increased by 330% and 389%, respectively, while the plastic viscosity was increased by 85% and 125%, respectively. The significant increase in yield stress and plastic viscosity can be attributed to the high absorption of WL PAM within the first 10 min after introduction to the fresh concrete.

Table 3-7. Yield stress and plastic viscosity of HPC made with different IC of SAPs

Mixture	Yield stress (Pa)	Plastic viscosity (Pa·s)
Reference	76	79
P-50-M3	330	146
P-100-M3	372	178
B-50-M3	264	116
B-100-M3	330	142

*Rheology test was conducted at approximately 5 min and 15 min of age (about 3 min after starting the initial slump measurement) for reference and other mixtures made with SAPs

Mechanical properties

Figure 3-8 shows the compressive strength of the investigated HPC mixtures made without and with 50% and 100% IC of WL PAM and BASF SAPs at different ages. The compressive strength of all mixtures was higher than 4000 psi at all investigated ages, which meets the requirement of Illinois Tollway. Results showed that the 100% IC of both SAPs were more beneficial and increased the compressive strength more than those with 50% of IC. Specifically, the 28-day compressive strength of the mixture made with 50% and 100% IC of BASF SAP was increased by 3% and 18%, respectively.

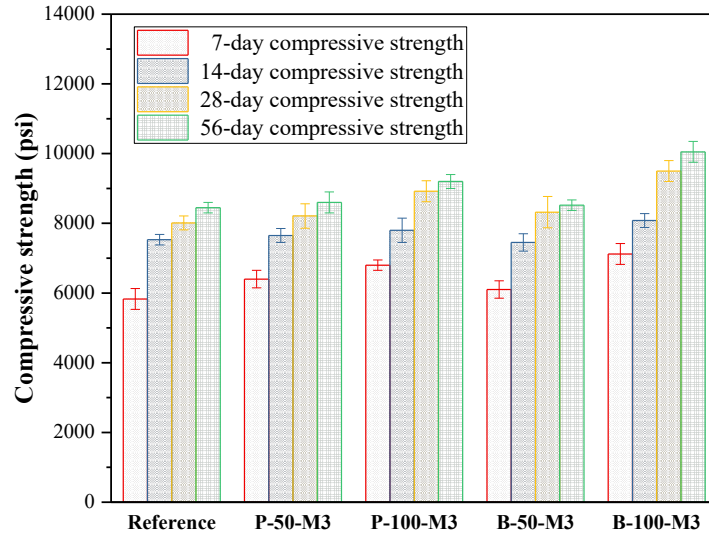
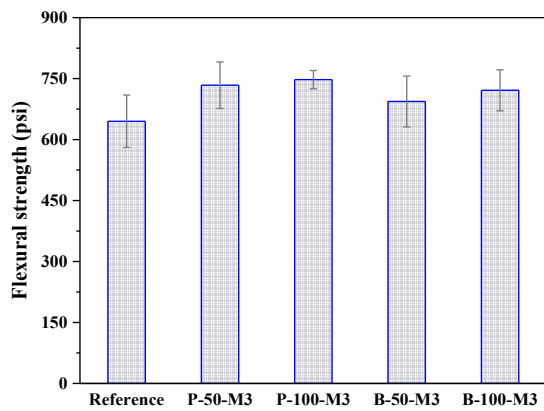
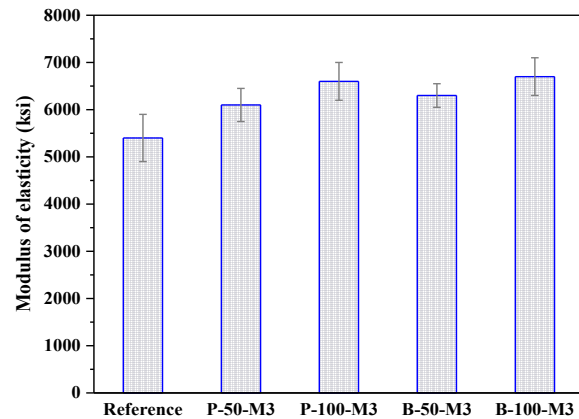


Figure 3-8. Compressive strength of HPC made with different IC of SAPs

Figure 3-9 shows the flexural strength and MOE of the investigated HPC mixtures made with/without IC of WL PAM and BASF SAPs at 28 days. Results showed that the flexural strength and MOE slightly increased after the addition of SAPs. The flexural strength and MOE were 645 psi and 5400 ksi for the reference mixture, respectively. The effect of 100% IC of WL PAM SAP on the flexural strength was maximum, where a 16% increase in flexural strength was recorded, as compared to the reference mixture. Besides, the use of 100% IC of BASF SAP had the most significant effect on the MOE, where a 24% increase in MOE was recorded, as compared to the reference mixture.



(a)



(b)

Figure 3-9. Flexural strength (a) and MOE (b) of HPC made with different IC of SAPs at 28 days of age

Viscoelastic properties

Figure 3-10 shows the autogenous shrinkage of the investigated HPC mixtures made with/without IC of WL PAM and BASF SAPs. Results showed that the effect of 100% IC of SAPs on reducing the 28-day autogenous shrinkage was more significant than 50% IC of the SAPs. For instance, a 26% reduction of autogenous shrinkage at 28 days was recorded for the use of 100% IC of BASF SAP, while only 10% reduction was recorded for the use of 50% IC of BASF SAP, compared to the reference mixture.

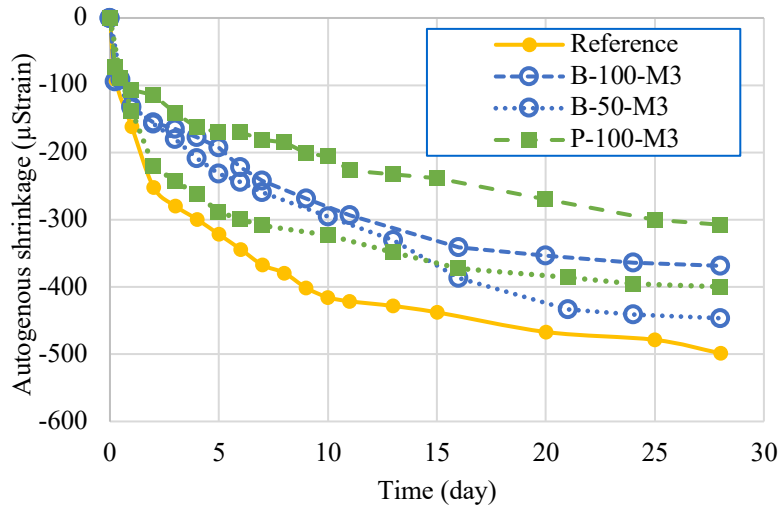


Figure 3-10. Autogenous shrinkage of HPC made with different IC of SAPs

Figure 3-11 shows the drying shrinkage of the investigated HPC mixtures made with/without different IC of WL PAM and BASF SAPs. The 21-day drying shrinkage of all mixtures was less than 300 µstrain, which meets the requirement of Illinois Tollway. Results also showed that the use of 100% IC of WL PAM and BASF SAPs were significant in reducing drying shrinkage but limited effect on drying shrinkage was observed when 50% IC of WL PAM and BASF SAPs was applied. For instance, 50% reduction of 21-day drying shrinkage was recorded for 100% IC of WL PAM SAP, whereas only 15% reduction was recorded for 50% of WL PAM SAP, compared to reference mixture.

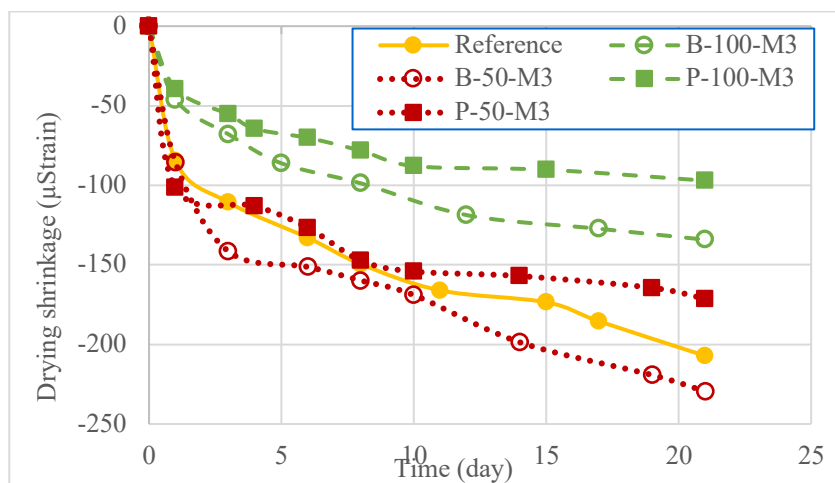


Figure 3-11. Drying shrinkage of HPC made with different IC of SAPs (initial length was recorded at 7 days of age after air drying)

Bulk resistivity

Table 3-8 summarizes the electrical surface resistivity and bulk resistivity of the investigated HPC mixtures made with/without different IC of WL PAM and BASF SAPs at 28 days of age. Table 3-9 lists the surface resistivity limits for chloride ion penetrability indication. The surface resistivity of all the mixtures was ranged from 55 to 59 Ohm·m, indicating the chloride ion permeability was very low based on specification. Results also showed that the bulk resistivity was significantly increased with the addition of SAP. For instance, the use of 100% IC of WL PAM SAP increased the bulk resistivity by 16%, compared to the reference mixture. Overall, the increase in the surface resistivity and bulk resistivity after SAP addition indicated that the impermeability of HPC was improved with the use of both SAPs.

Table 3-8. Electrical resistivity of HPC made with different IC of SAPs at 28-days of age

Mixture	Surface resistivity (Ohm·m)	Uniaxial resistivity (Ohm·m)
Reference	55.1	147.3
P-50-M3	57.2	170.0
P-100-M3	58.6	173.0
B-50-M3	58.8	156.4
B-100-M3	59.1	165.5

Table 3-9. Surface resistivity limits for chloride ion penetrability indication based on AASHTO TP 95-11

Chloride ion permeability	Surface resistivity (Ohm·m)
High	<12
Moderate	12-21
Low	21-37
Very low	37-254
Negligible	>254

Major findings of B-2-1

Table 3-10 lists the performance summary of HPC made with 50% and 100% IC of SAPs. The results from the shrinkage test showed that 100% of IC was most effective in reducing autogenous and drying shrinkage than 50% of IC. Also, 100% of IC was more effective in increasing the mechanical properties. The 14-day compressive strength of all the mixtures was higher than 4000 psi, and the drying shrinkage at 28 days of the age of all the mixtures was less than 300 μ strain, which can meet the requirement of Tollway.

Table 3-10. Performance summary of HPC made with 50% and 100% IC of SAPs

Mixture	SP dosage (%)	28-d compressive strength (%)	28-d MOE (%)	28-d flexural strength (%)	28-d autogenous shrinkage (%)	21-d drying shrinkage (%)
Reference	100	100	100	100	100	100
P-50-M3	147	102	113	114	80	81
P-100-M3	160	109	118	116	62	48
B-50-M3	147	102	117	108	89	110
B-100-M3	173	116	124	112	74	64

*P and B denote WL PAM and BASF SAPs; 50 and 100 denote 50% and 100% of IC; M3 denote 3-min extended mixing time

3.2.2 B-2-2 Determine acceptable mixing time

In B-2-2, three extended mixing times (e.g., 3 min, 5 min, and 7 min) were used to disperse the two candidate SAPs, WL PAM and BASF in the mixture. The performance of HPC in terms of workability, viscoelastic properties, mechanical properties, transport properties was used to determine the optimum mixing time for SAPs dispersion.

Fresh properties

Table 3-11 summarizes fresh properties of the investigated HPC mixtures (100% IC of BASF and WL PAM) with three extended mixing times (3, 5, and 7 min) after SAP addition. The fresh properties include the initial slump, air content, and unit weight. Results showed that the total SP content was increased with a longer extended mixing time after SAP addition to maintaining an initial slump within the target value of 8 inches. For instance, 60% higher SP dosage was added to the mixture made with 100% IC of WL PAM and 3-min extended mixing time, whereas 127% higher SP dosage was added for a mixture made with 100% IC of WL PAM with 7-min extended mixing time, as compared to the reference mixture. The higher SP dosage used for longer extended mixing time can be attributed to the higher moist absorption of SAP during the

longer mixing time. WL PAM and BASF SAPs continually absorbed water in filtrated solution within 30 minutes.

Similarly, the continued absorption within 30 min of WL PAM and BASF SAPs resulted in a greater slump loss. For instance, approximately 6 in. of slump loss was recorded for a mixture made with WL PAM SAP and different extended mixing time at 40 min. Besides, the longer extended mixing time slightly increased the air content. For instance, with 7-min extended mixing time, the air content was increased by 0.5% for a mixture made with BASF SAP, as compared to the same mixture with 3-min extended mixing time.

Table 3-11. Fresh properties of HPC made with SAPs and different extended mixing time

Mixture	Slump (in.)			Air volume (%)		Unit weight (lb/ft ³)	SP content (fl oz/yd ³)		
	Initial*	20 min	40 min	Initial*	40 min		Before SAP addition	After SAP addition	Total
Reference	8.5	7.8	7.0	5.6	6.4	145.4	15	-	15
P-100-M3	8.6	5.8	2.6	5.1	5.6	146.1	15	9	24
P-100-M5	8.6	5.0	2.1	5.5	5.6	145.8	15	13	28
P-100-M7	8.8	5.9	2.5	5.8	6.5	145.6	15	19	34
B-100-M3	8.6	7.2	6.3	5.2	5.5	145.7	15	11	26
B-100-M5	8.2	6.8	5.4	5.5	6.0	145.2	15	11	26
B-100-M7	8.4	7.0	6.2	5.7	6.4	145.3	15	13	28

*Initial slump and air content measurement was conducted 2 min after the cement and water contact for the reference concrete, and 12 min, 14 min, and 16 min for the other mixtures made with SAP and 3-min, 5-min, and 7-min extended mixing time, respectively

Figure 3-12 shows the surface settlement (%) of the investigated HPC mixtures with different extended mixing time after SAP addition. Results showed that no obvious change in surface settlement for mixtures made with SAPs with different extended mixing times. For instance, the total surface settlement of mixture made with 100 IC of BASF SAP with 3-7 minutes extended mixing time was ranged from 0.10% to 0.12%.

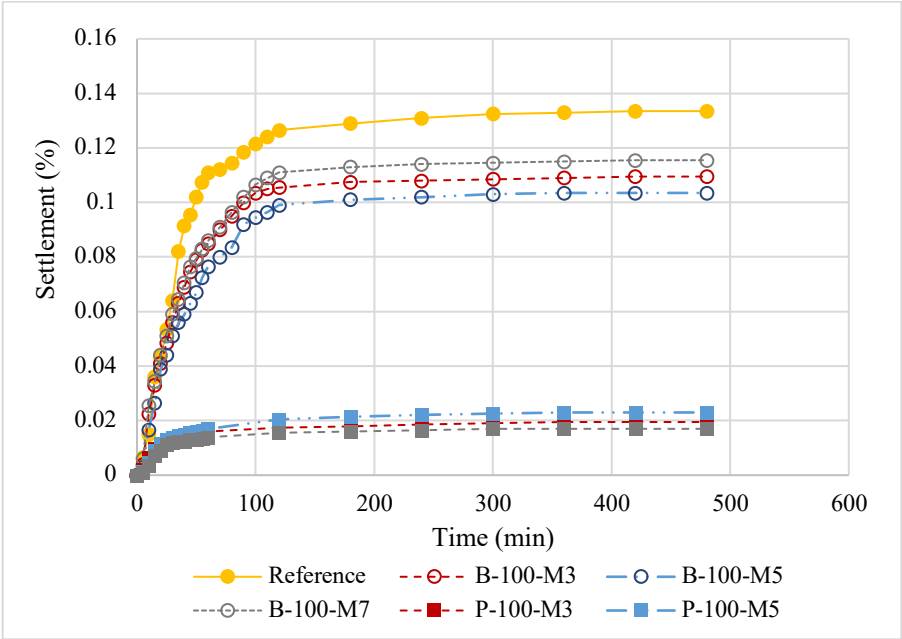


Figure 3-12. Surface settlement of HPC made with SAPs and different extended mixing time

Rheology

Table 3-12 summarizes the yield stress and plastic viscosity of the HPC mixtures made with two SAPs (WL PAM and BASF) and different extended mixing times. Results showed that the plastic viscosity of the mixtures made with two SAPs was increased with the longer extended mixing time, whereas a limited effect on yield stress was observed. For instance, a 64% increase in plastic viscosity was recorded for the mixture made with WL PAM SAP for the 7-min extended mixing time, compared to the same mixture with 3-min extended mixing time. This can be attributed to the continuous moist absorption of SAPs during the longer extended mixing time. However, the increased dosage of SP with the longer extended mixing time (as shown in Table 3-11) had a significant effect on reducing the yield stress, and thus, no obvious change was observed for the yield stress.

Table 3-12. Yield stress and plastic viscosity of the HPC mixtures made with SAPs and different extended mixing time

Mixture	Yield stress (Pa)	Plastic viscosity (Pa·s)
Reference	76	79
P-100-M3	372	178
P-100-M5	356	234
P-100-M7	363	292
B-100-M3	330	142
B-100-M5	338	153
B-100-M7	345	158

Mechanical properties

Figure 3-13 shows the compressive strength of the investigated HPC mixtures made with different extended mixing times (e.g., 3 min, 5 min, and 7 min) at different ages. Results showed that the different extended mixing times did not have an obvious effect on compressive strength. For instance, the deviation of compressive strength for the mixture made with the WL PAM SAP was within 5% for the different extended mixing times. This indicated that the extended mixing time of 3 min was sufficient for the homogeneous dispersion for the two SAPs.

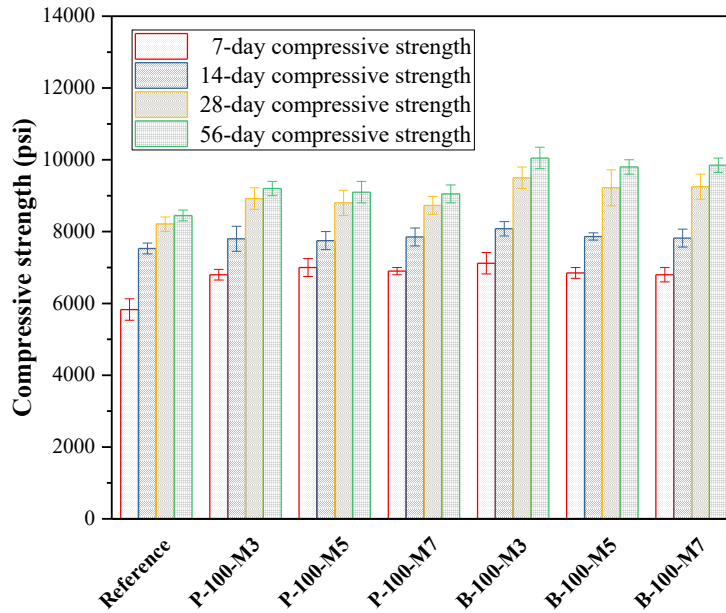


Figure 3-13. Compressive strength of HPC made with SAPs and different extended mixing time

Additionally, the three extended mixing times did not have a strong effect on flexural strength and MOE at age of 28 days, as shown in Figure 3-14. The flexural strength and MOE at age of 28 days increased with the addition of two SAPs for the three extended mixing times.

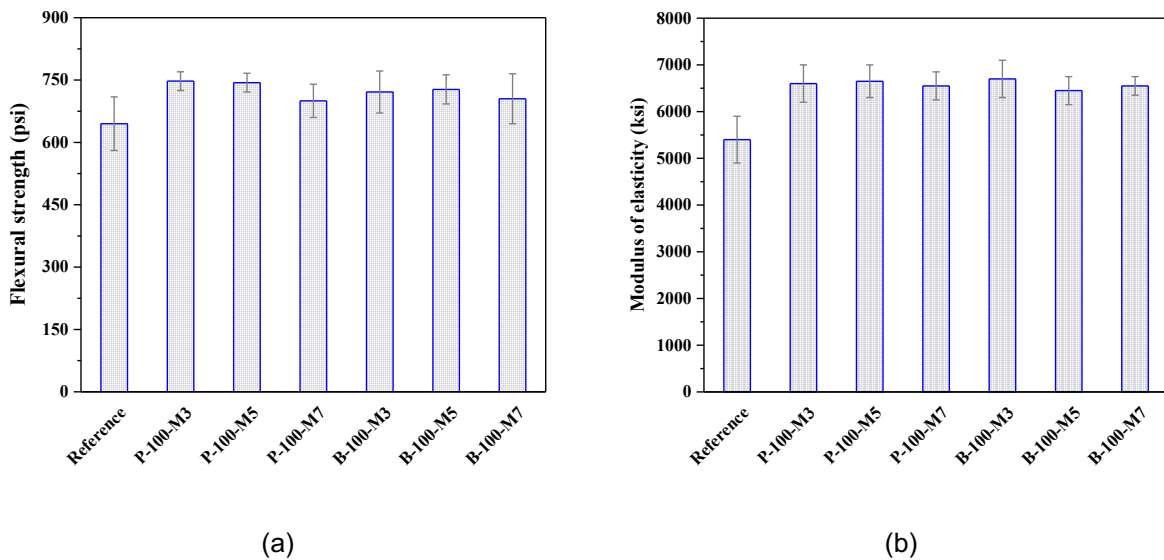


Figure 3-14. Flexural strength (a) and MOE (b) of HPC made with SAPs and different extended mixing time at 28 days of age

Viscoelastic properties

Figure 3-15 shows the autogenous shrinkage of the investigated HPC made three different extended mixing times. Results showed that autogenous shrinkage was significantly reduced with SAP addition for all the three extended mixing times, as compared to the reference mixture. For instance, the 28-day autogenous shrinkage of the mixture made with WL PAM SAP was reduced by 30% to 50% for all the extended mixing time. This also indicated that the 3-min extended mixing time was sufficient for the homogeneous dispersion of two SAPs.

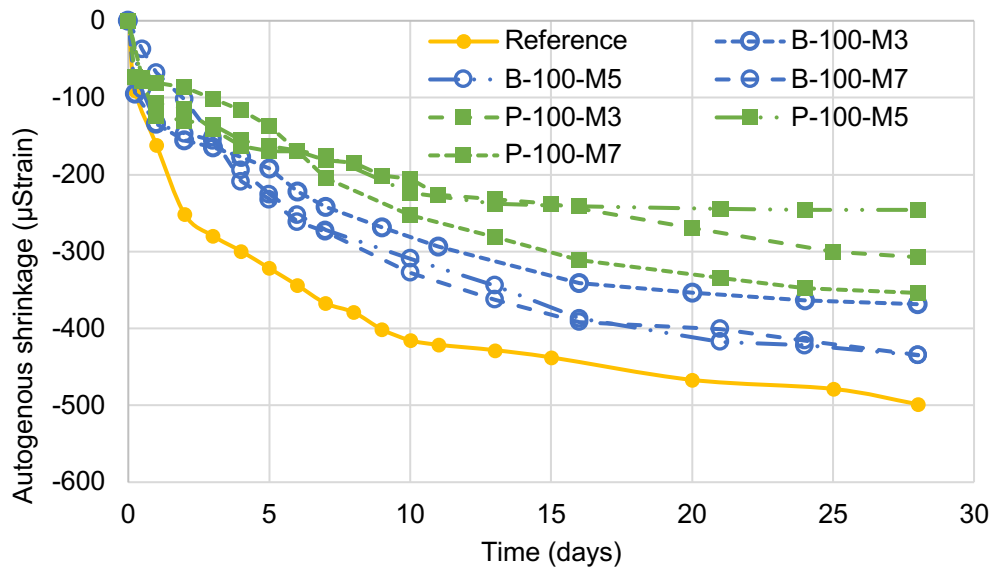


Figure 3-15. Autogenous shrinkage of HPC made with SAPs and different extended mixing time

Figure 3-16 presents the drying shrinkage of the investigated HPC mixtures made three different extended mixing times. The initial length was recorded at 7 days after being cured in lime-saturated solution. The 21-day drying shrinkage of all mixtures was less than 300 µstrain, which meets the requirement of Illinois Tollway. The drying shrinkage was significantly reduced with the addition of SAPs for all the extended mixing time. For instance, the 28-day drying shrinkage was reduced by 43% to 76% for the mixture made with WL PAM SAP with all the extended mixing time.

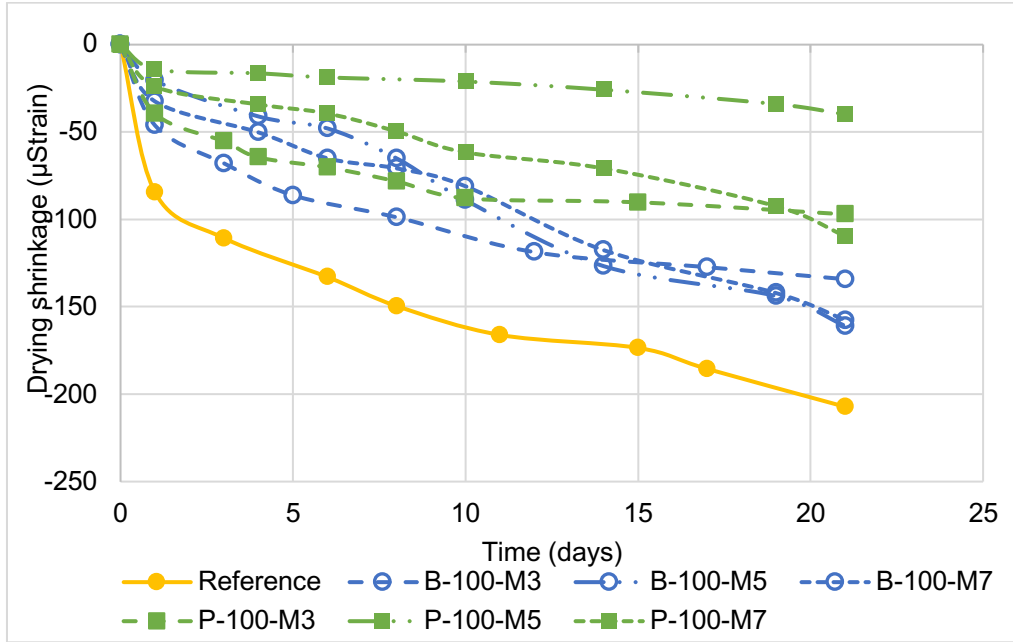


Figure 3-16. Drying shrinkage of HPC made with SAPs and different extended mixing time (Initial length was recorded at 7 days of age after air drying)

Electrical Bulk and surface resistivity

Table 3-13 summarizes the electrical surface resistivity and bulk resistivity of the investigated HPC mixtures made with different extended mixing times. Results showed that the surface resistivity of the mixtures made with SAPs and three extended mixing times was ranged from 56 to 59 Ohm·m, indicating a good resistance to chloride permeability. Additionally, the bulk resistivity was significantly increased with the addition of SAPs for all three extended mixing times. For instance, the bulk resistivity was ranged from 167 to 182 Ohm·m for the mixture with WL PAM SAP with all the three extended mixing times, compared to the value of 147 Ohm·m for the reference mixture. Overall, no apparent difference for electrical resistivity was found between the extended mixing time from 3 minutes to 7 minutes.

Table 3-13. Electrical resistivity of HPC made with SAPs and different extended mixing time

Mixture	Surface resistivity (Ohm·m)	Uniaxial resistivity (Ohm·m)
Reference	55.1	147.3
P-100-M3	58.6	173.0
P-100-M5	58.3	181.7
P-100-M7	57.5	167.1
B-100-M3	59.1	165.5
B-100-M5	56.8	165.9
B-100-M7	56.1	163.3

Major findings of B-2-2

Table 3-14 lists the performance summary of the investigated HPC made with different extended mixing times. Results showed that the longer extended mixing time resulted in a higher SP dosage to maintain the initial slump. However, no significant effect on the mechanical properties and drying shrinkage was found for the different extended mixing times. Therefore, 3-min extended mixing time was selected due to the sufficient dispersion for SAPs and lower dosage of SAP.

Table 3-14. Performance summary of HPC made with SAPs and different extended mixing time

No.	SP dosage (%)	28-d compressive strength (%)	28-d MOE (%)	28-d flexural strength (%)	28-d autogenous shrinkage (%)	21-d drying shrinkage (%)
Reference	100	100	100	100	100	100
P-100-M3	160	109	118	116	62	48
P-100-M5	187	107	123	115	49	62
P-100-M7	226	106	121	109	70	52
B-100-M3	173	116	124	112	74	64
B-100-M5	173	108	119	113	87	76
B-100-M7	187	110	121	109	87	74

*P and B denote WL PAM and BASF SAPs; 50 and 100 denote 50% and 100% of IC; M3, M5, and M7 denote 3-min, 5-min, and 7-min extended mixing time

3.2.3 B-2-3 Investigate frost durability using SAP

Fresh properties

Table 3-15 summarizes the fresh properties of the investigated SAP- HPC mixtures made with SAP, AEA, and SAP+AEA. The fresh properties included the initial slump, air content, and unit weight. Results showed that the SAP-HPC mixtures without AEA had lower air content and higher unit weight, compared to mixtures made with AEA and SAP+AEA. The initial air content of the mixtures made without AEA was ranged from 2.9% to 3.4%, and approximately 2% reduction was recorded compared to the mixtures with AEA. The addition of both SAPs slightly increased the air content of the HPC mixtures, compared to the reference mixture without AEA. For instance, without air-entraining, a 0.5% increase in air content was recorded for the mixture made with BASF SAP, compared to the reference mixture without AEA. Besides, the unit weight of the mixtures made without AEA was increased by approximately 5%, as compared to the

HPC mixtures with AEA. Overall, the addition of SAPs was only found to slightly increase the air content of fresh concrete.

Table 3-15. Fresh properties of the HPC mixtures made with and without AEA

Mixture	Slump (in.)			Air volume (%)		Unit weight (lb/ft ³)
	Initial*	20 min	40 min	Initial*	40 min	
Reference	8.5	7.8	7.0	5.6	6.4	145.4
Ref-without AEA	8.4	7.6	7.2	2.9	3.2	154.5
P-100-M3	8.6	5.8	2.6	5.1	5.6	146.1
P-100-without AEA	8.2	5.3	1.9	3.3	3.5	152.5
B-100-M3	8.6	7.2	6.3	5.2	5.5	145.7
B-100-without AEA	8.3	7.0	6.1	3.4	3.5	153.2

*Initial slump and air content measurement was conducted 2 min and 12 min after the cement and water contact for the reference concrete and the other mixtures made with SAP, respectively.

Rheology

Table 3-16 summarizes the yield stress and plastic viscosity of the HPC mixtures made with SAP, AEA, and SAP+AEA. Results showed that the reduction of air content had a limited effect on yield stress but increased the plastic viscosity for all the mixtures with and without SAPs. For instance, a 41% increase in plastic viscosity was recorded for the reference mixture without AEA, compared to the same mixture with AEA. Additionally, without air-entraining, the addition of both SAPs also significantly increased yield stress and plastic viscosity. For instance, without air-entraining, 359% and 81% increase in yield stress and plastic viscosity was recorded, respectively, compared to the reference mixture.

Table 3-16. Yield stress and plastic viscosity of the HPC mixtures made with and without AEA

Mixture	Yield stress (Pa)	Plastic viscosity (Pa·s)
Reference	76	79
Ref-without AEA	81	112
P-100-M3	372	176
P-100-without AEA	386	203
B-100-M3	330	142
B-100-without AEA	343	176

*Rheology test was conducted at approximately 5 min and 15 min of age (about 3 min after starting the initial slump measurement) for reference and other mixtures made with SAPs

Mechanical properties

Figure 3-17 shows the compressive strengths of the HPC mixtures made with SAP, AEA, and SAP+AEA at different ages. As shown in Figure 3-17, higher compressive strength was observed for the mixtures made with SAP only, as compared to those mixtures made with SAP+AEA. For instance, a 17% increase in 56-day compressive strength was observed for the mixture made with BASF SAP only, as compared to the mixture made with BASF SAP and AEA. This can be attributed to the lower entrained air volume for the mixtures without AEA. Even so, the 7-day and 14-day compressive strengths of all the mixtures were higher than 4000 psi at all ages, which can meet the requirement of Illinois Tollway.

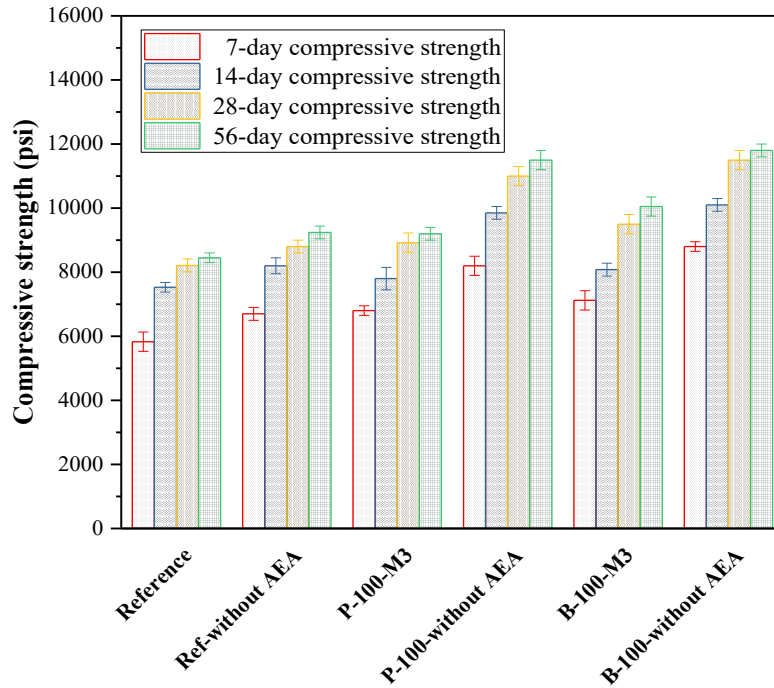


Figure 3-17. Compressive strength of the HPC mixtures made with and without AEA

Figure 3-18 shows the flexural strength and MOE of the investigated HPC mixtures made with SAP, AEA, and SAP+AEA at 28 days. Results showed that higher MOE but no apparent influence on flexural strength was observed for the mixtures made with only SAP, as compared to those mixtures made with SAP+AEA. For instance, a 10% increase of MOE was recorded for the mixture made with WL PAM SAP and without AEA, compared to the same mixture made with AEA. Besides, without air-entraining, the addition of SAPs also increased the flexural strength by 16% to 20% and improve the MOE by 20% to 22%.

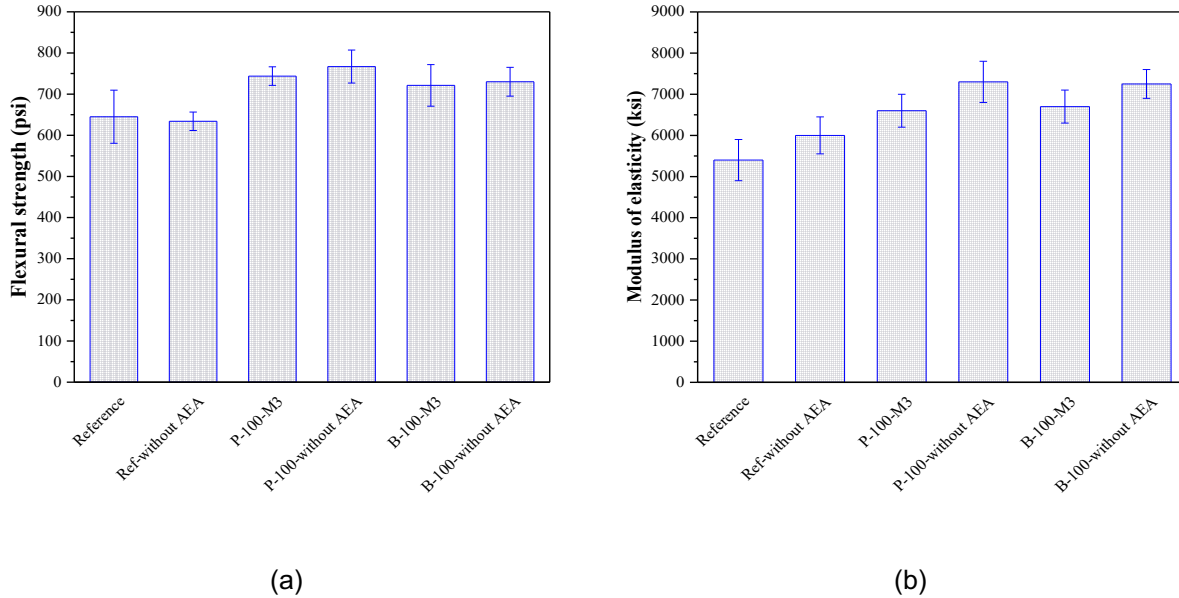


Figure 3-18. Flexural strength (a) and MOE (b) of the HPC mixtures made with and without AEA at 28 days of age

Viscoelastic properties

Figure 3-19 shows the autogenous shrinkage of the HPC mixtures made with SAP, AEA, and SAP+AEA. Results showed that no apparent influence on autogenous shrinkage was observed for the mixtures made with SAP only, as compared to those mixtures made with SAP+AEA. However, without air-entraining, the addition of both SAPs significantly reduced the autogenous shrinkage by 27% to 37%. For instance, a 32% reduction of 28-day autogenous shrinkage was recorded for the mixture made with WL PAM SAP and without AEA, compared to the reference mixture without AEA. Overall, the addition of AEA had a limited effect on the autogenous shrinkage for all the mixtures made with and without SAPs.

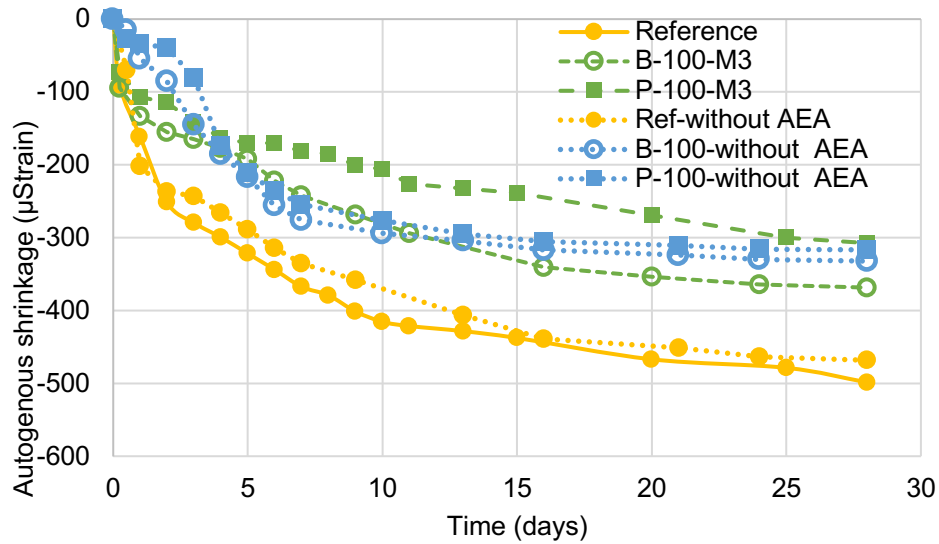


Figure 3-19. Autogenous shrinkage of the HPC mixtures made with and without AEA

Figure 3-20 shows the drying shrinkage of the HPC mixtures made with SAP, AEA, and SAP+AEA. Results showed that a reduction in drying shrinkage was observed for the mixtures made without AEA, as compared to those mixtures made with AEA. For instance, a 13% reduction of 21-day drying shrinkage was recorded for the reference mixture made without AEA, as compared to the same mixture made with AEA. This can be attributed to the dense structure of hardened concrete, which inhibited the water evaporation upon drying. Besides, a significant reduction in drying shrinkage was observed for mixtures made with SAP only, compared to the reference mixture. The minimum drying shrinkage was recorded for the mixture made with WL PAM SAP and without AEA, where 72% reduction of 21-day drying shrinkage was recorded as compared to the reference mixture made without AEA.

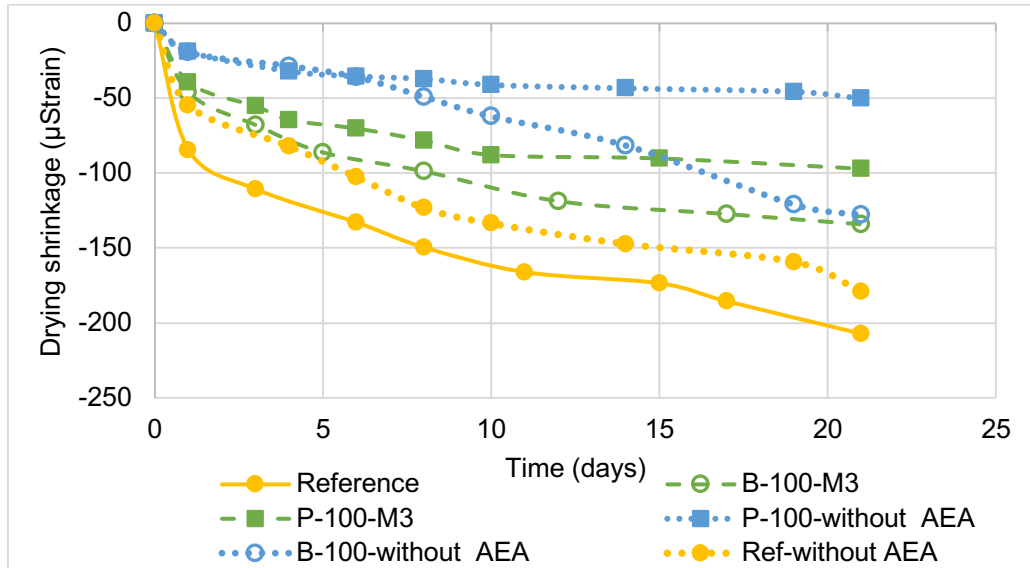


Figure 3-20. Drying shrinkage of the HPC mixtures made with and without AEA (initial length was recorded at 7 days of age after air drying)

Electrical Bulk and surface resistivity

Table 3-17 summarizes the surface resistivity and bulk of the HPC mixtures made with and without AEA. Results showed that the reduction of air content slightly increased the surface resistivity and bulk resistivity. For instance, a 12% and 8% increase in the surface resistivity and bulk resistivity was recorded for the mixture made with BASF SAP without AEA, respectively, as compared to the same mixture made with AEA. Besides, the addition of both SAPs had a significant effect on increasing the bulk resistivity, regardless of AEA. The maximum value of bulk resistivity was recorded for the mixture made with WL PAM SAP and without AEA, with approximately 11% increase compared to the reference mixture without AEA.

Table 3-17. Electrical resistivity of HPC made with SAPs and different extended mixing time

Mixture	Surface resistivity (Ohm·m)	Bulk resistivity (Ohm·m)
Reference	55.1	147.3
Ref-without AEA	60.3	168.2
P-100-M3	58.6	173.0
P-100-without AEA	64.5	185.5
B-100-M3	59.1	165.5
B-100-without AEA	66.2	179.5

Frost durability

Six mixtures were tested according to ASTM C666, approach A. They included reference (R), reference without AEA (RN), PAM (P), PAM without AEA (PN), BASF (B), and BASF without AEA (BN). Two specimens (labeled 1 and 2) were tested for freeze-thaw durability for each mixture. The results from the test are shown in Figure 3-21 and Figure 3-22. Mixtures without air-entrainer failed (Relative dynamic modulus less than 60%) before the end of the test. The mixtures without air entrainer but with an SAP performed better than the reference without AEA. The mixture with PAM SAP failed around 90 cycles and the mixture with BASF SAP failed around 150 cycles. Mixtures with air entrainment with and without SAP showed good frost durability with a durability factor greater than 80%. Use of SAP without AEA improved the frost durability but was not as effective as using an AEA.

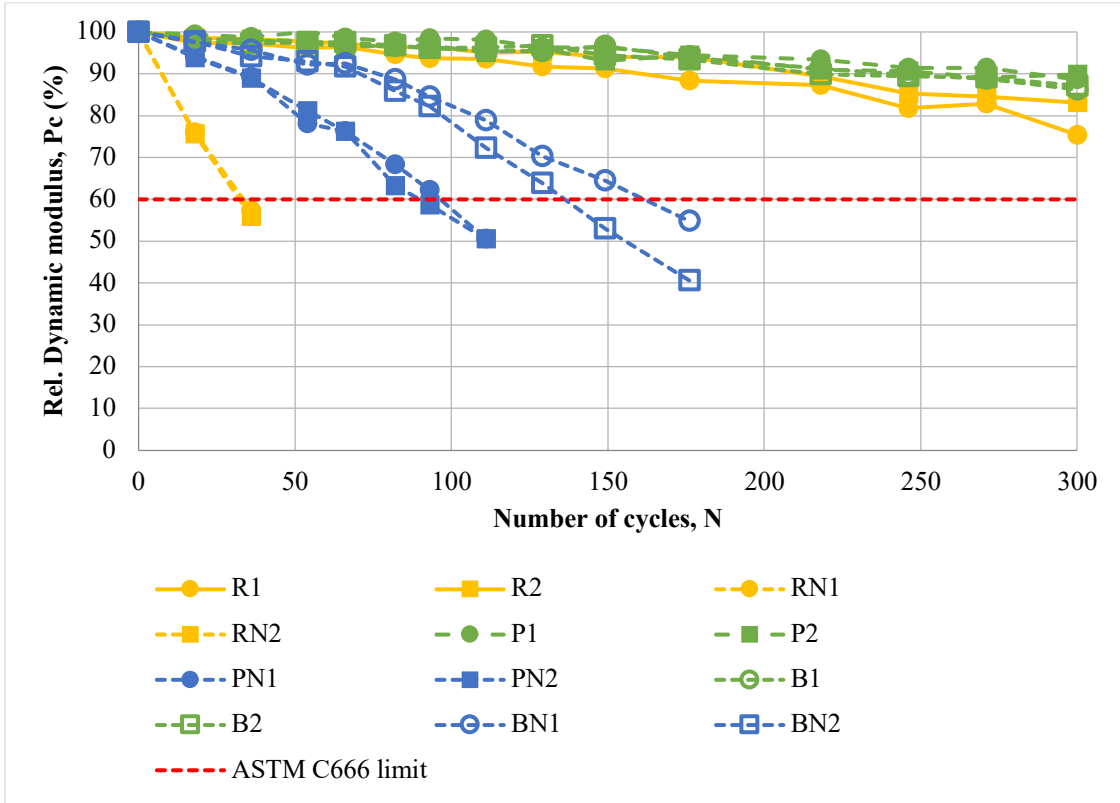


Figure 3-21. Relative dynamic modulus of HPC mixtures made with and without AEA

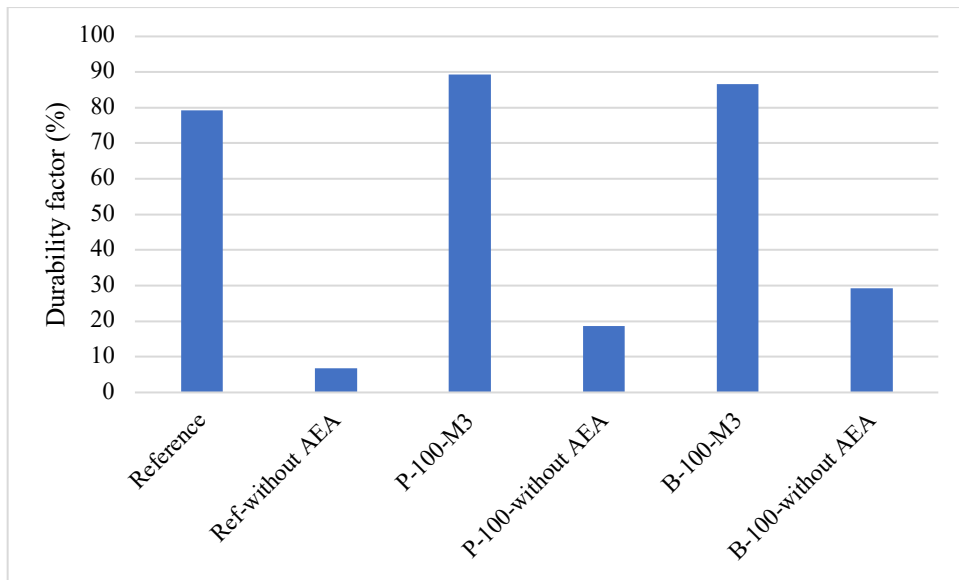


Figure 3-22. Durability factor of HPC mixtures made with and without AEA

Air void system

The results of the air void analysis are shown in Table 3-18. Results show that use of SAP increases the hardened air content significantly. This is due to the empty voids left behind by dehydrated SAP. The PAM mixtures were observed to have a relatively higher hardened air content than BASF mixtures, this is likely not only because the PAM SAP has larger particle size, but also possibly because PAM particles were dispersed more evenly during mixing than BASF SAP.

The tollway's requirement for air-void system requires the spacing factor to be less than 0.008 in., specific surface greater than $600 \text{ in}^2/\text{in}^3$ and total air content not less than 4% (these are waived if the durability factor from the freeze thaw test is equal or greater than 90% after 300 cycles). The results obtained show that when SAP is used with an AEA, the spacing factor is within the requirement with 0.003 in. for PAM and 0.005 in. for BASF. These are lower than the 0.006 in. spacing factor of the reference mixture with AEA. Note that the specific surface values in Table 3-18 are somewhat low. This is a consequence of the resolution of the digital images used for the analysis, and the spacing factor is the more useful value for predicting performance. All the mixtures with AEA satisfied the Tollway's requirement of at least 4% air content.

The SAP mixtures without AEA have a reasonably good air-void system with a spacing factor of 0.01 but do not perform well in the frost durability test. The irregular voids left behind by dehydrated SAP are not a substitute for air voids created by using an AEA.

The scanned images are shown in Appendix A.

Table 3-18 Hardened void analysis results for mixtures with and without AEA

	Fresh air content	Hardened air content	Aggregate content	Paste content	Specific surface	Spacing factor
Unit	%	%	%	%	1/in.	in.
Reference	6.4	8.7	64.5	26.8	541	0.006
Ref-without-AEA	3.2	3.1	72.1	24.9	407	0.017
P-100-M3	5.6	16.2	63.2	20.6	371	0.003
P-100-without AEA	3.5	7.5	67.5	25.0	345	0.010
B-100-M3	5.5	10.9	65.1	24.0	463	0.005
B-100 - without AEA	3.5	6.5	65.3	28.2	443	0.010

Major findings of Task

Table 3-19 lists the performance summary of HPC made with and without SAPs and AEA. Results showed that SAPs was also effective in reducing the drying shrinkage and increasing the mechanical properties of HPC made with and without AEA. Also, the mixtures made with SAPs and without AEA performed better frost durability than reference without AEA. However, SAPs cannot be as effective in improving frost durability as AEA.

Table 3-19. Performance summary of HPC made with and without SAPs and AEA

Mixture	28-d compressive strength (%)	28-d MOE (%)	28-d flexural strength (%)	21-d drying shrinkage (%)	28-d bulk resistivity (%)	Durability factor (%)	Hardened air content (%)	Spacing factor (%)
Reference	100	100	100	100	100	100	100	100
Ref-without AEA	110	111	102	86	114	9	36	291
P-100-M3	111	122	118	48	118	113	186	61
P-100-without AEA	137	135	120	24	126	24	86	181
B-100-M3	119	124	110	64	112	109	125	82
B-100-without AEA	144	134	115	62	122	37	75	168

*P and B denote WL PAM and BASF SAPs; 100 denotes 100% of IC; M3 denotes 3-min extended mixing time

3.3 Subtask B-3: Optimization of external curing regime

In this subtask, combined effect of external moist curing and IC using SAP on compressive strength and drying shrinkage was investigated. Three periods of external moist curing (e.g., without moist curing, 2 days and 6 days in lime-saturated water after demolding at 1 day) were selected.

Mechanical properties

Figure 3-23 shows the compressive strengths of the HPC mixtures made with and without SAPs at different ages cured with different moist curing periods. Specifically, the samples for the same mixture were cured without moist curing (right after demolding), 2 days, and 6 days in lime-saturated solution after demolding. Results showed that the 7-day and 14-day compressive

strength of all mixtures with different moist curing periods were higher than 4000 psi, which can meet the requirement of Illinois Tollway. Besides, the compressive strength was also increased with a longer moist curing period for all the mixtures with and without SAPs. For instance, the maximum value of 56-day compressive strength was recorded for the mixture made with BASF SAP and cured 7 days in lime-saturated solution, where 14% and 30% reduction were observed for the same mixture treated with 2 days in lime-saturated solution and without moist curing, respectively.

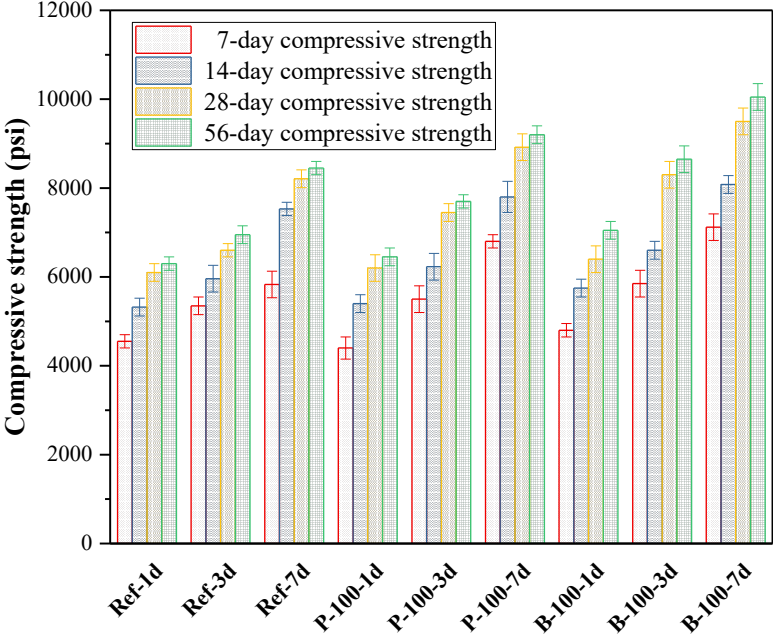


Figure 3-23. Compressive strength of the HPC mixtures with different moist curing periods (1-d, 3-d, 7-d correspond to 1-d in mold and 0, 2, and 6 days in lime-saturated solution)

Viscoelastic properties

Figure 3-24 shows the shrinkage of the HPC mixtures cured with different moist curing periods. The initial length was recorded after the samples were subjected to air drying. Results showed that the IC of both SAPs can effectively reduce the shrinkage of HPC as the exterior moist curing acted. For instance, the HPC mixtures made with both SAPs but without moist curing had the lower 28-d shrinkage, with the value of 170-180 μ strain, compared to the reference mixture with 6-day moist curing. Besides, a 35% reduction of shrinkage was recorded for the mixture made with WL PAM SAP with 2-day moist curing, compared to the reference mixture with 6-day

moist curing. This indicated that the use of SAP as an IC agent can significantly reduce the exterior moist curing period.

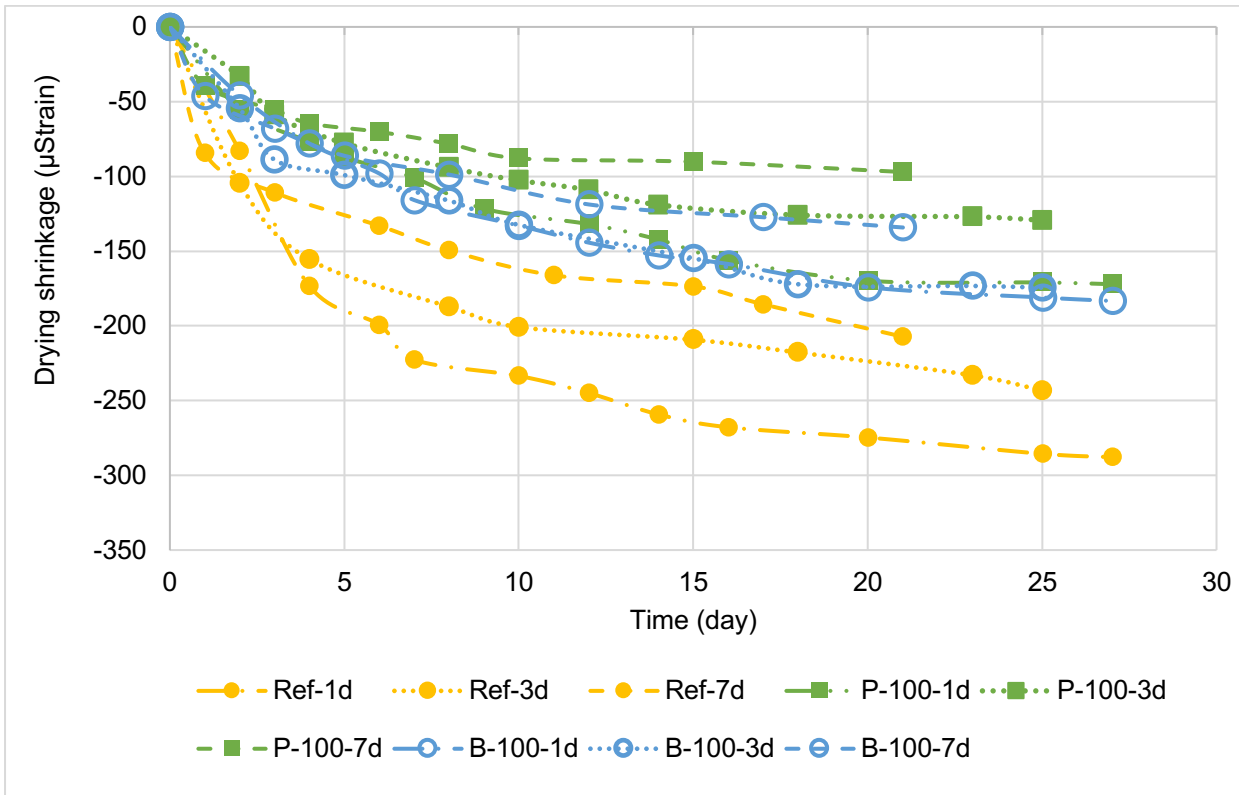


Figure 3-24. Drying shrinkage of the HPC mixtures with different moist curing periods (1-d, 3-d, 7-d correspond to 1-d in mold and 0, 2, and 6 days in lime-saturated solution)

Major findings of subtask B-3

Table 3-20 lists the performance summary of HPC made with SAPs and different external curing periods. The IC of SAP can improve the compressive strength and reduce the shrinkage of HPC effectively as the exterior moist curing. This indicated that the use of SAP as an IC agent can significantly reduce the exterior moist curing period. Specifically, 28-d compressive strength and drying shrinkage of HPC mixtures made with 100% IC of SAP and cured 2 days in lime-saturated water were comparable to reference mixture cured 6 days in lime-saturated water.

Table 3-20. Performance summary of HPC made with SAPs and different external curing period

No.	Moist curing (days)			7-d compressive strength (%)	28-d compressive strength (%)	28-d drying shrinkage (%)
	0	2	6			
Ref-1d	√			100	100	100
Ref-3d		√		118	108	93
Ref-7d			√	128	131	74
P-100-1d	√			97	102	74
P-100-3d		√		121	128	48
P-100-7d			√	149	146	35
B-100-1d	√			105	105	78
B-100-3d		√		129	136	60
B-100-7d			√	156	156	42

*P and B denote WL PAM and BASF SAPs; 50 and 100 denote 50% and 100% of IC; 1d, 3d and 7d denote 1-d in mold, 1-d in mold and 2-d in lime-saturated water, 1-d in mold, and 6-d in lime-saturated water, respectively

3.4 Subtask B-4: Comparison of HPC mixtures with LWS and SAP

In this subtask, the two selected SAPs (PAM and BASF) were compared with lightweight sand (LWS). All the mixtures included AEA, had 100% IC and 3-min extended mixing time and were

studied with no moist curing to study the full effect of internal curing. All the tests in this subtask were carried out at UIUC unless mentioned otherwise.

Fresh properties

Table 3-21 summarizes the fresh properties of the investigated SAP- HPC mixtures made with SAP and LWS. The fresh properties included the initial slump, air content, and unit weight. Results showed that the slump loss was faster with SAP than LWS and the unit weight of concrete mixture made with LWS was noticeably lower as expected.

Table 3-21. Fresh properties of HPC with SAP and LWS

Mix ID	Slump (in.)			Air content (%)	Unit weight (lb/ft ³)
	Initial	+20 min	+40 min	Initial	
Ref	8.5	6.5	4.0	6.5	145.6
PAM	8.0	4.0	2.0	5.8	146.4
BASF	8.0	5.0	3.5	4.8	147.2
LWS	8.5	7.0	6.0	-	136.8

Mechanical properties

Figure 3-25 shows the compressive strengths of the HPC mixtures made with SAP and LWS at different ages. As seen in Figure 3-25, in mixtures with SAP, higher compressive strengths were obtained when compared to the reference as well as the LWS mixture. While the LWS mixture satisfies the Tollway requirement of 4000 psi at 14-days, the mixtures with SAP performed significantly better with the PAM SAP having close to 70% higher compressive strength. In this subtask, the specimens were all subjected to no moist curing and the effect of internal curing can be clearly seen in the obtained results.

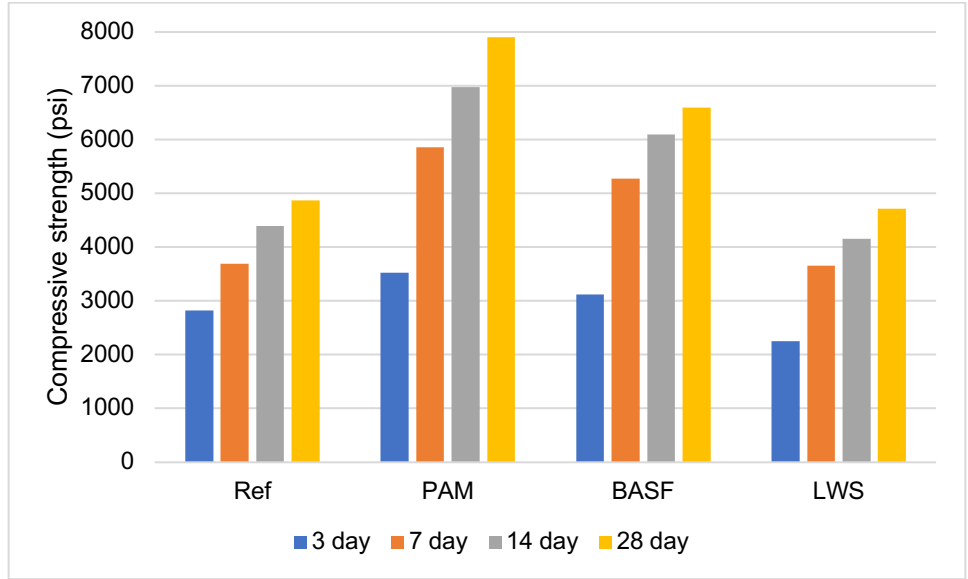


Figure 3-25. Compressive strength of the HPC made with SAPs and LWS

Figure 3-26 and Figure 3-27 show the flexural strength and the MOE of the investigated HPC mixtures made with SAP, and LWS at 28 days, respectively. Results showed that using SAPs and LWS did not dramatically influence the flexural strength or the MOE of the concrete. The mixtures with SAP performed slightly better than LWS and reference mixtures. Mixtures with SAP had about 20% higher flexural strength whereas the mixture with LWS had similar flexural strength as the reference mixture. Mixtures with SAP had about 10% higher MOE whereas the mixture with LWS had about 10% lower MOE than the reference mixture.

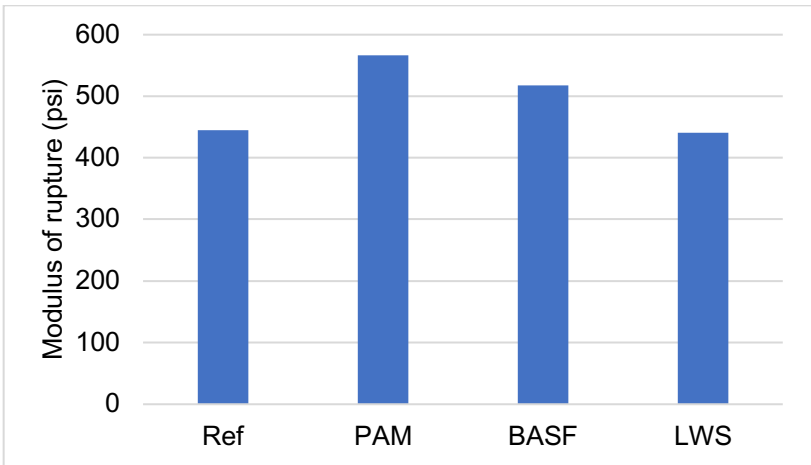


Figure 3-26. Flexural strength of the HPC made with SAPs and LWS

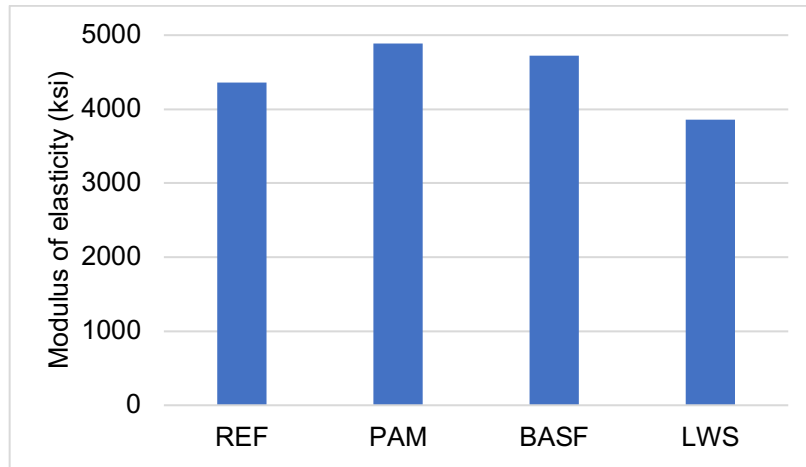


Figure 3-27. Modulus of elasticity of the HPC made with SAPs and LWS

Viscoelastic properties

Figure 3-28 and Figure 3-29 respectively show the autogenous shrinkage and drying shrinkage of the HPC mixtures made with SAP and LWS. These measurements were carried out at Missouri S&T. In both the tests, the mixtures with SAP performed better than both LWS and reference mixtures. 28-day autogenous shrinkage of HPC with PAM and BASF SAPs was 56% and 38% lower than the reference respectively. The LWS mixture had a 28% lower autogenous shrinkage compared to reference. For drying shrinkage, all the mixtures met the Tollway requirement (less than 300 μ strain at 21-day air drying after 7-day curing). 25-day drying shrinkage of HPC with PAM and BASF SAPs was 47% and 30% lower than the reference respectively. The LWS mixture had a slightly lower drying shrinkage compared to the reference.

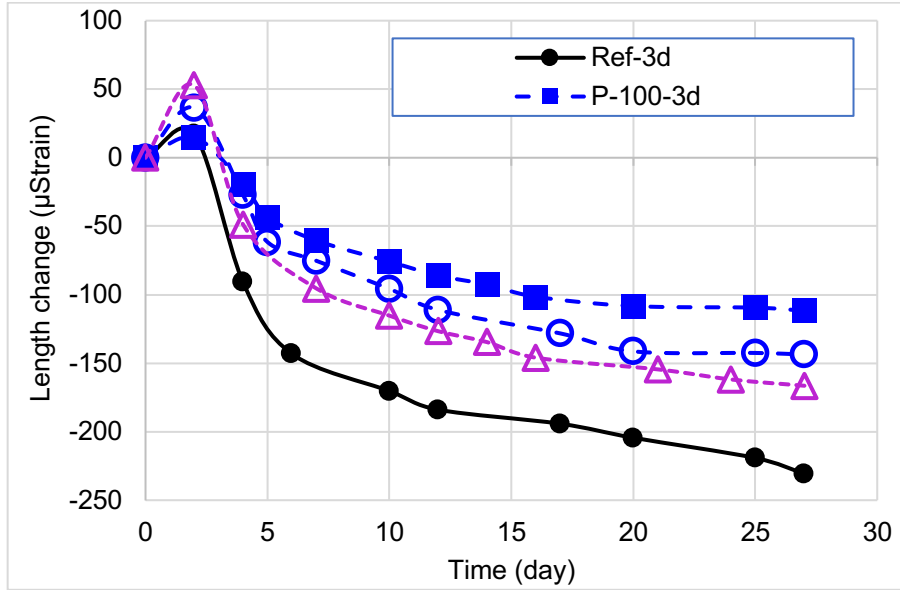


Figure 3-28. Autogenous shrinkage of HPC made with SAPs and LWS (initial length measured at 1 day)

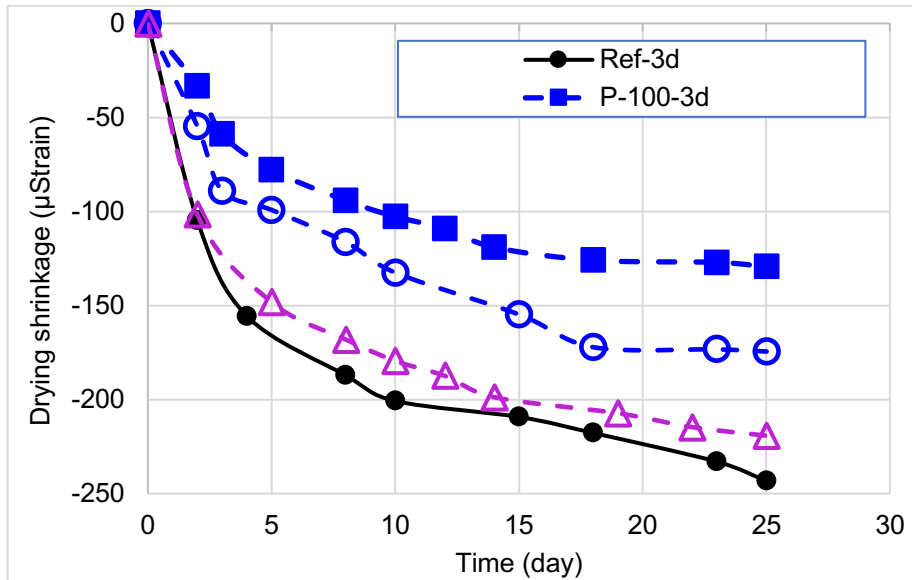


Figure 3-29. Drying shrinkage of HPC made with SAPs and LWS (initial length measured at 3 days)

The results from the ring test are shown in Figure 3-30. None of the rings cracked and the strains recorded were relatively low.

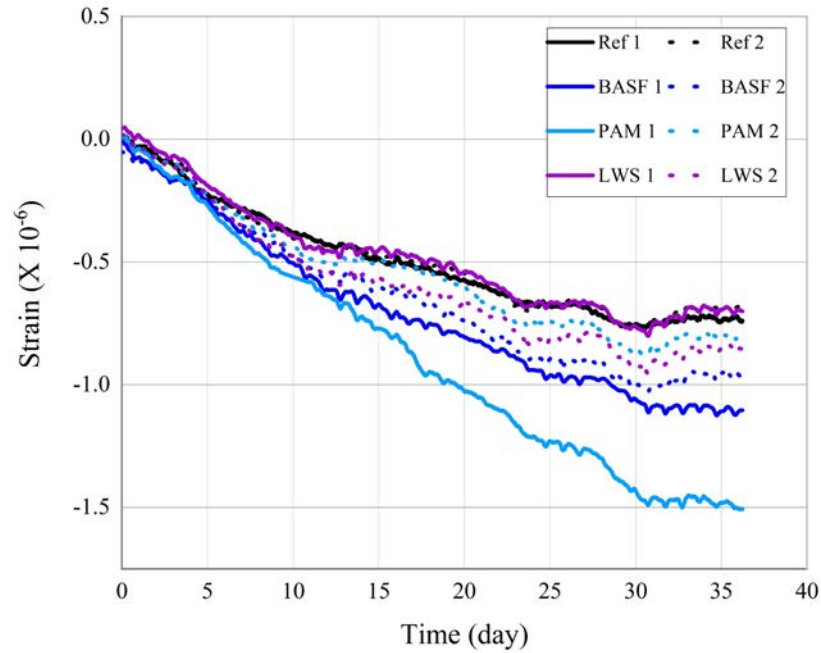


Figure 3-30. Restrained shrinkage over time (Ring test)

Durability

The four mixtures were tested according to ASTM C666, approach A. Two specimens (labeled 1 and 2) were tested for freeze-thaw durability for each mixture. The results from the test are shown in Figure 3-31 and Figure 3-32. None of the mixtures failed (Relative dynamic modulus less than 60%) before the end of the test. All the mixtures had air entrainment and showed good frost durability with a durability factor greater than 95% (Tollway requirement > 80%).

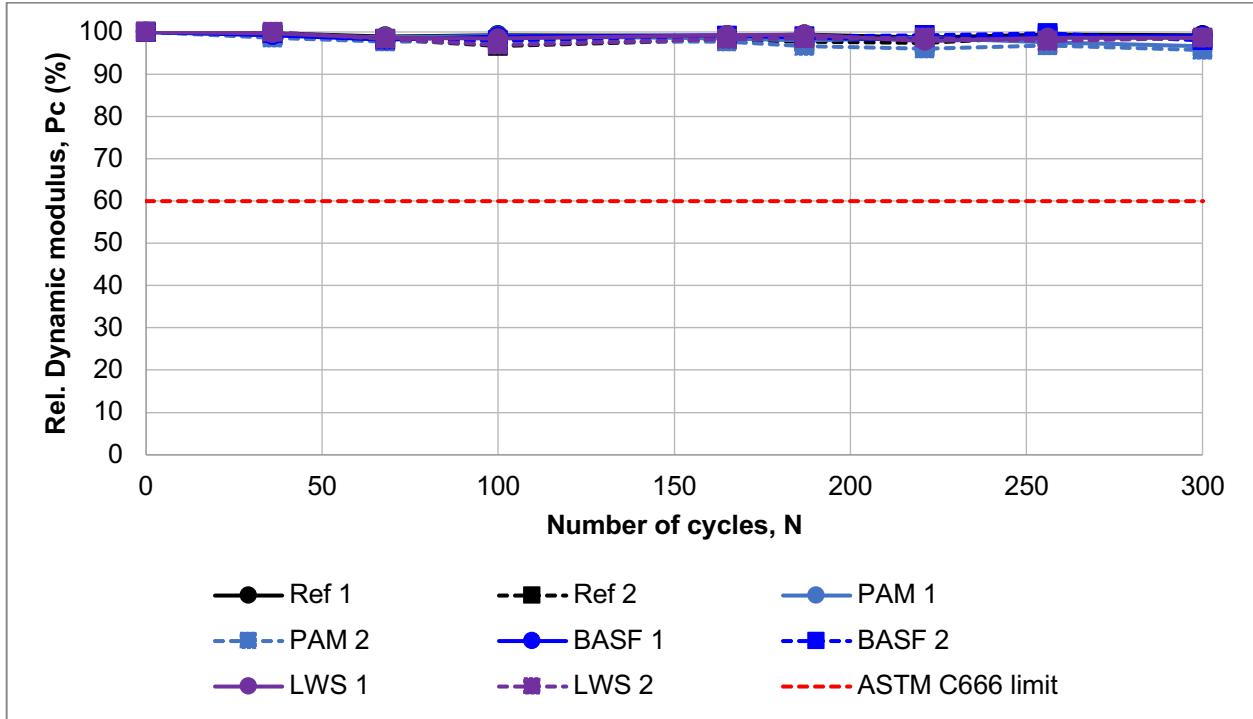


Figure 3-31. Relative dynamic modulus of HPC mixtures made with SAPs and LWS

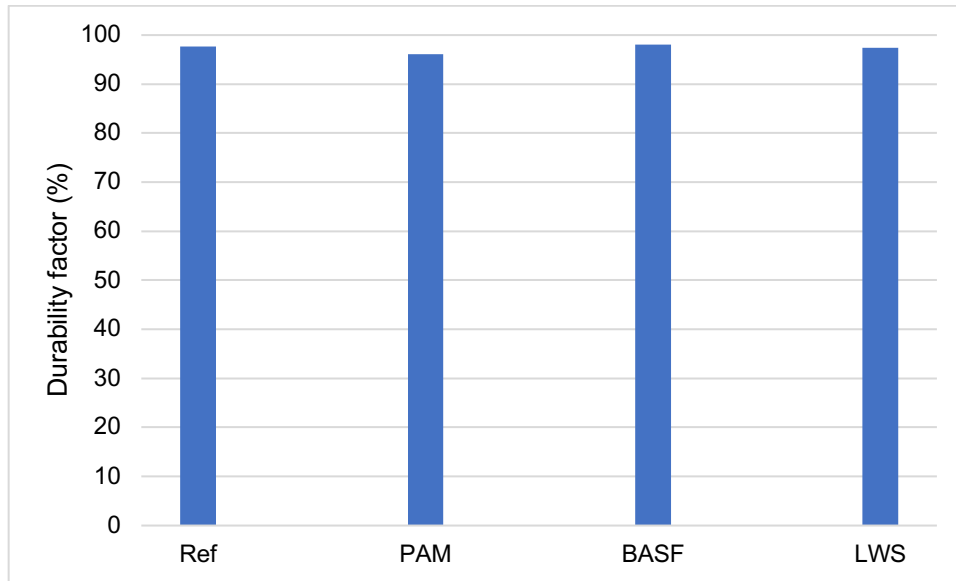


Figure 3-32. Durability factor of HPC mixes made with SAPs and LWS

Air void system

The results of the air void analysis are shown in Table 3-22. The spacing factor for all the mixes was found to range between 0.005 to 0.012 in. exhibiting good frost durability. The higher value obtained with PAM was likely a sampling issue and the sections tested had a particularly higher aggregate content thus increasing the spacing factor.

The scanned images are shown in Appendix B.

Table 3-22. Hardened void analysis results for mixtures with SAP and LWS

	Fresh air content	Hardened air content	Aggregate content	Paste content	Specific surface	Spacing factor
Unit	%	%	%	%	1/in.	in.
Ref	6.5	10.7	60.3	29.0	590	0.005
PAM	5.8	8.6	63.9	27.4	259	0.012
BASF	4.8	6.7	58.7	34.6	510	0.009
LWS	-	9.4	60.8	29.9	573	0.006

Major findings of Task

Table 3-23 lists the performance summary of HPC made with and without SAPs and AEA. Results show that SAPs were effective in improving the mechanical properties of the HPC compared to LWS. They are also more effective in reducing shrinkage. Including SAPs in HPC has similar effect to LWS in frost durability.

Table 3-23. Performance summary of HPC made with SAPs and LWS

Mixture	28-d compressive strength (%)	28-d MOE (%)	28-d flexural strength (%)	25-d drying shrinkage (%)	28-d autogenous shrinkage (%)	Durability factor (%)
Reference	100	100	100	100	100	100
PAM	162	112	127	54	57	98
BASF	135	108	116	70	73	100
LWS	97	88	99	89	53	100

4. FIELD TESTING RESULTS AND DICUSSION

Two field tests were carried out during this project period. One at the beginning of the project to determine the feasibility of implementing SAP in a concrete truck and to identify potential complications with the mixing procedure. Second, to test the performance of the developed HPC mixtures on a large scale. Instrumented test slabs were cast and the performance of HPC with SAP with and without a curing compound was investigated.

4.1 Field test 1: Feasibility of HPC with SAP in the field

The purpose of this trial was to determine the feasibility of implementing SAP in the field for internal curing in high performance concrete (HPC), and to identify any potential complications with the mixing procedure. This trial was conducted on November 19th, 2019 at Ozinga Concrete Materials located in Des Plaines, IL.

Over the course of the day, three truckloads (approx. 8 cu. yds. each) of HPC were batched in total. Each batch was used to test three SAP products: (1) WL PAM/Type S, (2) Hydromax, and (3) BASF. For every batch, HPC was pulled from the truck at four stages to record slump, temperature, and air content, and to cast cylinders for subsequent testing. The first stage (A) tested the base HPC mixture prior to any SAP additions. Stages B-D tested the HPC following SAP addition at the beginning (B), middle (C), and end (D) of the truckload. Stages C and D were achieved by discarding approximately 1/3 of the truckload prior to testing fresh properties and casting cylinders. In total there were 12 sample types, summarized in Table 4-1 below.

Table 4-1. Sample summary

Sample ID	SAP type	Description
1 – A	None	Base HPC in truck # 1
1 – B	WL PAM	Beginning of load
1 – C		Middle of load
1 – D		End of load
2 – A	None	Base HPC in truck # 2
2 – B	Hydromax	Beginning of load
2 – C		Middle of load
2 – D		End of load
3 – A	None	Base HPC in truck # 3
3 – B	BASF	Beginning of load
3 – C		Middle of load
3 – D		End of load

Mixture Design and Procedure

The base HPC mixture listed in Table 4-2 remained the same for each of the three truckloads. The batch ticket for each truck is attached in Appendix C.

Table 4-2. Summary of the HPC mixture design

Material	Design Quantity
Type I Cement	345 lb
Fly Ash – Class C	80 lb
Slag – Grade 100	110 lb
Coarse Aggregate (CM11)	1810 lb
Fine Aggregate (FM02)	1364 lb
Water	25.3 Gal
Superplasticizer: (GCP ADVA® Cast 575)	1.5 oz./cwt.
Water Reducing admixture: (GCP WRDA® 82)	2 oz./cwt.
Air Entraining Admixture: (GCP Darex® II)	0.75 oz./cwt.
Hydration Stabilizer: (GCP Recover®)	2 oz./cwt.

For each batch the amount of SAP required was calculated using Eq. X1.2 from ASTM C 1761/C1761M-17 [123]. This equation considers the absorption and desorption behavior of each SAP product determined via laboratory testing prior to the mixing day. Note, the SAP dosage decreases with an increase in the SAP absorption capacity. The SAP dosages are summarized in Table 4-3.

Table 4-3. SAP dosages

SAP	Absorption Capacity (g/g)	M _{SAP} (lb/yd ³)
Wastelock PAM/Type S	19.80	2.05
BASF	34.45	1.10
Hydromax	16.81	2.58

The same mixing procedure was followed for all three batches (1-3). First, the base HPC mixture was batched and added to a truck on site at central mixing plant. The remaining procedure involved modifying the HPC mixture in the mixing truck. There were four stages (A-D) in which slump, temperature, and air content was recorded and cylinders were cast for subsequent testing. For each sample type, ten 6 x 12 in. cylinders were cast for compressive strength testing at 3, 7, 14, and 28 days, as well as five 4 x 8 in. cylinders for air void analysis. In Stage A, the base HPC mixture was tested and cast into cylinders. Then, the predetermined amount of SAP was added to the back of the mixing truck and incorporated with 40 revolutions. Immediately following the SAP addition, the HPC was tested again. As expected from preliminary laboratory testing, the addition of SAP led to an immediate slump loss, therefore additional superplasticizer was added to the truck and incorporated with another 40 revolutions. In Stage B, the HPC, now containing the SAP and the additional superplasticizer, was tested, and cast into cylinders. A third of the truck (~2.5 – 3 cu. yds.) was then discarded prior to Stage C, during which the middle of the load was tested and cast into cylinders. Finally, another third of the truck was discarded prior to Stage D, during which the end of the load was tested and cast into cylinders.



Figure 4-1. Mixing procedure: (left) arrival of mixing truck containing the base HPC mixture, (middle) addition of SAP to back of mixing truck, (right) testing fresh properties and casting cylinders.

Fresh Properties

The fresh properties of each batch are summarized in Table 4-4 below. The fresh properties of each mix revealed aspects of the base HPC mixture that would impact the overall strength of the material. In Batches 2 and 3 the air content was higher than normal (greater than 8%). In Batch 1 a miscalculation of the moisture content of the sand increased the w/c from the target w/c of 0.40 to 0.45. After observing high air content in the first two batches, for Batch 3, a lower dosage of air entraining admixture was used – 0.56 oz./cwt. A detailed account of each batch is provided in this section.

Table 4-4. Summary of Fresh Properties

Sample ID	SAP Type	Air Content (%)	Slump (in.)
1 – A	None	7.8	8.75
1 – B	WLPAM	9.4	7.50
1 – C		9.5	4.50
1 – D		10.2	4.25
2 – A	None	10.7	7.00
2 – B	Hydromax	11.5	9.25
2 – C		13.5	8.50
2 – D		14.5	8.00
3 – A	None	8.8	5.50
3 – B	BASF	6.2	7.50
3 – C		5.6	3.75
3 – D		5.1	2.50

Batch 1 was used to test WL PAM. At Stage A, the base HPC mixture had a slump of 8.75 in. and an air content of 7.8%. The predetermined amount of 16.41 lbs. of WL PAM was added to the back of the truck and incorporated with 40 revolutions. Immediately following the addition of SAP, the slump dropped to 3.25 in. and the air content increased to 8.6%. To combat the slump loss, 40 oz of superplasticizer was added to the truck and incorporated with another 40 revolutions. After the addition of superplasticizer, the slump increased to 7.5 in. and the air content further increased to 9.4%, at the beginning of the load, Stage B. In the middle of the load, Stage C, the air content remained steady, but the slump was reduced to 4.5 in. At the end of the load, Stage D, the slump remained steady at 4.25 in. however the air increased slightly to 10.2%. A summary of the fresh properties can be seen in Appendix D.

Batch 2 was used to test Hydromax. Here, at Stage A, the base HPC mixture started with a slump of 7 in. and an air content of 10.7%. A predetermined amount of 20.67 lbs of Hydromax was added to the back of the mixing truck as shown in Figure 4-2. The SAP was mixed into the HPC with 40 revolutions. Immediately following the addition of SAP, the slump dropped to 2 in. and the air content decreased to 8%. To combat the slump loss, 40 oz of superplasticizer was then added to the truck and incorporated with another 40 revolutions. At this point it was observed that some of the SAP was stuck on the fins, which are responsible for the mixing action within the truck. The fins were scraped manually with a shovel and the HPC was mixed with an additional 20 revolutions. The slump and air content which were found to be 9.25 in. and 11.5% respectively, at the beginning of the load, Stage B. In the middle of the load, Stage C, the slump decreased slightly to 8.5 in. and the air content increased to 13.5%. At the end of the load, Stage D, the slump decreased slightly to 8 in. and the air increased to 14.5%. A summary of the fresh properties can be seen in Appendix D.



Figure 4-2. Addition of HydroMax

The final truckload, Batch 3, was used to test the BASF SAP. The load size for this batch was inadvertently changed from 8 to 9 cu. yds. However, the SAP dosage remained at that calculated for the 8 cu. yds. At Stage A, the base HPC mixture started with a slump of 5.5 in. and an air content of 8.8%. A predetermined amount of 8.82 lbs BASF SAP was added to the back of the mixing truck and incorporated with 40 revolutions. Prior to the addition of extra

superplasticizer, the slump was determined to be approximately 0.5” via the VERIFI® apparatus attached to the back of the truck (seen in Figure 4-3). To combat the slump loss, 100 oz of superplasticizer was added to the truck immediately and incorporated with another 40 revolutions. At this point it was observed that a substantial portion of the BASF SAP was stuck on the fins of the truck, as shown in Figure 4-4. The fins were scraped manually with a shovel and the HPC was mixed with an additional 10 revolutions. The mixture was then tested for slump and air content which were found to be 7.5 in. and 6.2% respectively at the beginning of the load, Stage B. In the middle of the load, Stage C, the slump decreased to 3.75 in. and the air content continued to decrease to 5.6%. At the end of the load, Stage D, the slump decreased to 2.5 in. and the air decreased to 5.1%. A summary of the fresh properties can be seen in Appendix D.



Figure 4-3. GCP applied technologies VERIFI® apparatus



Figure 4-4. BASF SAP stuck to fins of mixing truck

Compressive strengths

The compressive strengths for all 12 samples were tested at 3, 7, 14, and 28 days and are tabulated in Table 4-5. One set of specimens were dry cured (no external moisture) and tested at 14 days to study the effect of internal curing by SAP and the results are shown in Table 4-6.

Table 4-5. Moist cured compressive strength

Sample ID	SAP Type	Compressive Strength (psi)			
		3-day	7-day	14-day	28-day
1 – A	None	2234	3126	4016	4898
1 – B	WL PAM	2072	2803	3761	4253
1 – C		2036	2750	3537	3830
1 – D		1916	2709	3126	3883
2 – A	None	1792	2550	3289	3822
2 – B	Hydromax	2184	3050	3807	4360
2 – C		2193	2893	3750	3889
2 – D		1949	2662	3184	3846
3 – A	None	2505	3657	4685	4730
3 – B	BASF	3394	5333	6696	6631
3 – C		3817	5592	7003	7797
3 – D		3884	5606	6983	7122

Table 4-6. 14 - day compressive strength (moist cured vs. air cured)

Sample ID	SAP Type	14-day Compressive Strength (psi)	
		Moist cured	Air cured
1 – A	None	4016	3507
1 – B	WL PAM	3761	3748
1 – C		3537	3349
1 – D		3126	3090
2 – A	None	3289	3022
2 – B	Hydromax	3807	3350
2 – C		3750	2923
2 – D		3184	2793
3 – A	None	4685	3928
3 – B	BASF	6696	5684
3 – C		7003	6081
3 – D		6983	5912

The results show little variance between the beginning, middle, and end of load sets as seen in Figure 4-5. Only the samples containing the BASF SAP met the Illinois Tollway compressive strength target of 4000 psi at 7 days. The BASF mixture had a lower air entrainer dosage than the other two mixtures. The air content of the base HPC used for all samples was high, falling at or above the maximum of 8% typically specified by the Illinois Tollway. As can be expected, the air content was further increased by the addition of superplasticizer. The addition of SAP also increased the air content in PAM and Hydromax but not in BASF mixture as seen in Table 4-4.

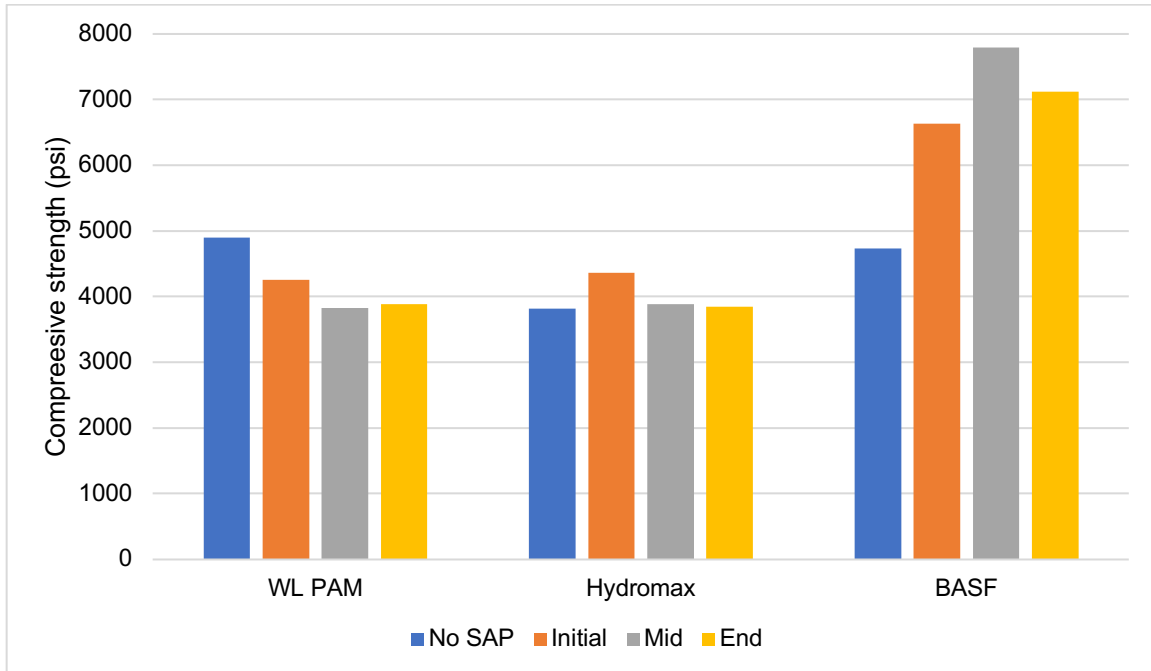


Figure 4-5. 28-day compressive strength

To compare the effect of internal curing with SAP, the compressive strength of the mixtures at 14 days were studied with and without moist curing. The results are shown in Figure 4-6. WasteLock PAM performed the best with 2% reduction in strength due to air curing. The companion reference mixture (1 - A) had a 13% reduction in strength. The 14-day compressive strength of air cured Hydromax and BASF specimen were 15% lower than the moist cured specimens. For Hydromax, this reduction was higher than the companion reference mixture (2 - A) which was only 8% lower. The BASF SAP performed marginally better with the reference mixture (3-A) seeing a 16% reduction.

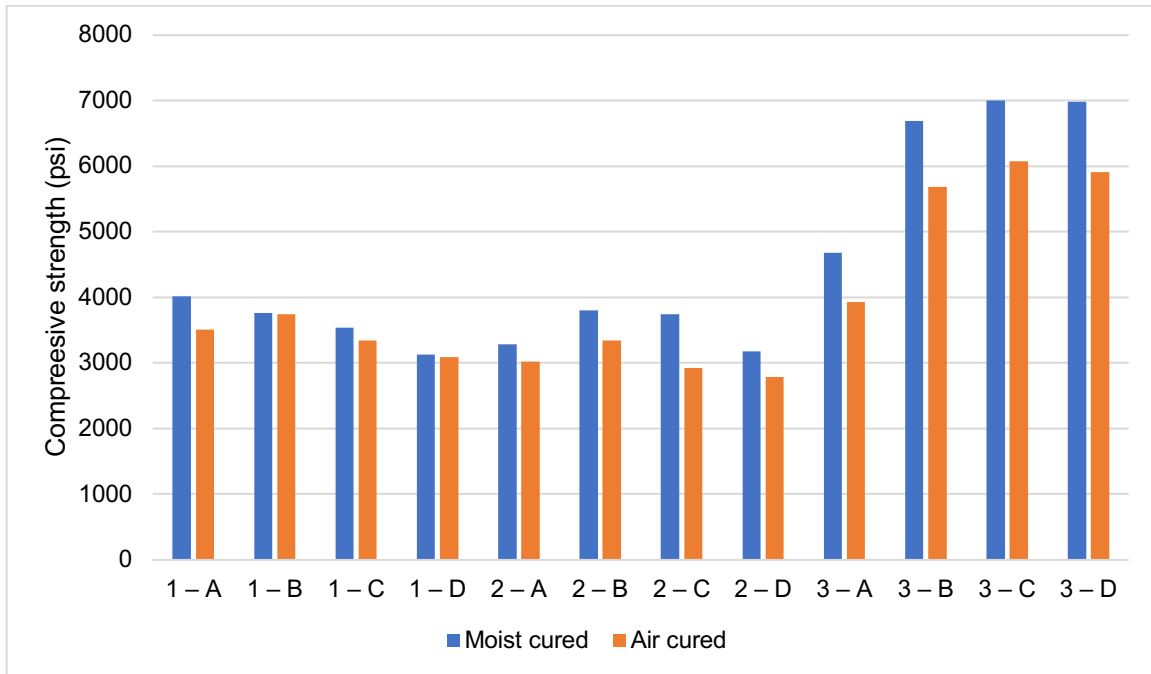


Figure 4-6. 14 - day compressive strength (moist vs. air curing)

The compressive strength data shows that overall, SAP has no deleterious effects on the performance of concrete and in the case of BASF, led to a significant increase in strength. These results, while preliminary, showed that SAP is a promising candidate for use in HPC.

Air void system

The results of the air void analysis are shown in Table 4-7.

Table 4-7. Hardened air void analysis results

	Fresh air content	Hardened air content	Aggregate content	Paste content	Specific surface	Spacing factor
Unit	%	%	%	%	1/ in.	In.
1 - A	7.8	8.4	63.8	27.8	772	0.004
1 - B	9.4	12.1	59.6	28.3	517	0.005
1 - C	9.5	12.6	62.1	25.3	573	0.004
1 - D	10.2	11.9	60.9	27.2	646	0.004
2 - A	10.7	16.5	63.7	19.8	734	0.002
2 - B	11.5	13.3	63.3	23.3	752	0.002
2 - C	13.5	16.7	61.7	21.6	548	0.002
2 - D	14.5	17.2	65.1	17.7	563	0.002
3 - A	8.8	9.7	64.2	26.1	767	0.004
3 - B	6.2	4.2	70.4	25.4	786	0.006
3 - C	5.6	5.5	61.9	32.7	636	0.008
3 - D	5.1	5.7	65.2	29.1	627	0.007

It was found that the hardened air content was greater than the measured fresh air content in most cases. This is due to the empty voids left behind by the dehydrated SAP. This increase in air void was greater in the larger SAP (WL PAM and Hydromax) than in the BASF SAP.

The spacing factor was found to be less than 0.008 in. in all cases as required by the Illinois tollway specification. The specific surface was close to or greater than 600 in.²/in.³ in all cases as required by the specification.

Major findings

This initial trial was conducted early in this project to identify any potential complications with the mixing procedure so that they may be addressed in laboratory testing. Several issues such as slump loss, effect on air content, SAP dispersion, mixing time after SAP addition were identified and then investigated further in the laboratory testing. The preliminary results from this field testing showed that SAP is a promising candidate for use in future Illinois Tollway HPC mixtures.

4.2 Field test 2: Field implementation of HPC with SAP

The purpose of this trial was to construct and test slabs using concrete with SAP. This trial used three concrete mixtures: control, and two SAPs namely, WL PAM and BASF. Two instrumented test slabs were constructed with each of these mixtures. One of the two slab for each mixture was coated with a curing compound (CC) to study effectiveness of SAP at internal curing. This trial was conducted at Ozinga Concrete Materials located in Lemont, IL. The strain gages were set up on May 10, concrete was poured on May 11, and the lift off gages (LVDTs) and iButtons were installed on May 12, 2021.

Sensors and instrumentation

The slabs were each 20 feet long, 5 feet wide and 10 in. deep. Each slab was instrumented with four strain gages, one lift off gage, and two relative humidity/temperature sensors (iButton). The strain gages were installed in pairs at two different heights to capture potential bending in the slab. The strain gages and the lift off gages were hard wired to a data logger box. A schematic of the locations of these gages/sensors in each slab and the nomenclature used to identify them is shown in Figure 4-7.

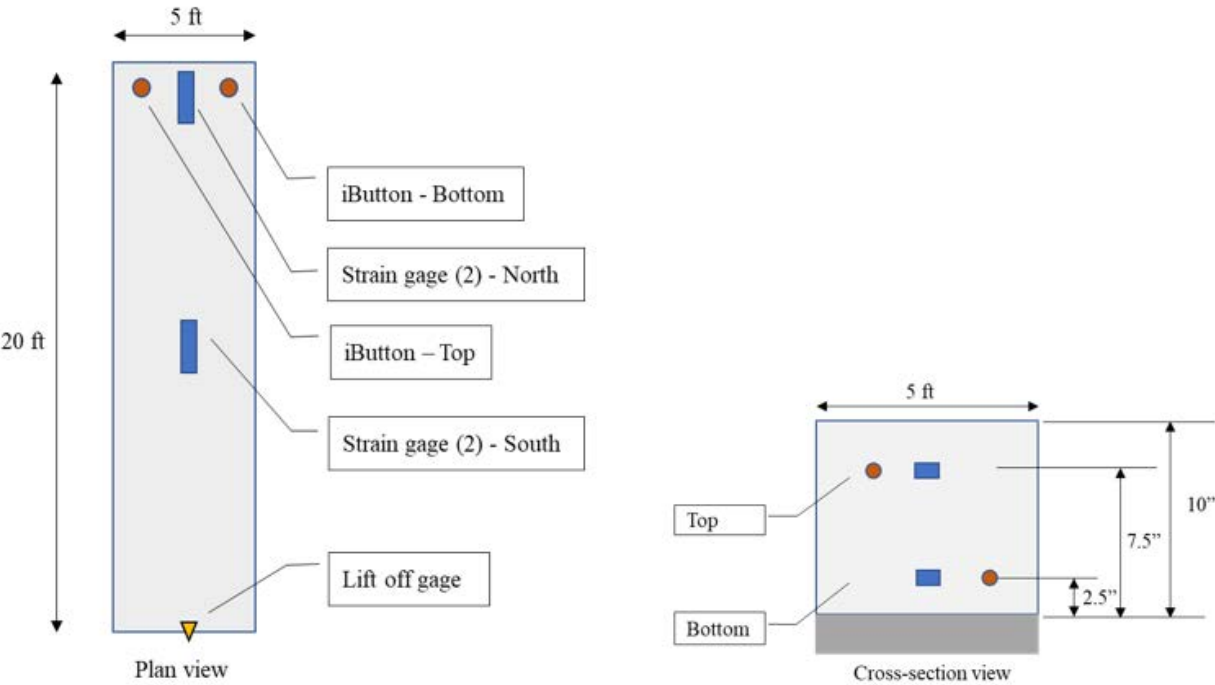


Figure 4-7. Schematic of the slab instrumentation

The strain gages used were from Tokyo Measuring Instruments Lab, model PMFL-60-2LJRTA and are shown in Figure 4-8. These waterproof gauges are designed to measure internal strain of concrete. They are embedded into the concrete by placing them in position and pouring concrete around them. These strain gauges have quarter-bridge configuration, 3-wire system, a gauge length of 5 inch, and a resistance of 120-ohm.



Figure 4-8. Strain gages (PMFL-60-2LJRTA)

The strain gages were positioned on a steel chair (commonly used as reinforcement bar support) at a height of 2.5" and 7.5" from the granular base as shown in Figure 4-9. The positioning chair and the gages were tied to a steel stake (driven into the granular base) to prevent it from moving during the concrete pour. The strain gages were secured loosely (allowing for movement in the longitudinal direction to record shrinkage of the concrete) to the chair by using zip ties as shown in Figure 4-10.



Figure 4-9. Strain gages mounted on positioning chair



Figure 4-10. Strain gage secured to positioning chair with zip tie

Each slab had two of these chairs oriented longitudinally in the middle of the slab width; one chair 1 foot from the north edge of the slab and the other at the middle of the slab (10 feet from

the ends). The final setup of the strain gages and the positioning chairs before concrete pour is seen in Figure 4-11.



Figure 4-11. Strain gages and positioning chairs setup (photographed facing south)

The strain gages were connected to LORD MicroStrain V-Link wireless nodes as seen in Figure 4-12. Up to four strain gages were connected to a single node. Each strain sensor was set up to be queried, and data stored every hour. The wireless nodes can directly collect the data from the sensor, store it in memory, and immediately transfer the data to wireless sensor data aggregator (WSDA-1500) using radiofrequency communication when there is no obstruction in communication. The data could be downloaded from the data aggregator when required. The wireless nodes sampled 32 data points per second for 3 continuous minutes every hour for each strain gauge.



Figure 4-12. LORD MicroStrain V-Link wireless node

To measure curling of the slabs, if any, lift off gages (LVDTs) from Trans-Tek, model 244-000 1.00 DCDT with a working range of 1 in. were used. An Adafruit Feather 32u4 Adalogger with built in micro-USB charging was used to record the data from these LVDTs. The datalogger works with the Arduino Integrated Development Environment (IDE). The data logging sketch was written in the 32u4 Adalogger through a serial/com port. A microSD card was used for recording the data which could be accessed when required to download data. The displacement was measured every second and averaged by an hour.

A 3 feet long stake was driven into the aggregate base close to the slab (roughly 3-6 in. away from the slab) and a nut was epoxied to the top of this stake to act as reference point for the LVDT measurements. A bolt was screwed into this nut to the required height to adjust the precise position for the LVDT when required. This is shown in Figure 4-13.



Figure 4-13. Reference point for lift off gage measurements

Each lift off gage was mounted on a base which was secured to an L-bracket. The L-bracket was secured to the slab a day after the concrete pour using Tapcon concrete screw anchors. The lift off gage was positioned such that the steel core of the LVDT attached to the reference point as shown in Figure 4-14. The plastic screw cap seen in Figure 4-14 was epoxied to the top of the bolt to make a secure connection to ensure the LVDT was always in touch with the reference point. The steel core was free to move within the LVDT to record the slab movements. The final lift off gage set up is shown in Figure 4-15.



Figure 4-14. Connection between reference point and lift off gage (LVDT)



Figure 4-15. Lift off gage (LVDT) installed on the slab

To record temperature and relative humidity (RH), a sensor with embedded battery power and memory was used. The sensor used was from iButtonLink technology, model DS1923-F5# iButton (referred hereafter as iButton) and is shown in Figure 4-16.

These iButtons were placed near the north end of the slabs (about 1 foot from the edges) at two heights (2.5" and 7.5" from the bottom of the slab). Immediately after the concrete was poured, a plastic pipe was inserted into the fresh concrete to create a hollow cylindrical space to the correct depth. This pipe was removed the day after the concrete pour and an iButton was placed into this void using a magnetic stick. The pipe was then reinserted on top of the iButton to create a seal. Figure 4-17 shown these steps in sequence. The iButton was then left to collect temperature and RH data from within the slab. At the end of the project, the pipe seal was removed, the iButton extracted with a magnetic stick and the data downloaded. Two iButtons were also placed outside the slabs to collect ambient temperature and RH data.



Figure 4-16. iButtons (temperature and relative humidity sensors)



Figure 4-17. Installation of iButtons (L-R: removing plastic pipe after concrete hardened, placing iButton using magnetic stick, covering the space above iButton using the plastic pipe to form a seal)

Mixture Design and Placement of HPC

The control mixture was Ozinga's IDOT Class BS concrete, selected because it could be readily produced with materials available at the Ozinga concrete plant in Lemont, IL. The control mixture remained the same for each of the three truckloads (9 cu. yd. each) and is given in Table 4-8. The amount of SAP required was calculated using Eq. X1.2 from ASTM C 1761/C1761M-17 [123]. The required amount of SAP (WL PAM – 1.14 lb./cu. yd. and BASF, 1.14 lb./cu. yd.) was batched in water soluble bags and was added to the back of the truck. The concrete was then subjected to an additional 40 revolutions to thoroughly disperse the SAP. However, it was observed that for the BASF SAP mixture, the SAP was stuck to the fins and an additional 40 revolutions were included. The batch ticket for each truck is attached in Appendix E.

Table 4-8. Summary of the HPC mixture design

Material	Design Quantity
Type I Cement	455 lb
Fly Ash – Class C	155 lb
Coarse Aggregate (CM11)	1851 lb
Fine Aggregate (FM02)	1129 lb
Water	27.5 Gal
Superplasticizer: (GCP ADVA® Cast 575)	4.5 oz./cwt.
Water Reducing admixture: (GCP ZYLA® 630)	2 oz./cwt.
Air Entraining Admixture: (GCP Darex® II)	2.79 oz./cwt.
Hydration Stabilizer: (GCP Recover®)	1 oz./cwt.

The fresh properties of the mixtures were measured before and after the addition of the SAP and is given in Table 4-9. During the pour of the BASF mixture, it was observed that the water-soluble bag failed to disintegrate, and a considerable amount of the BASF SAP did not disperse, as shown in Figure 4-18.

Table 4-9. Fresh properties

	Control	WL-PAM		BASF	
		Before SAP	After SAP	Before SAP	After SAP
Slump (in.)	5	7.75	4.75	>11	8
Air content (%)	8.5	6.5	7.5	10.2	9.5
Temperature (F)	61	60	60	62	64
SAM air (%)	8.8	7.5		10.3	
SAM	0.23	0.34		0.26	



Figure 4-18. Dispersion issue seen during the BASF mixture pour

For each mixture, 6 x 12 in. cylinders were cast for compressive strength testing at 3, 7, 14, and 28 days.

During the placement of the HPC, special attention was paid to not disturb the strain gages and the positioning chair. The concrete was carefully placed around the positioning chair and sensors and manually compacted by using a compacting rod as seen in Figure 4-19. All the slabs were finished with the help of floats, screed and brooms as shown in Figure 4-20. One of the two slabs of each HPC mixture was coated with a curing compound (Ozinga ENVIROCURE C309) by spraying it on the top surface as shown in Figure 4-21.



Figure 4-19. Compacting of HPC around the embedded strain gages

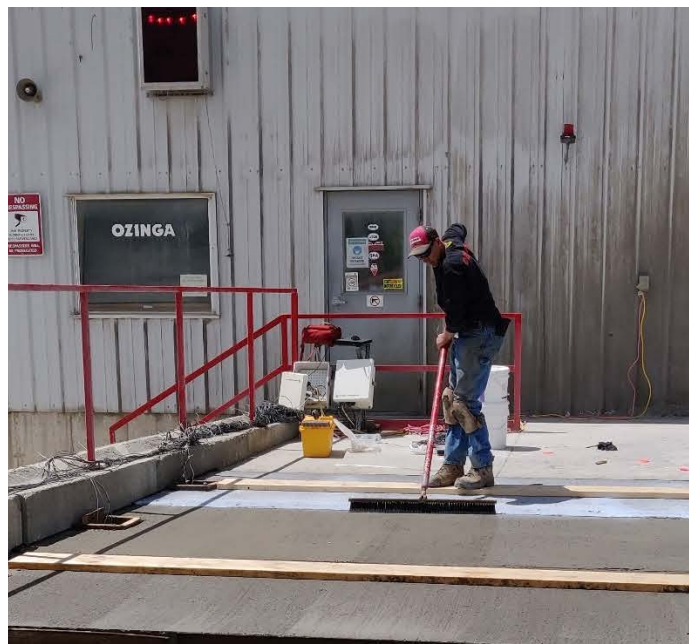


Figure 4-20. Finishing of the HPC slabs



Figure 4-21. Coating the top surface of the HPC slab with curing compound

Results and discussion

The compressive strengths of the HPC mixtures are shown in Figure 4-22. All the three mixtures met the Tollway requirement of 4000 psi at 14 days despite having higher than normal air contents as seen in Table 4-9.

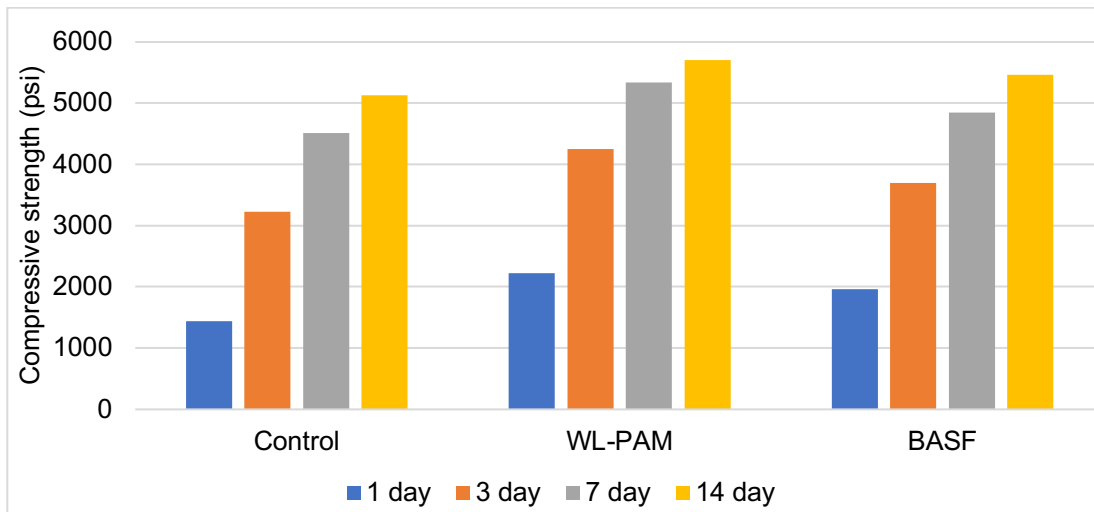


Figure 4-22. Compressive strength

The data from the embedded strain gages and lift off gages was collected periodically during the testing period of approximately 2.5 months. During the three visits to the site after the slabs were constructed, it was observed that the slabs and the surrounding site remained wet. Figure 4-23 shows the wetness around the test site on the day the test was ended (July 29, 2021). The right image of Figure 4-23 shows how SAP particles may swell after the concrete has hardened if there is exposure to rain water without high alkali levels as found in pore solution. Recalling that SAP absorption is sensitive to pH, the initial particle swelling occurs when alkalinity is high. If later the alkalinity is lowered by flushing the site with rainwater, the SAP particles will swell and exude from the concrete surface as shown in Figure 4-23. The particles may be perceived as slippery, but they are easily removed with clear water or brooming, and would not negatively impact surface friction or skid resistance.

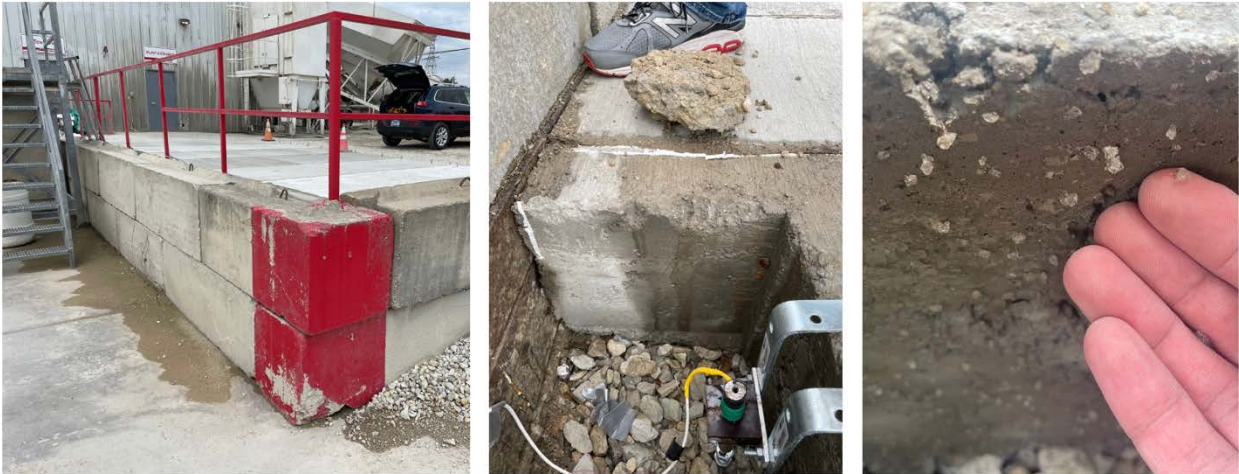


Figure 4-23. Wetness observed around the slabs

The ambient temperature and RH during the first month of testing, recorded by the iButton is shown in Figure 4-24, Figure 4-25, and Figure 4-25. The temperature and RH within the slab are shown in Figure 4-26 and Figure 4-27. The temperature within the slabs remained roughly the same across all the slabs and at different heights. The RH data confirmed the visual observation of wetness of the slabs and the surrounding. The RH of all but one slab (Control CC top) was consistently 100%. The slabs remained in a saturated condition during the testing period.

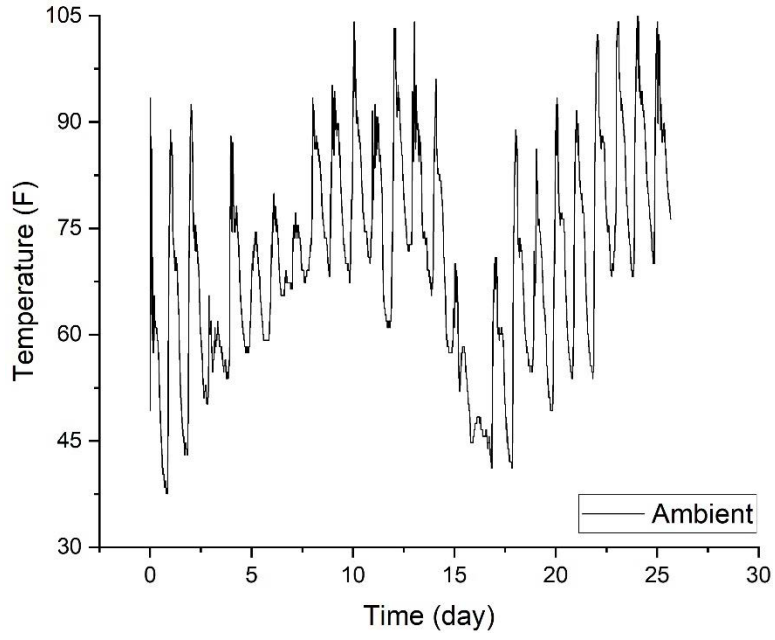


Figure 4-24. Ambient temperature near the HPC slabs

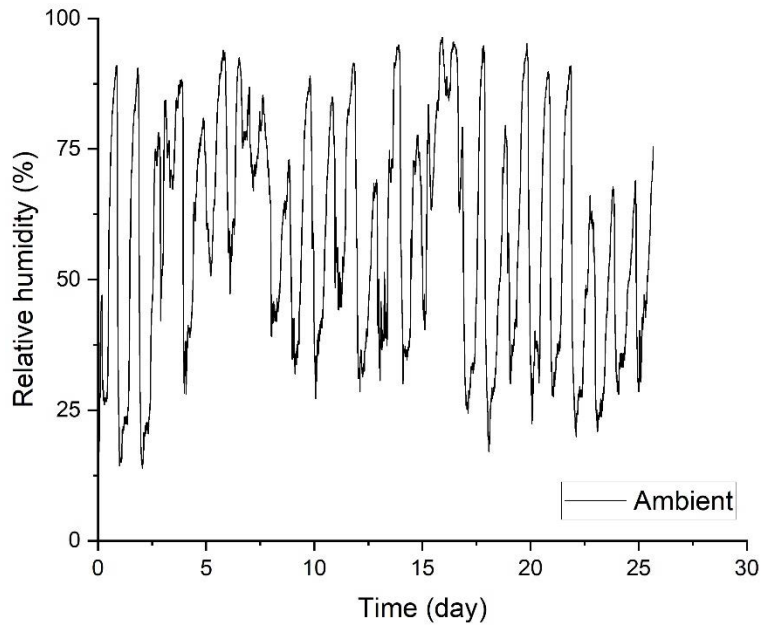


Figure 4-25. Ambient RH near the HPC slabs

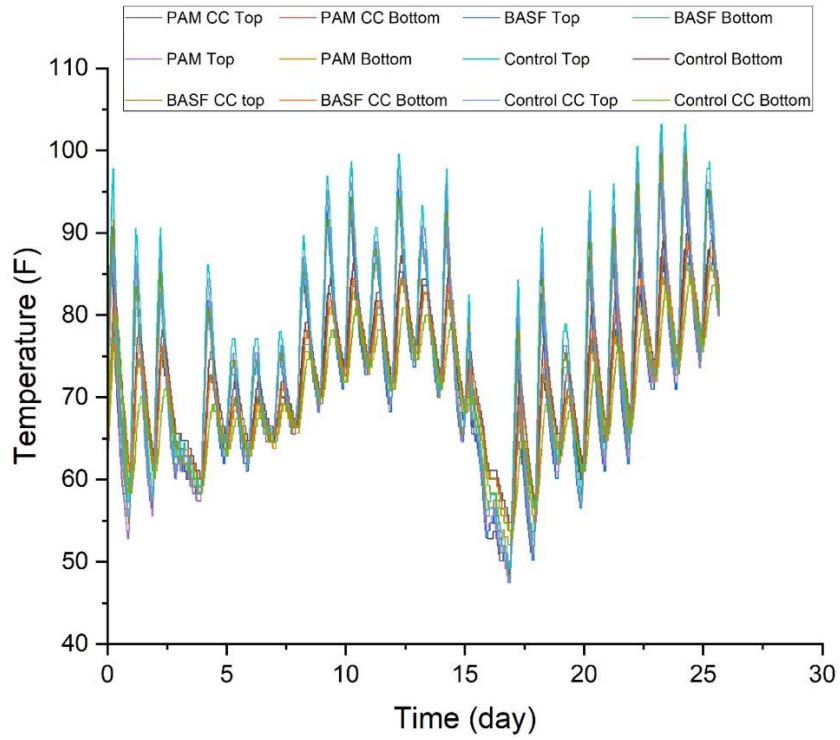


Figure 4-26. Temperature within the HPC slabs

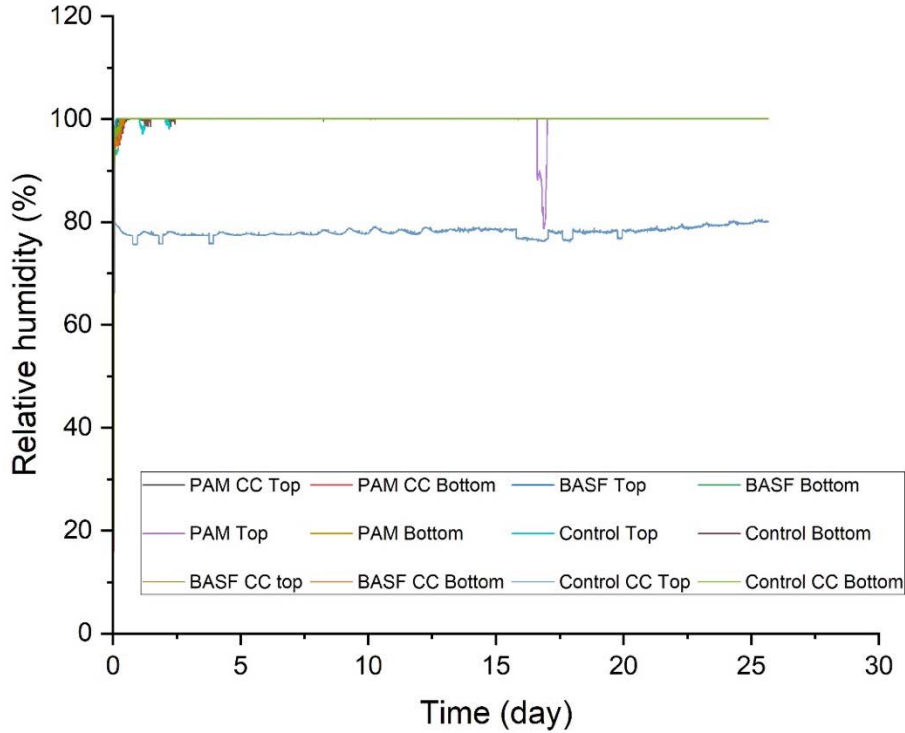


Figure 4-27. RH within the HPC slabs

The strain gage data is shown in Figure 4-28 Figure 4-30. No evidence of bending/curling is evident from the obtained results. The strain values recorded were extremely small and were more likely to have been from daily temperature cycles. No long-term strain trends were seen. The continuous saturated state of the slabs is likely to have prevented any shrinkage of the slabs. This made any observations on the effectiveness of SAP with and without a curing compound to internally cure the slabs limited. In general, the strain gages at the center of the slab and at the bottom recorded larger tensile strain while the strain gages at the top recorded larger compressive strain. The values obtained are close enough to only lead to a qualitative assessment and not to suggest bending/curling of the slabs. Any large strain seen in the data corresponds to a sharp vertical change in the strain which is likely due to a crack in the concrete.

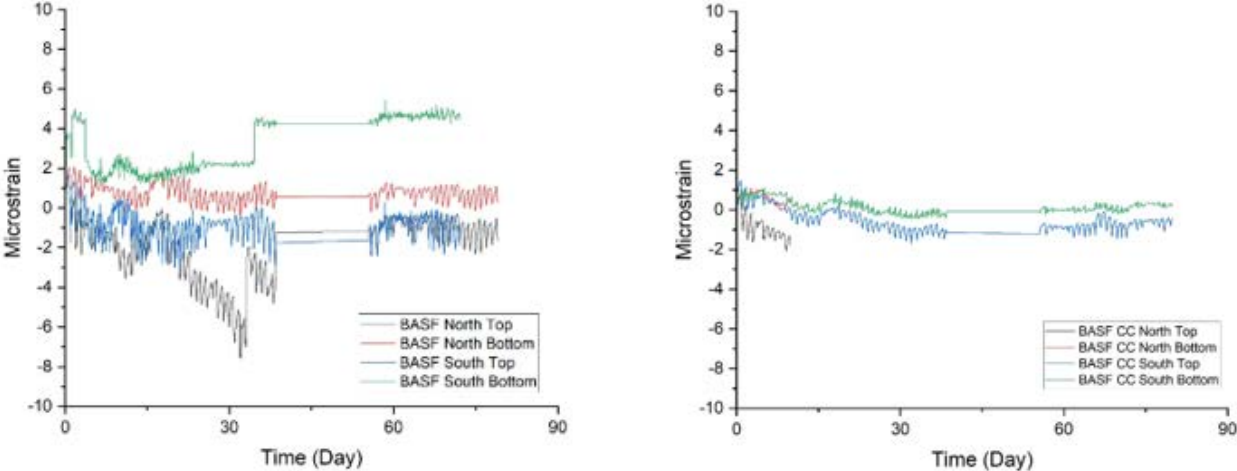


Figure 4-28. Strain measurements of the BASF slabs with and without CC

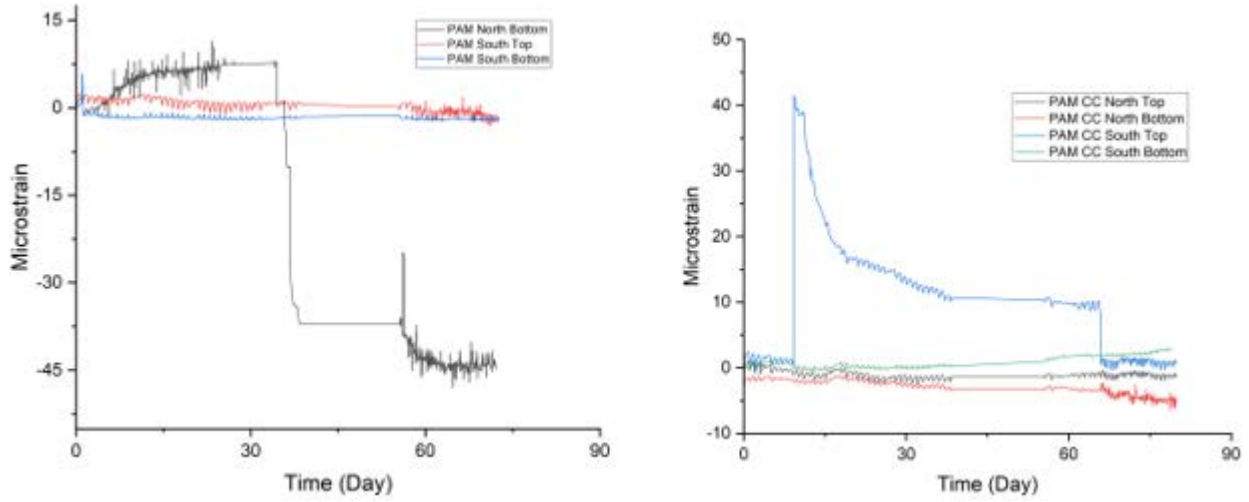


Figure 4-29. Strain measurements of the PAM slabs with and without CC

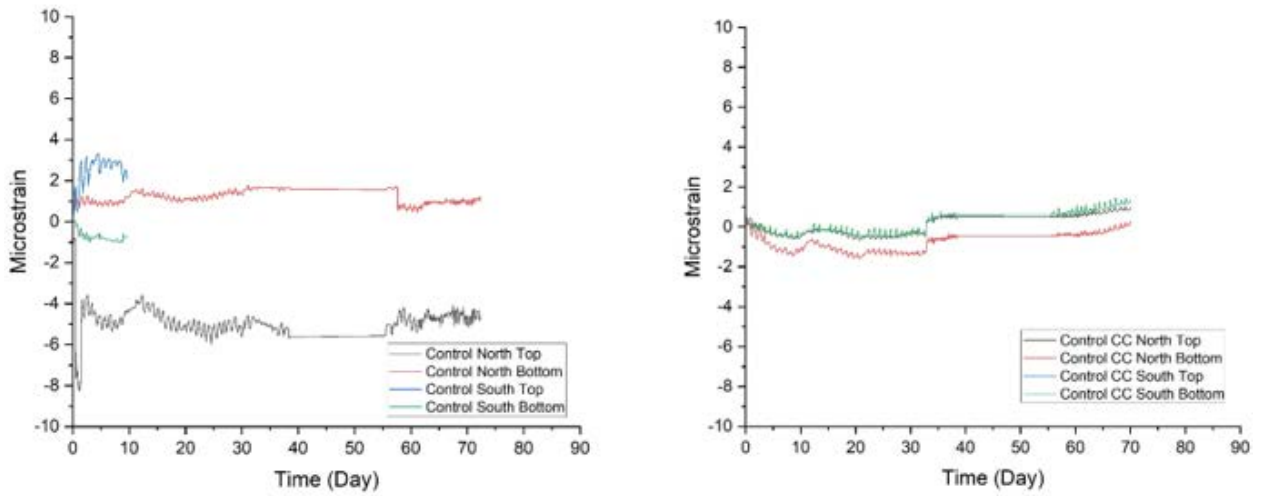


Figure 4-30. Strain measurements of the control slabs with and without CC

The lift-off gages (LVDTs) also confirm the strain gage data. Slab curl/deformation, if any, was very small. Comparisons between the mixtures and the use of curing compound is limited due to lack of change in dataset. The signal data from the LVDTs were noisy and hence a moving average filter (of 24 hours) was used to clean the data and is shown in Figure 4-31. The largest

movement was seen in the control mixture. In general, mixtures with a SAP had lower movement and when a curing compound was used in addition, the values were further reduced.

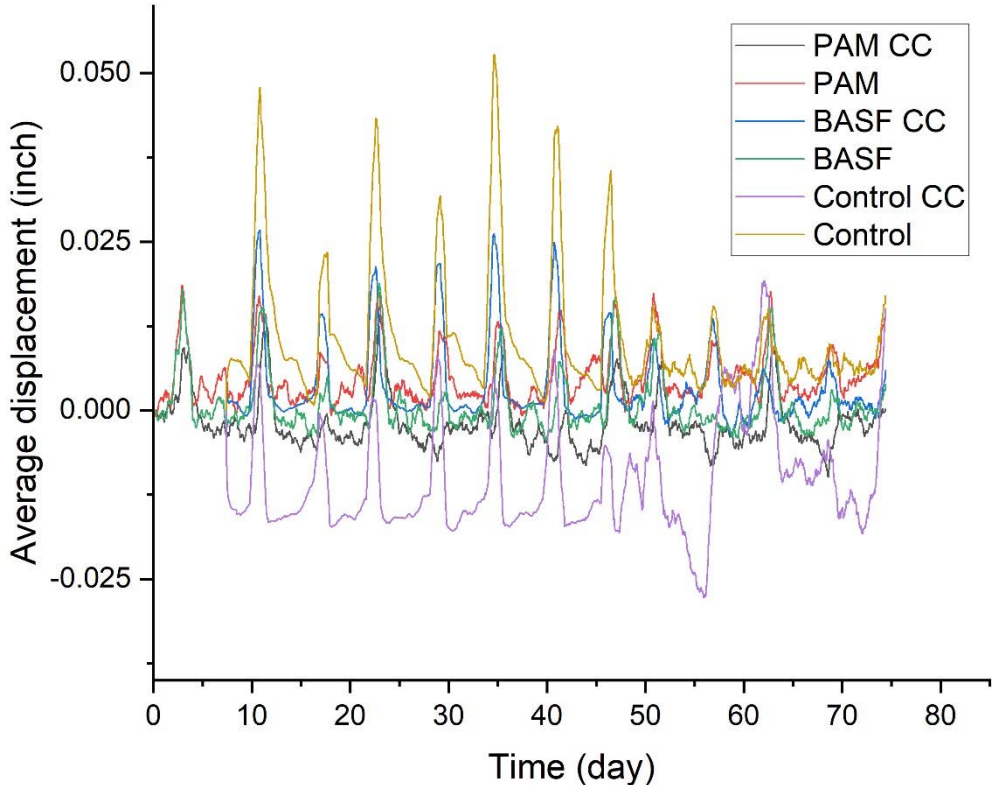


Figure 4-31. Lift-off gage data of the HPC slabs

Findings about material handling

This field trial was carried out towards the end of the project period to implement the laboratory findings in the field and to check the feasibility of using SAP at a larger scale. Expected issues such as slump loss after the addition of SAP was tackled by using a control mixture with a high initial slump. A key takeaway from this field trial was that delivery and dispersion of SAP at the back of the truck needed to be carefully monitored to achieve good distribution of the SAP. The water soluble bags proved to be problematic in that we observed SAP clumps and incompletely dissolved bags. When a large amount of dry SAP powder is in the bag, the initial water absorption may cause the SAP to compete for water with the bag itself, leading to an unacceptable clumping of the material. For this reason, we do not recommend use of water soluble bags. Instead, SAP can be manual added to the truck, taking care to disperse the SAP.

5. RECOMMENDED CHANGES TO TOLLWAY SPECIFICATIONS

The use of SAP requires changes to Tollway standard specification language to accommodate the use of a new material in the production of HPC and the corresponding changes in concrete performance. In general, specifications for the use of SAP in commercial production are not readily available. The suggestions for changes to Tollway reference documents are provided in Appendix F.

The main objective of this research was to study internal curing by SAP to improve the durability of Tollway structures and pavements. The research has demonstrated several advantages to use of SAP that will benefit future Tollway construction by both simplifying the concrete production process and enhancing the long-term durability of concrete. Based on these findings, and given the dry SAP addition approach recommended by the researchers, recommendations and cautions for practice have been prepared.

The primary modification to the Tollway specifications will be the implementation of an approved material supplier list¹, which will also contain the qualification test procedure required to characterize a new product. The test method protocol, referred to as the “Teabag” test has appeared in several publications but was prepared for the purposes of a standardized test recently by Weiss et al.² Test frequency for QA/QC testing purposes should be annually or if any noticeable changes are observed in the material appearance or concrete performance. The AquaSmart SAP product is recommended for included on the approved material list. AquaSmart was not selected for use in all laboratory comparisons or the field testing because it has unique characteristics because SAP is delivered as a coating on sand. The sand is included as a portion of the concrete fine aggregate, and the SAP is determined

Specification acceptance criteria for SAP materials will be based on the measured sorption characteristic given by the Teabag test, which is then used to calculate the recommended amount of dry SAP material to be added to provide sufficient water for complete cement hydration. Due to the performance testing requirements already contained in the Tollway

¹ Recommended Tollway SAP Approved Supplier List

² Weiss, W.J.; Montanari, L. Guide Specification for Internally Curing Concrete (InTrans Project No. 13-482); Iowa Department of Transportation: Ames, IA, USA, 2017

specifications for HPC³, the use of a low absorption or “poor performing” SAP will result in limited shrinkage mitigation for both linear and restrained ring shrinkage testing and therefore “poor performing” SAP will be excluded. The specification should also exclude the use of repulpable or dissolvable containers for SAP, which were found by this research team to be problematic.

³ Recommended Tollway HPC Specification, modified for SAP

6. SUMMARY AND CONCLUSIONS

This project demonstrated that SAP can benefit the properties of high performance concrete used for Tollway bridge structures. The most important benefit is that SAP absorbs water, maintains it in the microstructure, and then releases it as cement hydration demands. The desired outcome of internal curing with SAP is that shrinkage is reduced while strength and other mechanical properties are slightly improved. The workability of fresh concrete with SAP is affected, and users need to be prepared to use superplasticizer to offset slump loss.

The project demonstrated a successful approach for adding SAP internal curing benefits to HPC concrete mixtures. A contractor can modify an HPC mixture by adding SAP and then increasing superplasticizer to compensate for the water demand represented by the SAP. The resulting concrete can be mixed, placed, and finished using the same techniques. The hardened concrete will achieve similar if not slightly higher strength, lower shrinkage, and improved durability.

The project explored many aspects of material behavior. The effects of SAP types, different contents of IC water (i.e., SAP content), extended mixing time and external curing period on workability, mechanical properties, viscoelastic properties, and durability of HPC mixtures designated for bridge decks were investigated. The results showed that the internal curing provided by the SAP can reduce the shrinkage and risk of early-age shrinkage cracking. Specifically, the two SAP types namely BASF and WL PAM exhibited the ability on retaining the water within the window time for mixing were found to be more effective in improving the mechanical properties and reducing the shrinkage. Based on the test results from the research presented in this investigation, the following conclusions can be drawn:

1. WL PAM and BASF SAPs are recommended given the more significant reduction in autogenous and drying shrinkage with no apparent reduction in mechanical properties.
2. 100% IC of both WL PAM and BASF SAPs are more effective in reducing autogenous and drying shrinkage.
3. SAP was well dispersed with a short extended mixing time, indicating that the current Tollway requirement for 40 additional revolutions after addition of admixtures is sufficient for SAP.

4. 100% IC using WL PAM and BASF SAPs with 2-day external moist curing has a comparable effect on reducing drying shrinkage, compared to 6-day external moist curing. The detailed summary of each subtask is as follows:

Subask B-1: Pre-test of SAP for internal curing of HPC

Table 6-1 presents the performance summary of HPC made with five types of SAPS in Task B-1. The absorption and desorption kinetics of the five investigated SAPs, namely the Hydro., WL 770, WL PAM, Aqua100, and BASF SAPs infiltrated solutions made with ternary cementitious materials and chemical admixtures (water reducer, retarder, and air-entraining agents) were investigated.

Table 6-1. Performance summary of HPC made with different SAPs

Mixture	SP dosage (%)	28-day compressive strength (%)	56-day compressive strength (%)	28-day autogenous shrinkage (%)	21-day drying shrinkage (%)
Reference	100	100	100	100	100
WL-PAM	145	109	105	59	60
WL-770	130	96	91	73	125
Hydromax	145	114	112	88	115
BASF	175	116	113	72	80
WL-CP	226	110	108	74	111

The addition of SAP resulted in a significant increase in HRWR dosage ranging from 7 to 13 fl oz /yd³, with the highest value observed with the BASF SAP. In general, the results of the absorption kinetics showed that SAPs had different absorption capacities and rates. The maximum adsorption capacity was observed for the BASF and WL 770 SAPs, 35 and 30 g/g, respectively, although the peak was reached at different rates/times. The BASF SAP reached its

maximum absorption rate at 50 min, while the WL 700 SAP reached its peak after 1 min. The same absorption rate was recorded for the Hydro. SAP but at a lower capacity of 15 g/g. Considering the additional mixing time of 3 min during the introduction of SAP, a full benefit of the absorption capacity of the BASF SAP cannot be achieved. Therefore, in practice, the WL770 and Hydro. SAPs are better candidates given the fast absorption rate. On the other hand, the absorption capacity of the WL PAM SAP, within the window need for proper mixing, is higher than the Hydro. SAP and lower than the WL 770 SAP. However, the use of the WL PAM SAP is suggested as it can retain water for a longer duration. The results show that the desorption of the WL PAM SAP was initiated at 50 min., while this time was only 6 min. for the WL 770 and Hydro. SAPs. In conclusion, the WL PAM SAP is the best candidate among the investigated SAPs as it is more stable chemically in the pore solution and its absorption/desorption kinetics are favorable for the concrete mixing procedure of the Tollway project where 3 min. of additional mixing is allowed after the introduction of SAP.

The results from the shrinkage test also confirmed that the WL PAM product was the most effective SAP in inhibiting autogenous and drying shrinkage. Also, it contributed significantly to compressive strength development at the investigated ages. The BASF is another candidate SAP that showed acceptable performance in compressive strength and viscoelastic properties due to their high absorption capacity.

Subtask B-2: Performance of HPC with optimized SAPs

Key fresh and hardened properties, including workability, mechanical properties, viscoelastic properties, transport properties, and frost durability of HPC made with two types of SAP were evaluated. Tables 6-2 to 6-4 summarizes the performance summary of investigated mixtures corresponding to subtask B-2-1 to B-2-3, respectively.

Table 6-2. Performance summary of HPC made with 50% and 100% IC of SAPs

Mixture	SP dosage (%)	28-d compressive strength (%)	28-d MOE (%)	28-d flexural strength (%)	28-d autogenous shrinkage (%)	21-d drying shrinkage (%)
Reference	100	100	100	100	100	100
P-50-M3	147	102	113	114	80	81
P-100-M3	160	109	118	116	62	48
B-50-M3	147	102	117	108	89	110
B-100-M3	173	116	124	112	74	64

Table 6-3. Performance summary of HPC made with SAPs and different extended mixing time

Mixture	SP dosage (%)	28-d compressive strength (%)	28-d MOE (%)	28-d flexural strength (%)	28-d autogenous shrinkage (%)	21-d drying shrinkage (%)
Reference	100	100	100	100	100	100
P-100-M3	160	109	118	116	62	48
P-100-M5	187	107	123	115	49	62
P-100-M7	226	106	121	109	70	52
B-100-M3	173	116	124	112	74	64
B-100-M5	173	108	119	113	87	76
B-100-M7	187	110	121	109	87	74

Table 6-4. Performance summary of HPC made with and without SAPs and AEA

Mixture	28-d compressive strength (%)	28-d MOE (%)	28-d flexural strength (%)	21-d drying shrinkage (%)	28-d bulk resistivity (%)
Reference	100	100	100	100	100
Ref-without AEA	110	111	102	86	114
P-100-M3	111	122	118	48	118
P-100-without AEA	137	135	120	24	126
B-100-M3	119	124	110	64	112
B-100-without AEA	144	134	115	62	122

The 100% IC of both SAPs had a more significant influence in improving the mechanical properties and reducing the autogenous and drying shrinkage. However, 100% IC of both SAPs increased the SP dosage by 10% to 25%, as compared to those mixtures made with 50% IC. The higher SP dosage used for 100% IC can be attributed to the lower amount of free water due to the absorption of SAPs.

Additionally, no apparent difference was observed in hardened properties as the extended mixing time was increased from 3 to 7 min, indicating that 3 min extended mixing time was sufficient for homogenous dispersion of SAP. However, the longer extended mixing time resulted in the greater initial SP dosage to maintain the initial fluidity, which can be attributed to the moist absorption of SAP during mixing.

A significant improvement in strength and drying shrinkage was obtained for the mixtures made with only SAPs, compared to the mixtures made with SAP+AEA. However, SAP had limited effect on increasing the air content, and cannot act as AEA agent. The mixtures made with SAPs and without AEA performed better frost durability than reference without AEA. However, SAPs cannot be as effective in improving frost durability as AEA.

Subtask B-3: Optimization of external curing regime

Table 6-5 summarizes the performance summary of investigated mixtures corresponding to Task B-3. The IC of SAP can improve the compressive strength and reduce the shrinkage of HPC effectively as the exterior moist curing. This indicated that the use of SAP as an IC agent can significantly reduce the exterior moist curing period. Specifically, 28-d compressive strength and drying shrinkage of HPC mixtures made with 100% IC of SAP and cured 2 days in lime-saturated water were comparable to reference mixture cured 6 days in lime-saturated water.

Table 6-5. Performance summary of HPC made with SAPs and different external curing period

No.	Moist curing (days)			7-d compressive strength (%)	28-d compressive strength (%)	28-d drying shrinkage (%)
	0	2	6			
Ref-1d	√			100	100	100
Ref-3d		√		118	108	93
Ref-7d			√	128	131	74
P-100-1d	√			97	102	74
P-100-3d		√		121	128	48
P-100-7d			√	149	146	35
B-100-1d	√			105	105	78
B-100-3d		√		129	136	60
B-100-7d			√	156	156	42

Subtask B-4: Comparison of HPC mixtures with LWS and SAP

Table 6-6 summarizes the performance summary of investigated HPC mixtures in subtask B-4. Key fresh and hardened properties, including workability, mechanical properties, viscoelastic properties, and frost durability of HPC made with two SAPs and LWS were evaluated.

Table 6-6. Performance summary of HPC made with SAPs and LWS

No.	28-d compressive strength (%)	28-d MOE (%)	28-d flexural strength (%)	25-d drying shrinkage (%)	28-d autogenous shrinkage (%)	Durability factor (%)
Reference	100	100	100	100	100	100
PAM	162	112	127	54	57	98
BASF	135	108	116	70	73	100
LWS	97	88	99	89	53	100

The use of SAP in HPC significantly increased the compressive strength of the mixtures. It also improved the other mechanical properties of the HPC mixtures. The mixtures with SAP performed better than the LWS mixture in terms of both autogenous and drying shrinkage. The inclusion of SAPs made no significant change to the frost durability of the mixtures and provides the required frost resistance.

Task C: Field Trial

Two field trials were carried out. The trial in November 2019 showed that concrete with SAP could be successfully mixed at full scale with conventional truck mixers. The concrete testing confirmed that the concrete properties met ISTHA specification for strength gain and durability, and lower shrinkage was achieved. The trial in May 2021 showed that concrete with SAP could be successfully mixed, placed and finished for full scale concrete slabs. The concrete testing confirmed that the concrete properties met ISTHA specification for strength gain and durability. Drying shrinkage measurements from the May 2021 tests were hampered by the fact that the slabs did not dry very much within the three month window of observation. It was found that moist at the work site was persistently higher than expected, and thus high quality moist curing was observed for all the concretes under consideration. Nevertheless, the two field trials were successful in demonstrating full scale usage of SAP in concrete, and were useful for identifying the need for care to disperse SAP well during truck mixing. The results leads us to discourage

the use of water dissolvable bags, but use other methods to ensure that the SAP is well distributed when added to the back of the concrete truck.

The field trials also showed that the mixture proportioning principles were effective for producing concrete with SAP. The recommended principle for SAP dosage is to include enough SAP to absorb the amount of water associated with chemical shrinkage of the cement. The calculation requires that SAP absorption is known, and thus the SAP characterization would need to be completed by a contractor before designing the concrete mixture proportions.

Task D: Recommended Changes to Tollway Specifications

This study concluded that SAP can be used in Tollway concrete to provide internal curing benefits. Changes are recommended for existing Tollway Specifications, and are included in Appendix F.

REFERENCES

1. Rupnow, T.D., *Evaluation of Portland cement concrete with internal curing capabilities: tech summary*. 2016, Louisiana Transportation Research Center.
2. Jones, W.A., M.W. House, and W.J. Weiss, *Internal curing of high performance concrete using lightweight aggregates and other techniques*. 2014, Colorado. Dept. of Transportation. Research Branch.
3. Byard, B.E., et al., *Cracking tendency of bridge deck concrete*. Transportation research record, 2010. 2164(1): p. 122-131.
4. Hwang, S.-D., K.H. Khayat, and D. Youssef, *Effect of moist curing and use of lightweight sand on characteristics of high-performance concrete*. Materials and structures, 2013. 46(1): p. 35-46.
5. Bremner, T. and T. Holm. *Elastic compatibility and the behavior of concrete*. in *Journal Proceedings*. 1986.
6. Wasserman, R. and A. Bentur, *Interfacial interactions in lightweight aggregate concretes and their influence on the concrete strength*. Cement and Concrete Composites, 1996. 18(1): p. 67-76.
7. Chia, K.S. and M.-H. Zhang, *Water permeability and chloride penetrability of high-strength lightweight aggregate concrete*. Cement and concrete research, 2002. 32(4): p. 639-645.
8. Józwiak-Niedźwiedzka, D., *Scaling resistance of high performance concretes containing a small portion of pre-wetted lightweight fine aggregate*. Cement and Concrete Composites, 2005. 27(6): p. 709-715.
9. Jensen, O.M. and P. Lura, *Techniques and materials for internal water curing of concrete*. Materials and Structures, 2006. 39(9): p. 817-825.

10. Mechtcherine, V. and H.-W. Reinhardt, *Application of superabsorbent polymers (SAP) in concrete construction: state-of-the-art report prepared by Technical Committee 225-SAP*. Vol. 2. 2012: Springer Science & Business Media.
11. Jensen, O.M. and P.F. Hansen, *Water-entrained cement-based materials: I. Principles and theoretical background*. Cement and concrete research, 2001. 31(4): p. 647-654.
12. Jensen, O.M. and P.F. Hansen, *Water-entrained cement-based materials: II. Experimental observations*. Cement and Concrete Research, 2002. 32(6): p. 973-978.
13. Jensen, O.M., *Use of superabsorbent polymers in concrete*. Concrete international, 2013. 35(1): p. 48-52.
14. Mechtcherine, V., et al., *Effect of internal curing by using superabsorbent polymers (SAP) on autogenous shrinkage and other properties of a high-performance fine-grained concrete: results of a RILEM round-robin test*. Materials and Structures, 2014. 47(3): p. 541-562.
15. Mechtcherine, V., et al., *Effect of superabsorbent polymers (SAP) on the freeze–thaw resistance of concrete: results of a RILEM interlaboratory study*. Materials and Structures, 2017. 50(1): p. 1-19.
16. Mechtcherine, V., *Use of superabsorbent polymers (SAP) as concrete additive*. RILEM Technical Letters, 2016. 1: p. 81-87.
17. Hasholt, M.T., M.H.S. Jespersen, and O.M. Jensen. *Mechanical properties of concrete with SAP. Part I: Development of compressive strength*. in *International RILEM conference on use of superabsorbent polymers and other new additives in concrete*. 2010. Rilem publications.
18. Hasholt, M.T., M.H.S. Jespersen, and O.M. Jensen. *Mechanical properties of concrete with SAP. Part II: Modulus of elasticity*. in *International RILEM Conference on Use of Superabsorbent Polymers and Other New Additives in Concrete*. 2010. Rilem publications.
19. Hasholt, M.T., et al., *Can superabsorbent polymers mitigate autogenous shrinkage of internally cured concrete without compromising the strength?* Construction and Building Materials, 2012. 31: p. 226-230.

20. Khayat, K.H., et al., *Use of Lightweight Sand for Internal Curing to Improve Performance of Concrete Infrastructure*. 2018, Missouri. Department of Transportation. Construction and Materials Division.
21. Barrett, T.J., A.E. Miller, and W.J. Weiss, *Documentation of the INDOT experience and construction of the bridge decks containing internal curing in 2013*. 2015, Purdue University. Joint Transportation Research Program.
22. Guo, Y., et al., *Internal Curing as a New Tool for Infrastructural Renewal: Reducing Repair Congestion, Increasing Service Life, and Improving Sustainability*. 2014, NEXTRANS Center (US).
23. D'Ambrosia, M., J. Slater, and T. Dam, *High-performance concrete for bridge decks*. Report for the Illinois State Toll Highways Authority, CTLGroup, Skokie, IL, 2013.
24. Delatte, N.J., E. Mack, and J. Cleary, *Evaluation of high absorptive materials to improve internal curing of low permeability concrete*. 2007, United States. Federal Highway Administration.
25. Yaede, J.M., *Internal Curing of Concrete Bridge Decks in Utah: Mountain View Corridor Project*. 2013.
26. Streeter, D.A., W.H. Wolfe, and R.E. Vaughn, *Field performance of internally cured concrete bridge decks in New York State*. Special Publication, 2012. 290: p. 1-16.
27. Ideker, J.H., T. Deboodt, and T. Fu, *Internal curing of high-performance concrete for bridge decks*. 2013, Oregon. Dept. of Transportation. Research Section.
28. Tia, M., et al., *Internally cured concrete for pavement and bridge deck applications*. 2015, Florida. Dept. of Transportation.
29. Rao, C. and M. Darter, *Evaluation of internally cured concrete for paving applications*. Applied Research Associates, Inc., Champaign, IL, 2013.
30. Cleary, J. and N. Delatte, *Implementation of internal curing in transportation concrete*. Transportation Research Record, 2008. 2070(1): p. 1-7.

31. Jensen, O.M., P. Lura, and K. Kovler, *Volume changes of hardening concrete: Testing and mitigation*. 2006: RILEM.
32. Zhu, C., X. Li, and Y. Xie. *Influence of SAP on the Performance of Concrete and its Application in Chinese Railway Construction*. in *Application of superabsorbent polymers and other new admixtures in concrete construction, Proceedings of International Conference, RILEM Publications, PRO*. 2014.
33. Craeye, B., M. Geirnaert, and G. De Schutter, *Super absorbing polymers as an internal curing agent for mitigation of early-age cracking of high-performance concrete bridge decks*. *Construction and building materials*, 2011. 25(1): p. 1-13.
34. Jensen, O.M. *Use of superabsorbent polymers in construction materials*. in *1st International Conference on Microstructure Related Durability of Cementitious Composites*. 2008. Rilem publications.
35. Buchholz, F.L. and A.T. Graham, *Modern superabsorbent polymer technology*. John! Wiley & Sons, Inc, 605 Third Ave, New York, NY 10016, USA, 1998. 279, 1998.
36. Brannon-Peppas, L. and R.S. Harland, *Absorbent polymer technology*. 2012: Elsevier.
37. ZOHOURIAN, M.M. and K. Kabiri, *Superabsorbent polymer materials: a review*. 2008.
38. Buchholz, F.L. and N. Peppas. *Superabsorbent polymers: science and technology*. 1994. American Chemical Society; Symposium Series, 573.
39. Brannon-Peppas, L. and R.S. Harland, *Absorbent polymer technology*. Vol. 8. 2012: Elsevier.
40. Jensen, O.M. and P.F. Hansen, *Water-entrained cement-based materials I. Principles and theoretical background*. *Cement and Concrete Research*, 2001. 31(4): p. 647-654.
41. Jensen, O.M. and P.F. Hansen, *Water-entrained cement-based materials II. Experimental observations*. *Cement and Concrete Research*, 2002. 32(6): p. 973-978.
42. Wang, F.Z., et al., *Autogenous Shrinkage of Concrete with Super-Absorbent Polymer*. *Aci Materials Journal*, 2009. 106(2): p. 123-127.

43. Mechtcherine, V., et al., *Effect of internal curing by using superabsorbent polymers (SAP) on autogenous shrinkage and other properties of a high-performance fine-grained concrete: results of a RILEM round-robin test*. *Materials and Structures*, 2013. 47(3): p. 541-562.
44. Zhutovsky, S. and K. Kovler, *Effect of internal curing on durability-related properties of high performance concrete*. *Cement and Concrete Research*, 2012. 42(1): p. 20-26.
45. Snoeck, D., et al., *X-ray computed microtomography to study autogenous healing of cementitious materials promoted by superabsorbent polymers*. *Cement and Concrete Composites*, 2016. 65: p. 83-93.
46. Lee, H.X.D., H.S. Wong, and N.R. Buenfeld, *Self-sealing of cracks in concrete using superabsorbent polymers*. *Cement and Concrete Research*, 2016. 79: p. 194-208.
47. Snoeck, D., et al., *Visualization of water penetration in cementitious materials with superabsorbent polymers by means of neutron radiography*. *Cement and Concrete Research*, 2012. 42(8): p. 1113-1121.
48. Kumar, P.A., G.A. Kumar, and K. Vennela, *Role of water absorbing materials in vegetable production*. *Journal of Pharmacognosy and Phytochemistry*, 2018. 7(2): p. 3639-3644.
49. Mignon, A., et al., *pH-sensitive superabsorbent polymers: a potential candidate material for self-healing concrete*. *Journal of Materials Science*, 2015. 50(2): p. 970-979.
50. Zohuriaan-Mehr, M.J., et al., *Advances in non-hygienic applications of superabsorbent hydrogel materials*. *Journal of Materials Science*, 2010. 45(21): p. 5711-5735.
51. Farzarian, K., *On the Interaction between Superabsorbent Hydrogels and Cementitious Materials*. 2017.
52. Kang, S.H., S.G. Hong, and J. Moon, *Absorption kinetics of superabsorbent polymers (SAP) in various cement-based solutions*. *Cement and Concrete Research*, 2017. 97: p. 73-83.

53. Mechtcherine, V., E. Secrieru, and C. Schrofl, *Effect of superabsorbent polymers (SAPs) on rheological properties of fresh cement-based mortars - Development of yield stress and plastic viscosity over time*. Cement and Concrete Research, 2015. 67: p. 52-65.
54. Liu, J., et al., *An overview on the effect of internal curing on shrinkage of high performance cement-based materials*. Construction and Building Materials, 2017. 146: p. 702-712.
55. Liu, J., et al., *Shrinkage and strength development of UHSC incorporating a hybrid system of SAP and SRA*. Cement and Concrete Composites, 2019.
56. Mignon, A., et al., *Alginate biopolymers: Counteracting the impact of superabsorbent polymers on mortar strength*. Construction and Building Materials, 2016. 110: p. 169-174.
57. Aday, A.N., et al., *Carrageenan-based superabsorbent biopolymers mitigate autogenous shrinkage in ordinary portland cement*. Materials and Structures, 2018. 51(2): p. 37.
58. Kanellopoulou, I., et al., *Effect of submicron admixtures on mechanical and self-healing properties of cement-based composites*. Fatigue & Fracture of Engineering Materials & Structures, 2019.
59. Mignon, A., et al., *Development of amine-based pH-responsive superabsorbent polymers for mortar applications*. Construction and Building Materials, 2017. 132: p. 556-564.
60. Ashkani, M., et al., *Synthesis of poly (2-acrylamido-2-methyl propane sulfonic acid) with high water absorbency and absorption under load (AUL) as concrete grade superabsorbent and its performance*. Construction and Building Materials, 2019. 206: p. 540-551.
61. Irie, Y., et al., *Method for production of particulate hydrogel polymer and absorbent resin*. 1993, Google Patents.
62. Aoki, S. and H. Yamasaki, *Process for preparation of spontaneously-crosslinked alkali metal acrylate polymers*. 1978, Google Patents.
63. Mechtcherine, V., et al., *Effect of internal curing by using superabsorbent polymers (SAP) on autogenous shrinkage and other properties of a high-performance fine-grained*

concrete: results of a RILEM round-robin test. *Materials and Structures*, 2014. 47(3): p. 541-562.

64. Schroefl, C., D. Snoeck, and V. Mechtcherine, *A review of characterisation methods for superabsorbent polymer (SAP) samples to be used in cement-based construction materials: report of the RILEM TC 260-RSC*. *Materials and Structures*, 2017. 50(4): p. 197.

65. Liu, J., et al., *Shrinkage and strength development of UHSC incorporating a hybrid system of SAP and SRA*. *Cement & Concrete Composites*, 2019. 97: p. 175-189.

66. Liu, J., et al., *Effects of superabsorbent polymer on shrinkage properties of ultra-high strength concrete under drying condition*. *Construction and Building Materials*, 2019. 215: p. 799-811.

67. Richter, A., et al., *Review on Hydrogel-based pH Sensors and Microsensors*. *Sensors*, 2008. 8(1): p. 561.

68. Schröfl, C., D. Snoeck, and V. Mechtcherine, *A review of characterisation methods for superabsorbent polymer (SAP) samples to be used in cement-based construction materials: report of the RILEM TC 260-RSC*. *Materials and Structures*, 2017. 50(4).

69. Lee, H.X.D., H.S. Wong, and N.R. Buenfeld, *Effect of alkalinity and calcium concentration of pore solution on the swelling and ionic exchange of superabsorbent polymers in cement paste*. *Cement and Concrete Composites*, 2018. 88: p. 150-164.

70. Mechtcherine, V., E. Secrieru, and C. Schröfl, *Effect of superabsorbent polymers (SAPs) on rheological properties of fresh cement-based mortars — Development of yield stress and plastic viscosity over time*. *Cement and Concrete Research*, 2015. 67: p. 52-65.

71. Wong, J., *The influence of superabsorbent polymer (cassava starch) on the rheological behavior of cement pastes*. 2016.

72. Secrieru, E., et al., *Rheological characterisation and prediction of pumpability of strain hardening cement-based-composites (SHCC) with and without addition of superabsorbent polymers (SAP) at various temperatures*. *Construction and Building Materials*, 2016. 112: p. 581-594.

73. Schroefl, C., V. Mechtcherine, and M. Gorges, *Relation between the molecular structure and the efficiency of superabsorbent polymers (SAP) as concrete admixture to mitigate autogenous shrinkage*. Cement and Concrete Research, 2012. 42(6): p. 865-873.
74. Paiva, H., et al., *Rheology and hardened properties of single-coat render mortars with different types of water retaining agents*. Construction and Building Materials, 2009. 23(2): p. 1141-1146.
75. Snoeck, D., et al., *Effect of high amounts of superabsorbent polymers and additional water on the workability, microstructure and strength of mortars with a water-to-cement ratio of 0.50*. Construction and Building Materials, 2014. 72: p. 148-157.
76. Mechtcherine, V., L. Dudziak, and J. Schulze. *Internal curing by super absorbent polymers (SAP)—effects on material properties of self-compacting fibre-reinforced high*. in *International RILEM Conference on Volume Changes of Hardening Concrete: Testing and Mitigation*. 2006. RILEM Publications SARL.
77. Mönning, S., *Superabsorbing additions in concrete: applications, modelling and comparison of different internal water sources*. 2009.
78. Dudziak, L. and V. Mechtcherine. *Reducing the cracking potential of ultra-high performance concrete by using super absorbent polymers (SAP)*. in *Proceedings of the International Conference on Advanced Concrete Materials (ACM'09)*. 2009.
79. Dudziak, L. and V. Mechtcherine. *Enhancing early-age resistance to cracking in high-strength cement based materials by means of internal curing using super absorbent polymers*. in *RILEM Proc. PRO*. 2010.
80. Sikora, K.S. and A.J. Klemm, *Effect of superabsorbent polymers on workability and hydration process in fly ash cementitious composites*. Journal of Materials in Civil Engineering, 2015. 27(5): p. 04014170.
81. Fenyvesi, O. *Early age shrinkage cracking of concretes*. 2012. Conference of Junior Researchers in Civil Engineering, Budapest, Hungary.

82. Gribniak, V., G. Kaklauskas, and D. Bancinskas, *State-of-art review of shrinkage effect on cracking and deformations of concrete bridge elements*. Baltic Journal of Road and Bridge Engineering, 2007. 2(4): p. 183-193.
83. Dudziak, L., V. Mechtcherine, and W. Brameshuber, *Enhancing early-age resistance to cracking in high-strength cement-based materials by means of internal curing using super absorbent polymers*. Additions improving properties of concrete, RILEM Proceedings PRO, 2010. 77: p. 129-139.
84. Olivier, G., et al., *Combined effect of nano-silica, super absorbent polymers, and synthetic fibres on plastic shrinkage cracking in concrete*. Construction and Building Materials, 2018. 192: p. 85-98.
85. Snoeck, D., L. Pel, and N. De Belie, *Superabsorbent polymers to mitigate plastic drying shrinkage in a cement paste as studied by NMR*. Cement and Concrete Composites, 2018. 93: p. 54-62.
86. Beltzung, F. and F.H. Wittmann, *Early chemical shrinkage due to dissolution and hydration of cement*. Materials and Structures, 2001. 34(239): p. 279-283.
87. Kocaba, V., E. Gallucci, and K.L. Scrivener, *Methods for determination of degree of reaction of slag in blended cement pastes*. Cement and Concrete Research, 2012. 42(3): p. 511-525.
88. Le Chatelier, H., *Sur les changements de volume qui accompagnent le durcissement des ciments*. Bulletin Societe de l'encouragement pour l'industrie nationale, 1900. 5.
89. Wang, F.Z., et al., *Influence of superabsorbent polymers on the surrounding cement paste*. Cement and Concrete Research, 2016. 81: p. 112-121.
90. Nie, S., et al., *Internal curing – A suitable method for improving the performance of heat-cured concrete*. Construction and Building Materials, 2016. 122: p. 294-301.
91. Fu, T., *Autogenous deformation and chemical shrinkage of high performance cementitious systems*, in *Civil and Construction Engineering*. 2011, Oregon State University.

92. Esteves, L.P., *Internal curing in cement-based materials*. 2009, Universidade de Aveiro (Portugal).
93. Kong, X.-m., Z.-l. Zhang, and Z.-c. Lu, *Effect of pre-soaked superabsorbent polymer on shrinkage of high-strength concrete*. *Materials and Structures*, 2014. 48(9): p. 2741-2758.
94. Igarashi, S.-i. and A. Watanabe. *Experimental study on prevention of autogenous deformation by internal curing using super-absorbent polymer particles*. in *Volume changes of hardening concrete: testing and mitigation. Proceedings of the international RILEM conference, Denmark*. 2006.
95. Shen, D., et al., *Effect of internal curing with super absorbent polymers on autogenous shrinkage of concrete at early age*. *Construction and Building Materials*, 2016. 106: p. 512-522.
96. Soliman, A. and M. Nehdi, *Effect of partially hydrated cementitious materials and superabsorbent polymer on early-age shrinkage of UHPC*. *Construction and Building Materials*, 2013. 41: p. 270-275.
97. Schroefl, C., et al., *Sorption kinetics of superabsorbent polymers (SAPs) in fresh Portland cement-based pastes visualized and quantified by neutron radiography and correlated to the progress of cement hydration*. *Cement and Concrete Research*, 2015. 75: p. 1-13.
98. Lura, P., F. Durand, and O.M. Jensen, *Autogenous strain of cement pastes with superabsorbent polymers*. *International RILEM Conference on Volume Changes of Hardening Concrete: Testing and Mitigation*, 2006: p. 57-65.
99. Liu, J., et al., *Shrinkage and strength development of UHSC incorporating a hybrid system of SAP and SRA*. *Cement and Concrete Composites*, 2019. 97: p. 175-189.
100. Liu, J., et al., *The effect of SCMs and SAP on the autogenous shrinkage and hydration process of RPC*. *Construction and Building Materials*, 2017. 155: p. 239-249.
101. Snoeck, D., O.M. Jensen, and N. De Belie, *The influence of superabsorbent polymers on the autogenous shrinkage properties of cement pastes with supplementary cementitious materials*. *Cement and Concrete Research*, 2015. 74: p. 59-67.

102. Klemm, A. and K. Sikora. *The effect of cement type on the performance of mortars modified by superabsorbent polymers*. in *Concrete Repair, Rehabilitation and Retrofitting III: 3rd International Conference on Concrete Repair, Rehabilitation and Retrofitting, ICCRRR-3, 3-5 September 2012, Cape Town, South Africa*. 2012. CRC Press.
103. Soliman, A.M. and M.L. Nehdi, *Effect of drying conditions on autogenous shrinkage in ultra-high performance concrete at early-age*. *Materials and Structures*, 2011. 44(5): p. 879-899.
104. Ma, X.W., et al., *Effects of SAP on the properties and pore structure of high performance cement-based materials*. *Construction and Building Materials*, 2017. 131: p. 476-484.
105. Assmann, A. and H.W. Reinhardt, *Tensile creep and shrinkage of SAP modified concrete*. *Cement and Concrete Research*, 2014. 58: p. 179-185.
106. Kong, X.-m., Z.-l. Zhang, and Z.-c. Lu, *Effect of pre-soaked superabsorbent polymer on shrinkage of high-strength concrete*. *Materials and Structures*, 2014: p. 1-18.
107. Mönnig, S., et al. *Results of a comparative study of the shrinkage behaviour of concrete and mortar mixtures with different internal water sources*. in *International RILEM Conference on Volume Changes of Hardening Concrete: Testing and Mitigation*. 2006. RILEM Publications SARL.
108. Assmann, A., *Physical properties of concrete modified with superabsorbent polymers*, in *Uni Stuttgart - Universitätsbibliothek*. 2013.
109. Kong, X. and Q. Li, *Influence of super absorbent polymer on dimension shrinkage and mechanical properties of cement mortar*. *Journal of the Chinese Ceramic Society*, 2009. 5.
110. Beushausen, H. and M. Gillmer, *The use of superabsorbent polymers to reduce cracking of bonded mortar overlays*. *Cement and Concrete Composites*, 2014. 52: p. 1-8.
111. Farzarian, K. and A. Ghahremaninezhad, *Desorption of superabsorbent hydrogels with varied chemical compositions in cementitious materials*. *Materials and Structures*, 2018. 51(1): p. UNSP-3.
112. Jin, Z., et al., *Influence of SAP on the chloride penetration and corrosion behavior of steel bar in concrete*. *Corrosion Science*, 2020. 171.

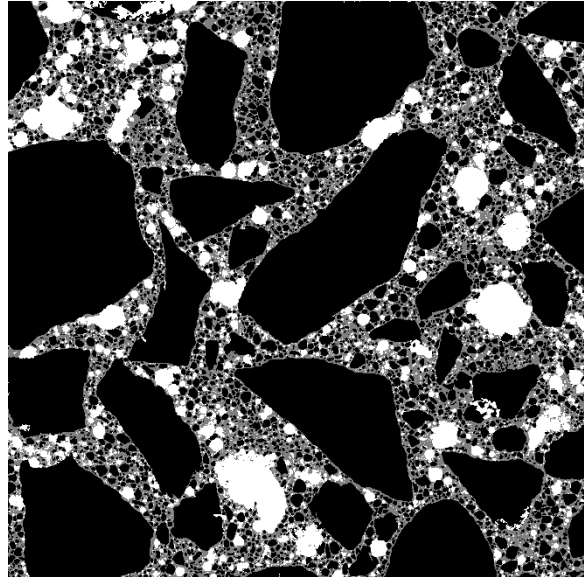
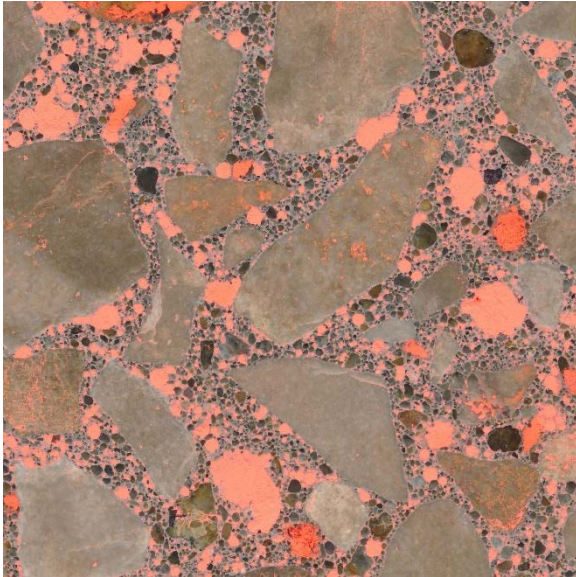
113. Ma, X., et al., *Effects of SAP on the properties and pore structure of high performance cement-based materials*. Construction and Building Materials, 2017. 131: p. 476-484.
114. Beushausen, H., M. Gillmer, and M. Alexander, *The influence of superabsorbent polymers on strength and durability properties of blended cement mortars*. Cement and Concrete Composites, 2014. 52: p. 73-80.
115. Laustsen, S., M.T. Hasholt, and O.M. Jensen, *Void structure of concrete with superabsorbent polymers and its relation to frost resistance of concrete*. Materials and Structures, 2015. 48(1): p. 357-368.
116. Bentz, D.P. and O.M. Jensen, *Mitigation strategies for autogenous shrinkage cracking*. Cement and Concrete Composites, 2004. 26(6): p. 677-685.
117. Riyazi, S., J.T. Kevern, and M. Mulheron, *Super absorbent polymers (SAPs) as physical air entrainment in cement mortars*. Construction and Building Materials, 2017. 147: p. 669-676.
118. Kim, I.S., et al., *An experimental study on absorptivity measurement of superabsorbent polymers (SAP) and effect of SAP on freeze-thaw resistance in mortar specimen*. Construction and Building Materials, 2020: p. 120974.
119. ASTM C494 / C494M-19, *Standard Specification for Chemical Admixtures for Concrete*, ASTM International, West Conshohocken, PA, 2019.
120. ASTM C150 / C150M-21, *Standard Specification for Portland Cement*, ASTM International, West Conshohocken, PA, 2021.
121. ASTM C618-19, *Standard Specification for Coal Fly Ash and Raw or Calcined Natural Pozzolan for Use in Concrete*, ASTM International, West Conshohocken, PA, 2019.
122. ASTM C989 / C989M-18a, *Standard Specification for Slag Cement for Use in Concrete and Mortars*, ASTM International, West Conshohocken, PA, 2018
123. ASTM C1761 / C1761M-17, *Standard Specification for Lightweight Aggregate for Internal Curing of Concrete*, ASTM International, West Conshohocken, PA, 2017.

124. ASTM C138 / C138M-17a, *Standard Test Method for Density (Unit Weight), Yield, and Air Content (Gravimetric) of Concrete*, ASTM International, West Conshohocken, PA, 2017.
125. ASTM C231 / C231M-17a, *Standard Test Method for Air Content of Freshly Mixed Concrete by the Pressure Method*, ASTM International, West Conshohocken, PA, 2017.
126. ASTM C143 / C143M-20, *Standard Test Method for Slump of Hydraulic-Cement Concrete*, ASTM International, West Conshohocken, PA, 2020.
127. ASTM C39 / C39M-14, *Standard Test Method for Compressive Strength of Cylindrical Concrete Specimens*, ASTM International, West Conshohocken, PA, 2014.
128. ASTM C617 / C617M-12, *Standard Practice for Capping Cylindrical Concrete Specimens*, ASTM International, West Conshohocken, PA, 2012.
129. ASTM C1609 / C1609M-12, *Standard Test Method for Flexural Performance of Fiber-Reinforced Concrete (Using Beam With Third-Point Loading)*, ASTM International, West Conshohocken, PA, 2012.
130. ASTM C469 / C469M-14, *Standard Test Method for Static Modulus of Elasticity and Poisson's Ratio of Concrete in Compression*, ASTM International, West Conshohocken, PA, 2014.
131. ASTM C1760-12, *Standard Test Method for Bulk Electrical Conductivity of Hardened Concrete*, ASTM International, West Conshohocken, PA, 2012.
132. ASTM C157 / C157M-17, *Standard Test Method for Length Change of Hardened Hydraulic-Cement Mortar and Concrete*, ASTM International, West Conshohocken, PA, 2017.
133. ASTM C1698-19, *Standard Test Method for Autogenous Strain of Cement Paste and Mortar*, ASTM International, West Conshohocken, PA, 2019.
134. ASTM C1581 / C1581M-18a, *Standard Test Method for Determining Age at Cracking and Induced Tensile Stress Characteristics of Mortar and Concrete under Restrained Shrinkage*, ASTM International, West Conshohocken, PA, 2018.

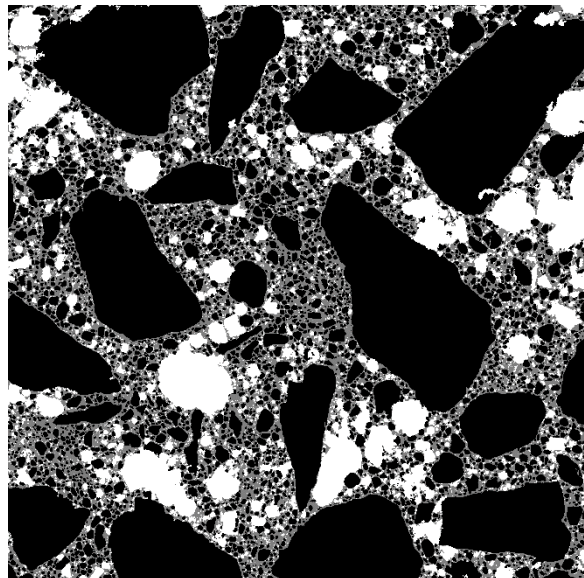
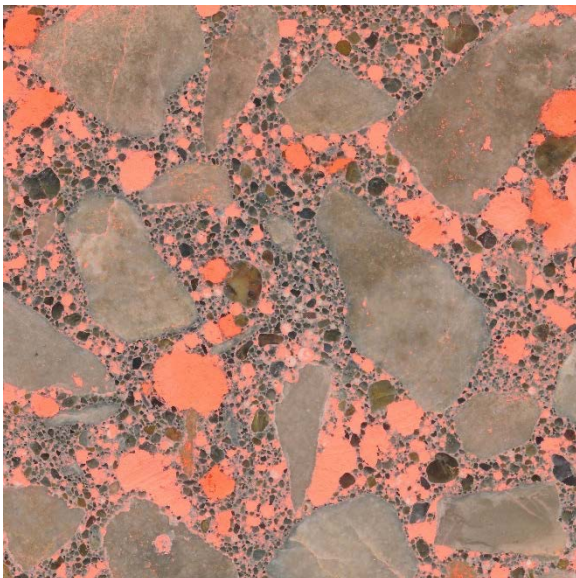
135. ASTM C666 / C666M-15, *Standard Test Method for Resistance of Concrete to Rapid Freezing and Thawing*, ASTM International, West Conshohocken, PA, 2015.
136. ASTM C457 / C457M-16, *Standard Test Method for Microscopical Determination of Parameters of the Air-Void System in Hardened Concrete*, ASTM International, West Conshohocken, PA, 2016.
137. Song, Y., et al., *Advances in measuring air-void parameters in hardened concrete using a flatbed scanner*. *Journal of Testing and Evaluation*, 2017. 45(5): p. 1713-1725.
138. Song, Y., et al., *Deep learning-based automated image segmentation for concrete petrographic analysis*. *Cement and Concrete Research*, 2020. 135: p. 106118.

APPENDIX

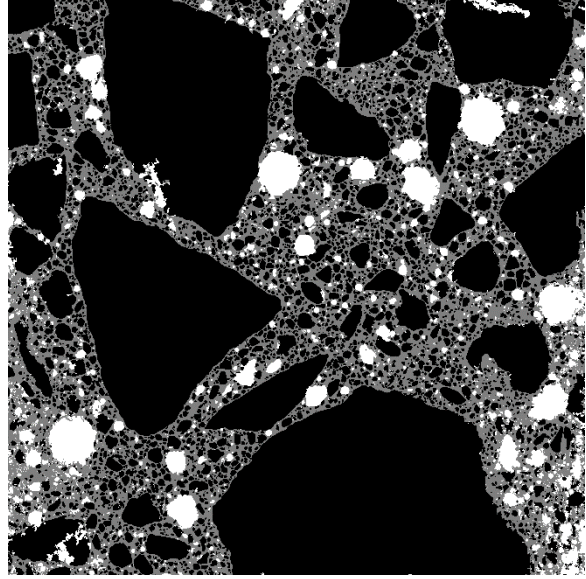
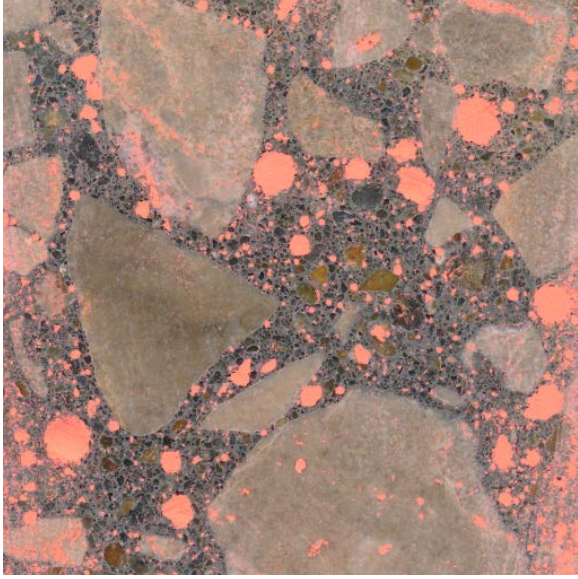
APPENDIX A - Air Void Segmentation Results – Subtask B2



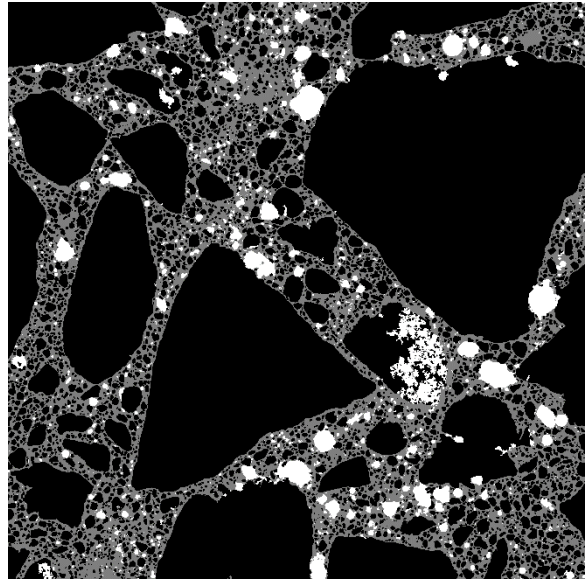
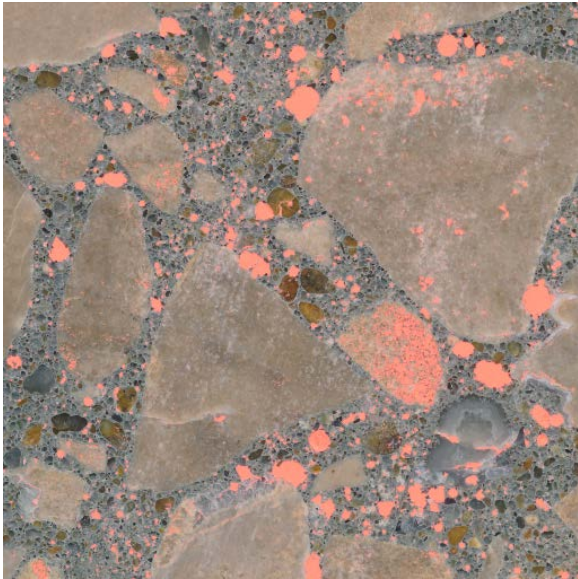
B2-P-100-M3-1



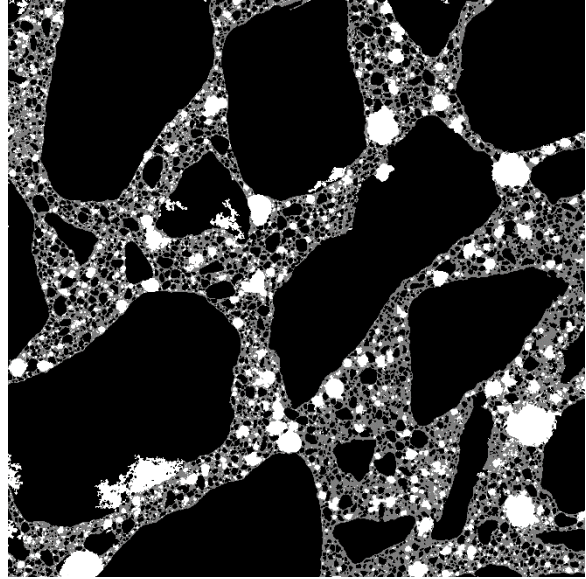
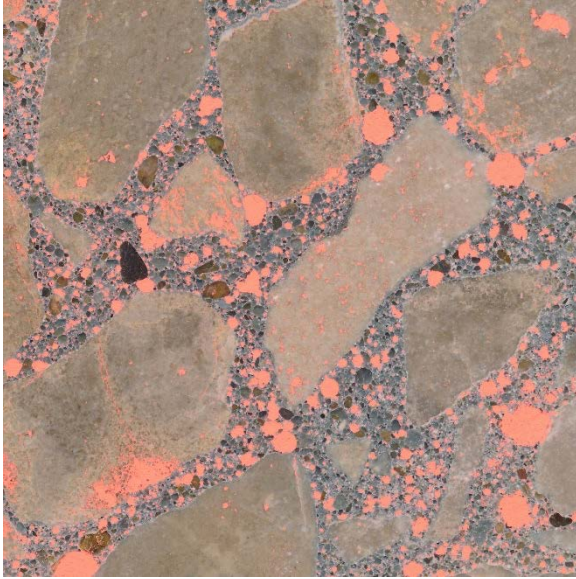
B2-P-100-M3-2



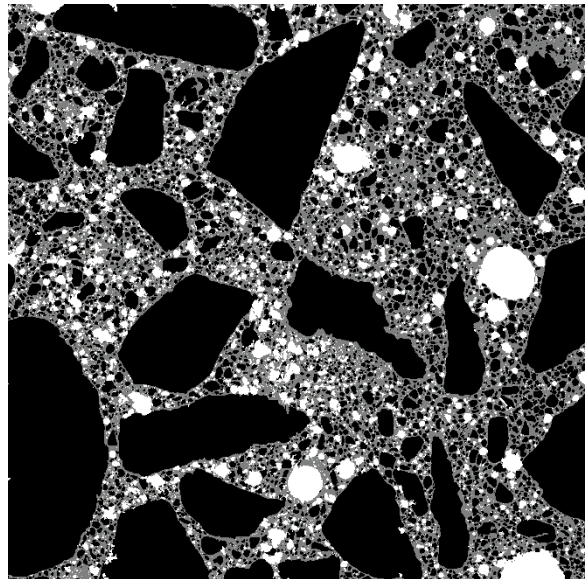
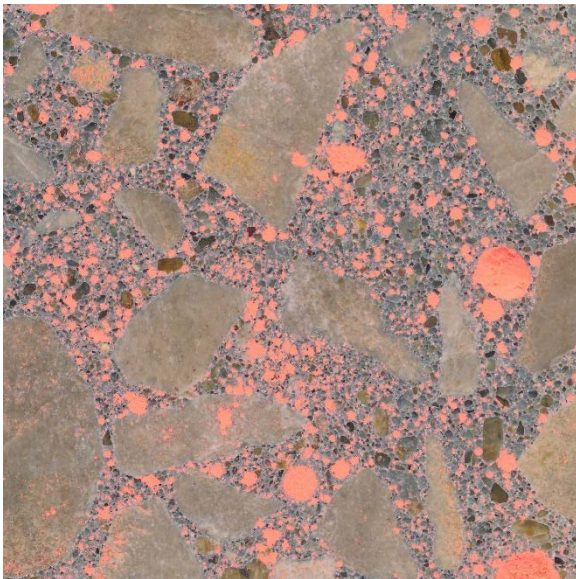
B2-P-100-without AEA-1



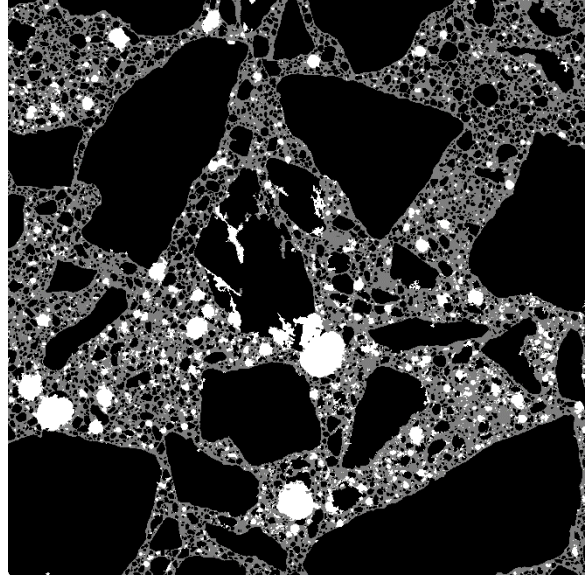
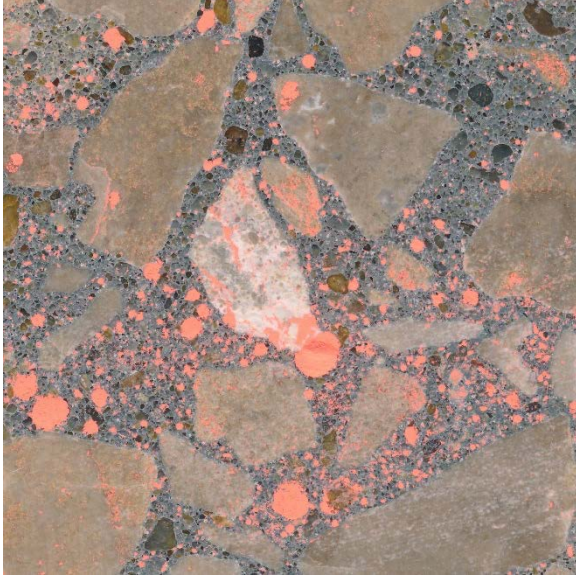
B2-P-100-without AEA-2



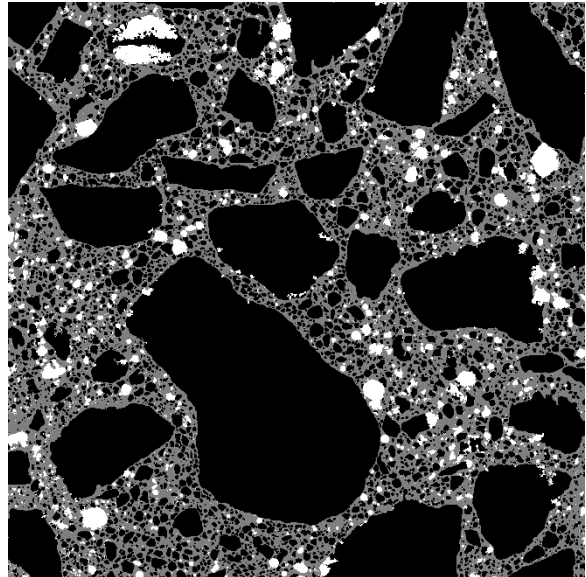
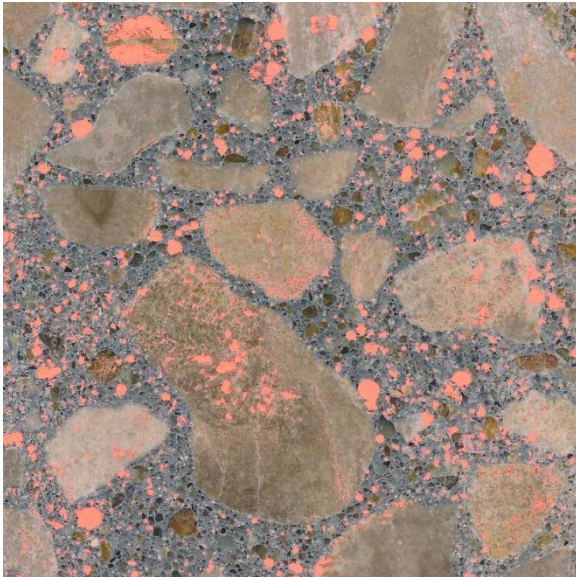
B2-B-100-M3-1



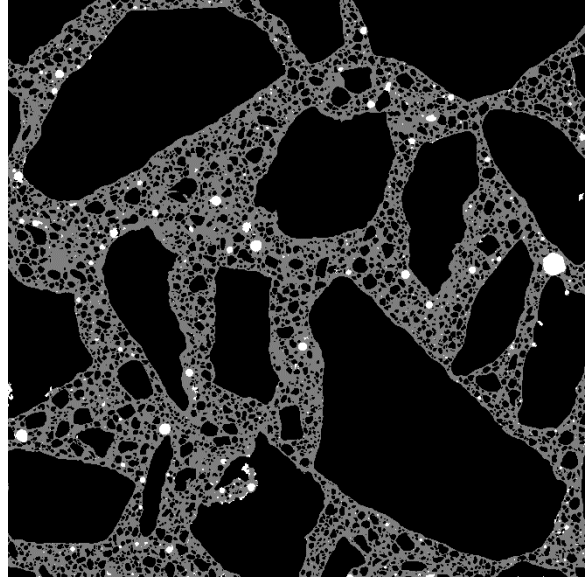
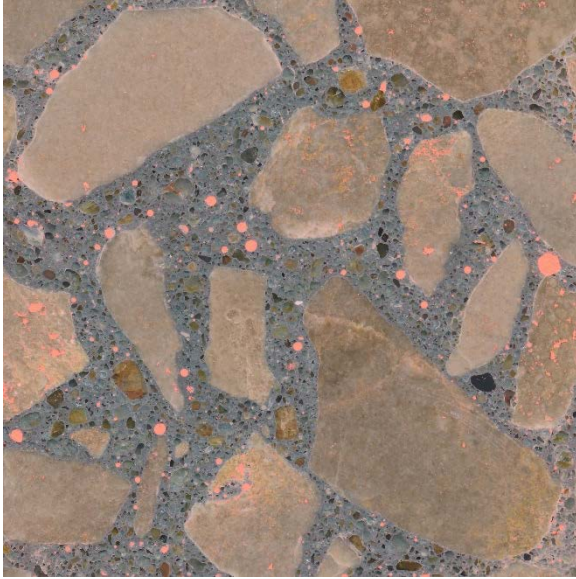
B2-B-100-M3-2



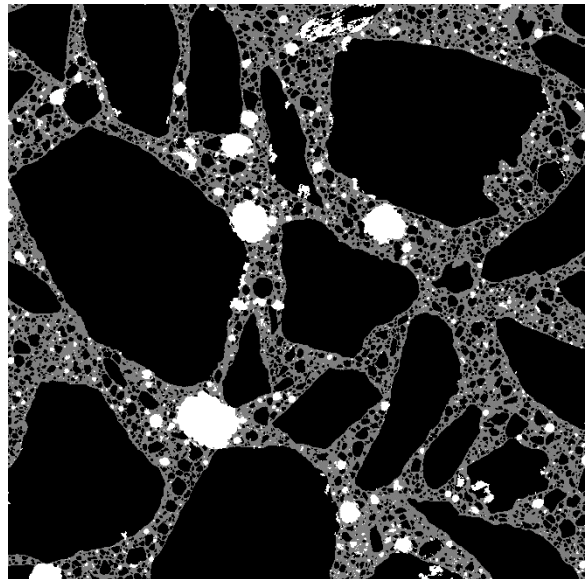
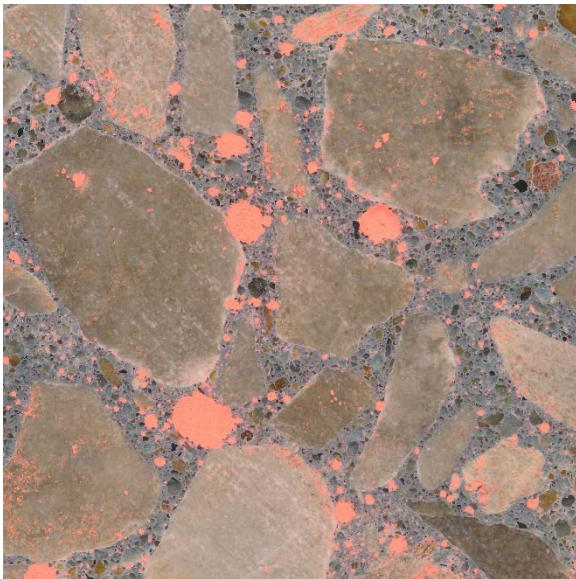
B2-B-100-without AEA-1



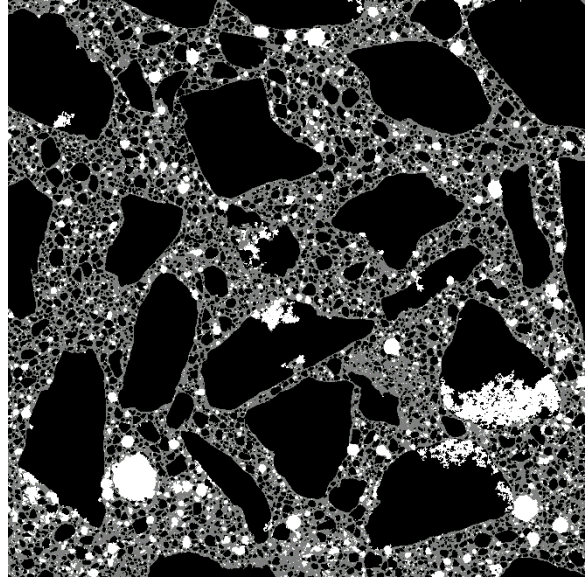
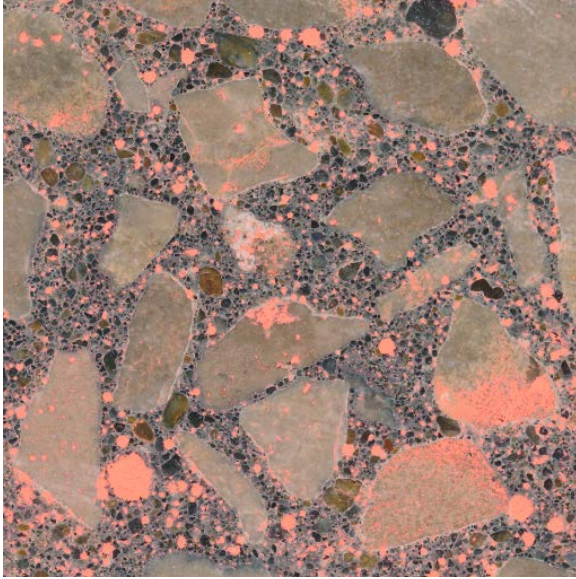
B2-B-100-without AEA-2



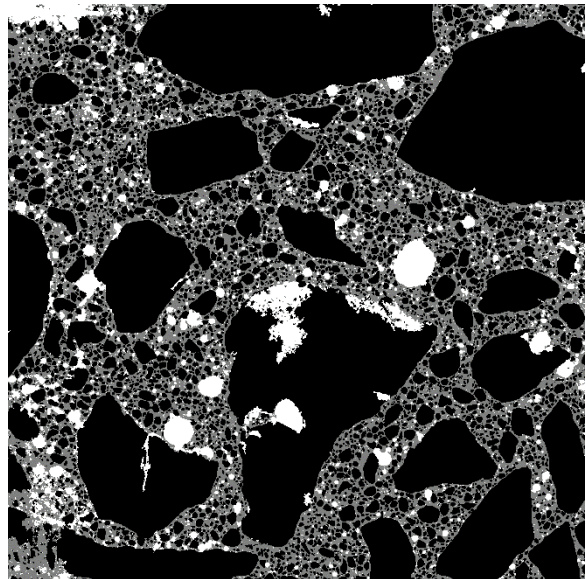
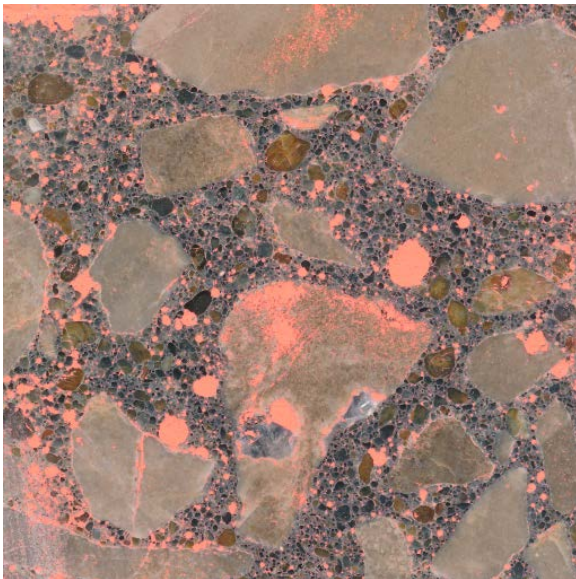
B2-R-without AEA-1



B2-R-without AEA-2

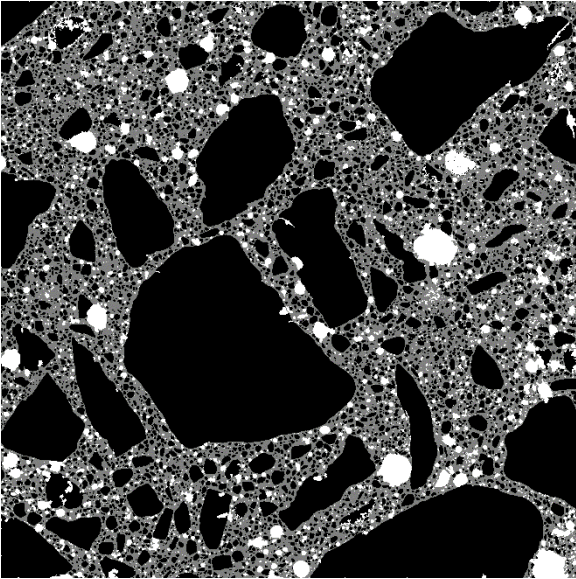
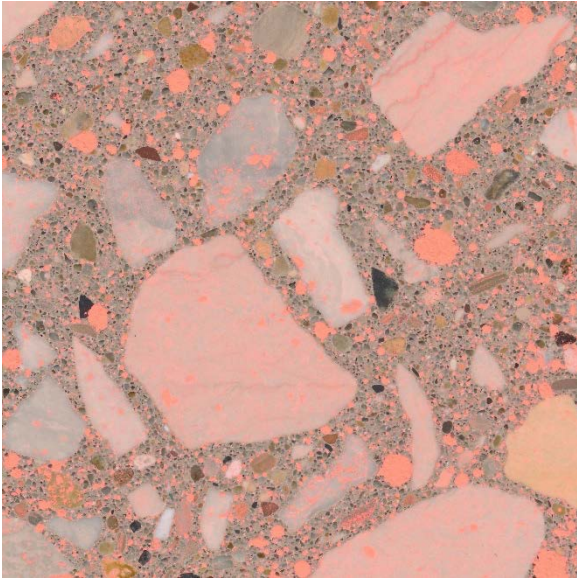


B2-R-1

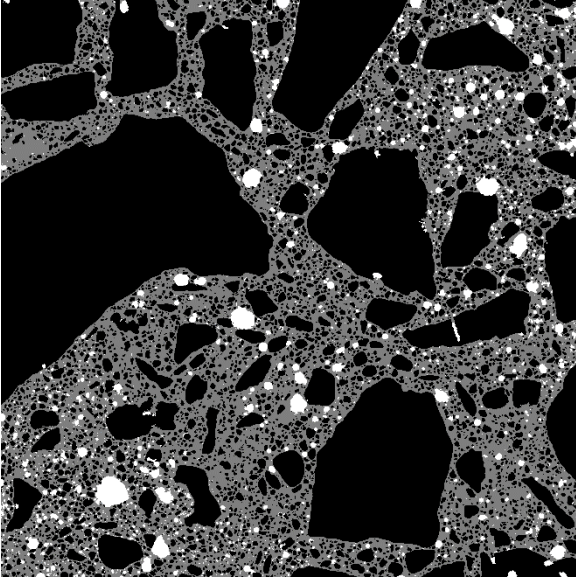
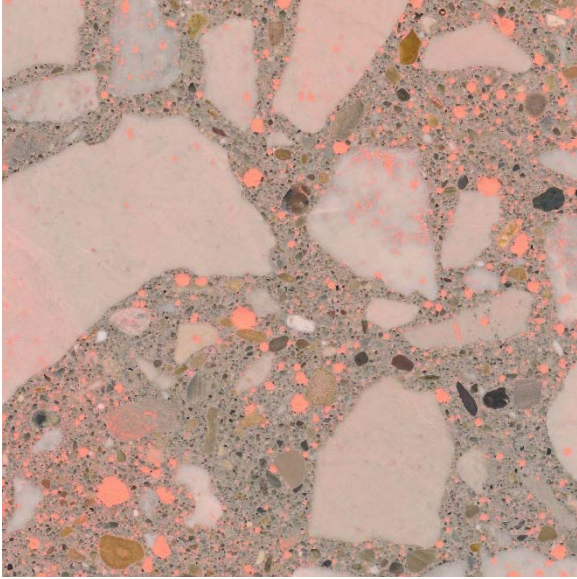


B2-R-2

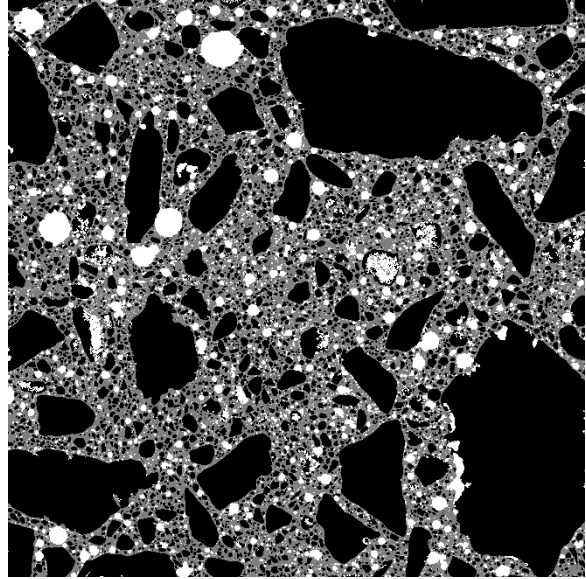
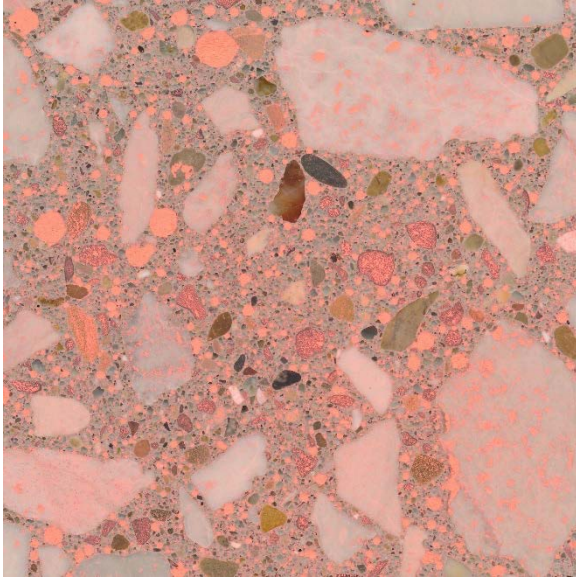
APPENDIX B - Air Void Segmentation Results – Subtask B-4



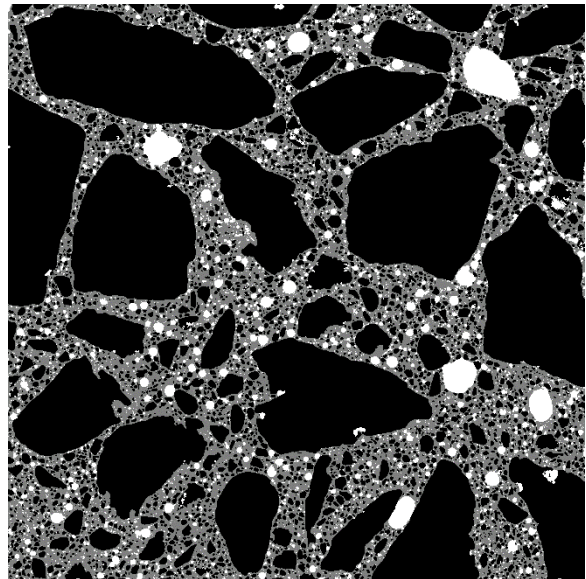
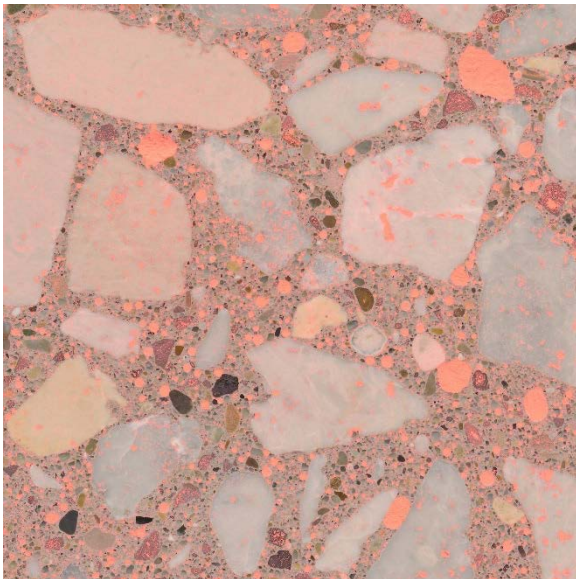
B4-BASF-1



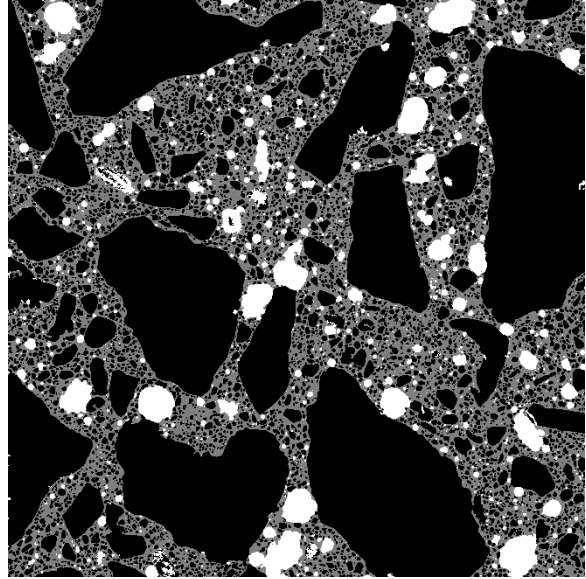
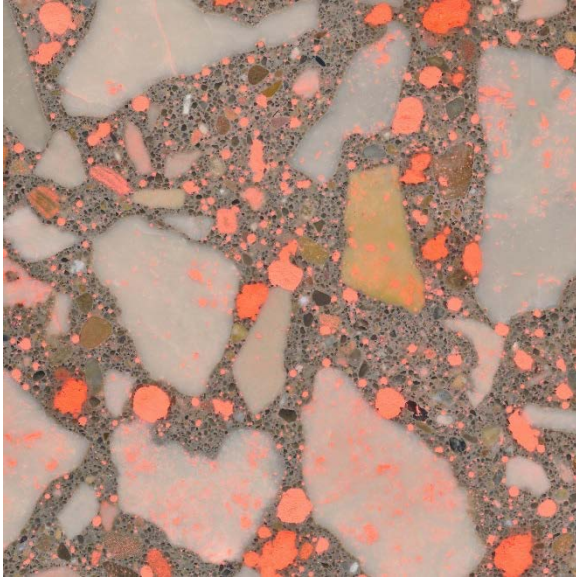
B4-BASF-2



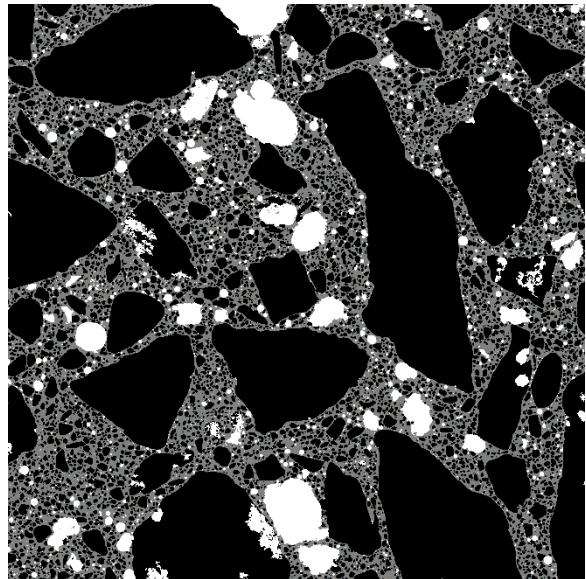
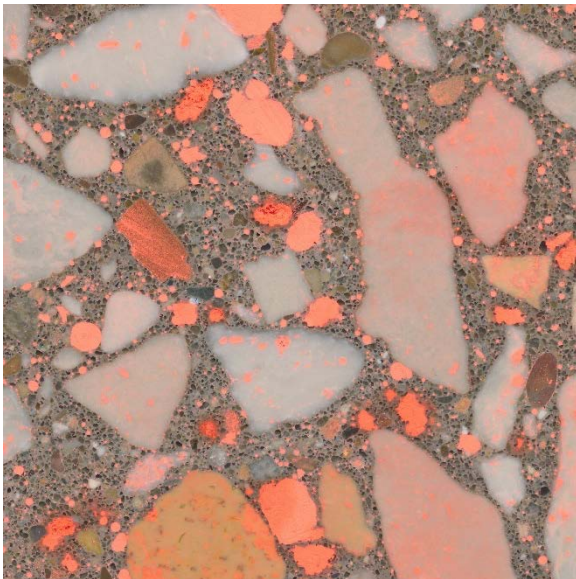
B4-LWS-1



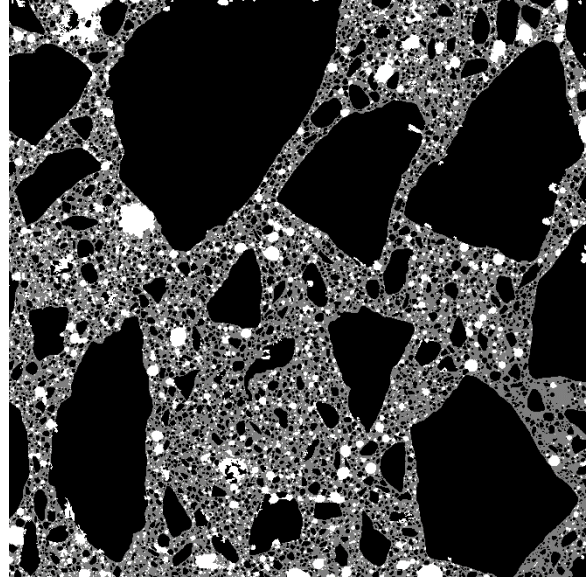
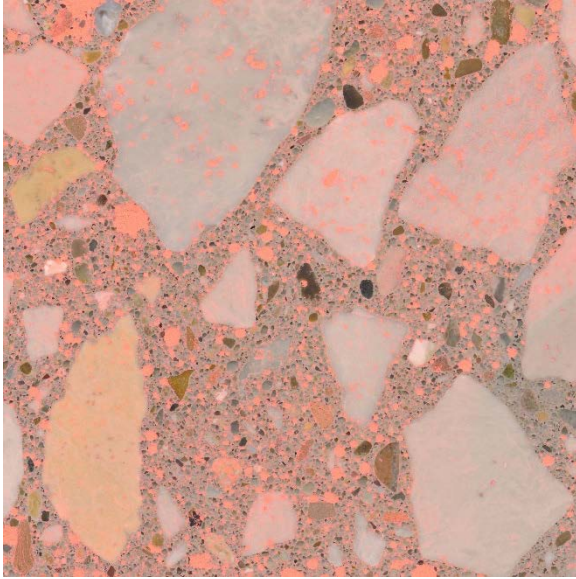
B4-LWS-2



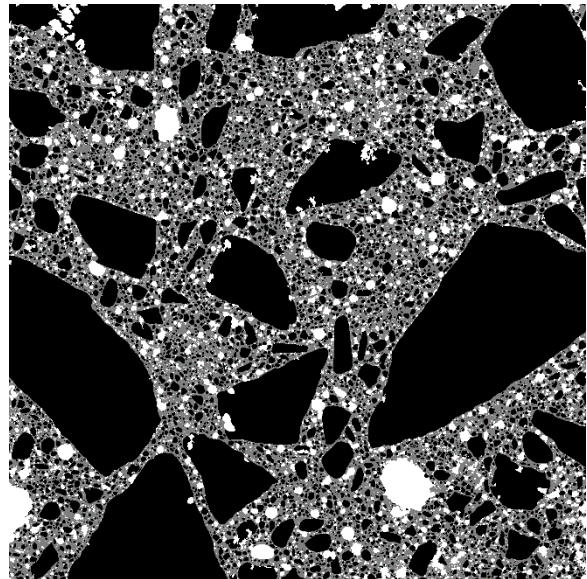
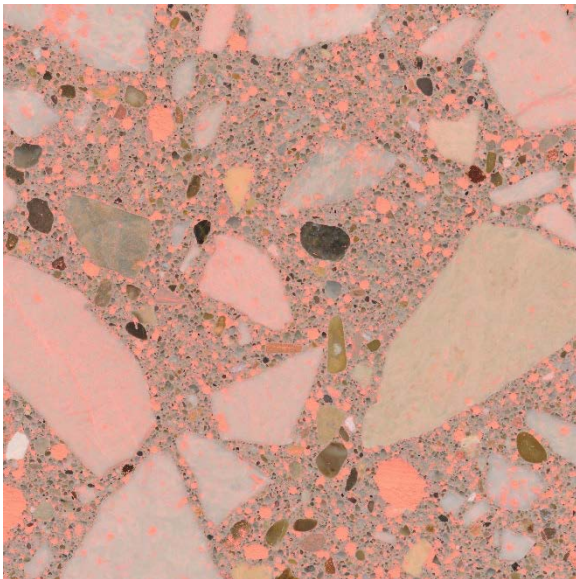
B4-PAM-1



B4-PAM-2



B4-R-1



B4-R-2

APPENDIX C – Field test 1 Batch Tickets

Truck	Driver	User	Disp Ticket Num	Ticket ID	Time	Date
1321	15055	user	237085	0	9:28	11/19/19
Load Size	Mix Code	Returned	Qty	Mix Age	Seq	Load ID
8.00 CY	4599SAP				W	108873

Material	Design Qty	Required	Batched	% Var	% Moisture	Actual	Wat
22CM11OVM	1810.00 lb	14624.80 lb	14680.00 lb	0.38%	1.00% M	145.35 lb	
27FM02MM	1364.00 lb	11078.39 lb	11140.00 lb	0.56%	1.52% E	167.31 lb	
HR-A575	1.50 /C	64.20 oz	62.00 oz	-3.43%			
CEM-FCMSG	345 lb	2760 lb	2795 lb	1.27%			
FLY-ASHELM	80 lb	640 lb	635 lb	-0.78%			
SLG-SKY	110.0 lb	880.0 lb	880.0 lb	0.00%			
WATER1	25.3 gl	171.4 gl	170.9 gl	-0.31%		1426.0 lb	
WR-82	3.00 /C	128.40 oz	126.00 oz	-1.87%			
AE-DX2	4.0 oz	32.0 oz	31.0 oz	-3.13%			
WRR-REC	2.0 /C	85.6 oz	86.0 oz	0.47%			

There was an issue with the sand moisture probe. Actual moisture is closer to 3.40% based on the second trial batch. Calculated w/cm is 0.45.

Actual	Num Batches:	1
Load 31575 lb	Design W/C: 0.395	Water/Cement: 0.403 A
Slump: 8.00 in #	Water in Truck: 0.0 gl	Adjust Water: 0.0 gl / Load
Actual W/C Ratio: 0.403	Actual Water: 1739 lb	Batched Cement: 4310 lb
		Design 1689.0 lb
		Actual 1738.7 lb
		To Add: 0.0 lb
		Trim Water: 0.0 gl / CY
		Allowable Water: 0 lb

Figure A.1. - Batch ticket for batch 1 HPC

Truck	Driver	User	Disp Ticket Num	Ticket ID	Time	Date
1321	15055	user	237122	0	11:08	11/19/19
Load Size	Mix Code	Returned	Qty	Mix Age	Seq	Load ID
8.00 CY	4599SAP				W	108910

Material	Design Qty	Required	Batched	% Var	% Moisture	Actual	Wat
22CM11OVM	1810.00 lb	14624.80 lb	14630.00 lb	0.04%	1.00% M	144.85 lb	
27FM02MM	1364.00 lb	11282.62 lb	11270.00 lb	-0.11%	3.40% A	370.21 lb	
HR-A575	1.50 /C	64.20 oz	62.00 oz	-3.43%			
CEM-FCMSG	345 lb	2760 lb	2800 lb	1.45%			
FLY-ASHELM	80 lb	640 lb	640 lb	0.00%			
SLG-SKY	110.0 lb	880.0 lb	880.0 lb	0.00%			
WATER1	25.3 gl	146.9 gl	146.4 gl	-0.34%		1222.0 lb	
WR-82	3.00 /C	128.40 oz	128.00 oz	-0.31%			
AE-DX2	4.0 oz	32.0 oz	31.0 oz	-3.13%			
WRR-REC	2.0 /C	85.6 oz	85.0 oz	-0.70%			

Actual	Num Batches:	1
Load 31461 lb	Design W/C: 0.395	Water/Cement: 0.402 A
Slump: 8.00 in #	Water in Truck: 0.0 gl	Adjust Water: 0.0 gl / Load
Actual W/C Ratio: 0.402	Actual Water: 1737 lb	Batched Cement: 4320 lb
		Design 1689.0 lb
		Actual 1737.1 lb
		To Add: 0.0 lb
		Trim Water: 0.0 gl / CY
		Allowable Water: 0 lb

Figure A.2. - Batch ticket for batch 2 HPC

Truck	Driver	User	Disp Ticket	Num	Ticket ID	Time	Date
1321	15055	user	237159	0	0	12:54	11/19/19
Load	Size	Mix Code	Returned	Qty	Mix Age	Seq	Load ID
9.00	CY	4599SAP				W	108947

Material	Design Qty	Required	Batched	% Var	% Moisture	Actual	Wat
22CM11OVMM	1810.00 lb	16452.90 lb	16410.00 lb	-0.26%	1.00% M	162.48 lb	
27FM02MM	1364.00 lb	12720.57 lb	12720.00 lb	0.00%	3.62% A	444.55 lb	
HR-A575	1.50 /C	72.23 oz	72.00 oz	-0.31%			
CEM-HCMSG	345 lb	3105 lb	3090 lb	-0.48%			
FLY-ASHELM	80 lb	720 lb	725 lb	0.69%			
SLG-SKY	110.0 lb	990.0 lb	985.0 lb	-0.51%			
WATER1	25.3 gl	162.0 gl	162.3 gl	0.13%		1354.0 lb	
WR-82	3.00 /C	144.45 oz	142.00 oz	-1.70%			
AE-DX2	3.0 oz	27.0 oz	27.0 oz	0.00%			
WRR-REC	2.0 /C	96.3 oz	95.0 oz	-1.35%			

Load size was inadvertently changed from 8.00 to 9.00. SAP was dosed based on 8.00.

Actual Load	35305 lb	Num Batches:	1	Design	1900.2 lb	Actual	1961.0 lb	To Add:	0.0 lb
Slump:	8.00 in	#		Water/Cement:	0.409 A	Water in Truck:	0.0 gl	Adjust Water:	0.0 gl / Load
Actual W/C Ratio:	0.409	Actual Water:	1961 lb	Batched Cement:	4800 lb	Trim Water:	0.0 gl / CY	Allowable Water:	0 lb

Figure A.3. - Batch ticket for batch 3 HPC

APPENDIX D – Field test 1 Fresh Properties

Table B.1. - Batch 1: WasteLock PAM/TYPE S

Time	Concrete Temp (°F)	Slump (in.)	Air Content (%)	SAM Air Content (%)	SAM Number	Cylinder Set
9:43 AM	64	8.75	7.8	8.1	0.14	1-A
10:02 AM	Added 16.415 lbs. of SAP (Waste Lock PAM / Type S), Mixed with 40 revs					
10:08 AM	N/A	3.25	8.6	N/A	N/A	N/A
Added 40 oz. HR-A575, Mixed with 40 revs						
10:18 AM	63	7.5	9.4	10.5	0.04	1-B
Discharged 2.5 - 3 CY						
10:30 AM	65	4.5	9.5	10.4	0.17	1-C
Discharged 2.5 - 3 CY						
10:42 AM	65	4.25	10.2	10.6	0.15	1-D

Table B.2. - Batch 2: Evolution HydroMax

Time	Concrete Temp (°F)	Slump (in.)	Air Content (%)	SAM Air Content (%)	SAM Number	Cylinder Set
11:18 AM	64	7	10.7	9.1	0.08	2-A
11:36 AM	Added 20.695 lbs. of SAP (HydroMax), Mixed with 40 revs					
11:41 AM		2	8			
11:45 AM	Added 80 oz. HR-A575, Mixed with 40 revs					
Noticed SAP on fin, Scraped with shovel, Mixed with 20 revs						
11:59 AM	65	9.25	11.5	11	0.02	2-B
Discharged 2.5 - 3 CY						
12:14 PM	65	8.5	13.5	11	Error	2-C
Discharged 2.5 - 3 CY						
12:29 PM	66	8	14.5	-	-	2-D

Table B.3. - Batch 3: BASF SAP

Time	Concrete Temp (°F)	Slump (in.)	Air Content (%)	SAM Air Content (%)	SAM Number	Cylinder Set
1:02 PM	66	5.5	8.8	9	0.21	3-A
1:10 PM	Added 8.82 lbs. of SAP (BASF), Mixed with 40 revs					
Approx. slump of 0.5"						
1:21 PM	Added 100 oz. HR-A575, Mixed with 40 revs					
Noticed SAP on fin, Scraped with shovel, Mixed with 10 revs						
1:32 PM	68	7.5	6.2	6.1	0.03	3-B
Discharged 2.5 - 3 CY						
1:46 PM	68	3.75	5.6	5.5	0.1	3-C
Discharged 2.5 - 3 CY						
1:59 PM	69	2.5	5.1	5.3	0.21	3-D

APPENDIX E – Field test 2 Batch Ticket

Truck	Driver	User	Disp Ticket	Num	Ticket ID	Time	Date
1701	16119	user	397972	0	0	10:58	5/11/21
Load Size	Mix Code	Returned	Qty	Mix Age	Seq	Load ID	
9.00 CY	508Z				DH	124191	

Material	Design Qty	Required	Batched	% Var	% Moisture	Actual	Wat
22CM11BVR	1851 lb	16826 lb	16630 lb	0.03%	1.00% M		20 gl
27FM02TH	1129 lb	10644 lb	10670 lb	0.25%	4.75% M		58 gl
FLY-OZJOP	155 lb	1395 lb	1455 lb	> 4.30%			
CEM-HCMMSG	455 lb	4095 lb	4065 lb	-0.24%			
WATER1	27.5 gl	155.8 gl	158.4 gl	> 1.68%		158.4 gl	
AE-DX2	17.00 oz	153.00 oz	153.00 oz	0.00%			
WR-Z630	2.00 /C	109.80 oz	108.00 oz	-1.64%			
NCAE	3.00 %	1976.40 oz	1968.00 oz	-0.43%			
WRR-REC	1.00 /C	54.90 oz	55.00 oz	0.18%			
HR-A575	4.50 /C	247.05 oz	246.00 oz	-0.43%			

Actual		Num Batches:	1				Manual	10:58:34
Load	34520 lb	Design W/C:	0.376	Water/Cement:	0.356	A	Design	247.5 gl
Slump:	4.00 in	Water in Truck:	0.0 gl	Adjust Water:	0.0	gl / Load	Actual	236.4 gl
							Trim Water:	0.0 gl /
								CY
							To Add:	11.1 gl

Batch ticket from field test 2 (typical for 3 truck loads)

APPENDIX F. Recommended Changes to Tollway Specifications

Several changes are recommended the Tollway document entitled PERFORMANCE-RELATED SPECIAL PROVISION FOR HIGH PERFORMANCE CONCRETE MIXTURES FOR CONCRETE SUPERSTRUCTURE (Illinois Tollway GBSP).

1. Add AASHTO reference standards for SAP materials and tests as they become available.
2. Revise Note 4 in the table shown under the MATERIALS header to read:
 - Note 4: Shrinkage reducing admixtures (SRA), corrosion inhibitors, superabsorbent polymers (SAP), and slump retention admixtures from Illinois Tollway approved sources may be used. SAP shall be added in a manner such that the product is dispersed and does not form balls or clumps during mixing. This shall be demonstrated during trial batch qualifications. Dissolvable or repulpable bags are not permitted.
3. Add clarification that slump is measured after addition of all admixtures:

Slump Loss

Unless otherwise approved by the Illinois Tollway, the initial slump (measured within 10 minutes after the addition of water **and all admixtures**) shall be between 3 and 8 inches. The slump shall be no less than 3 inches for at least 45 minutes after the addition of water as measured by AASHTO T 119. The change in slump shall be no greater than 2 inches in 20 minutes and 4 inches from the initial measurement (measured within 10 minutes after the addition of water **and all admixtures**). The concrete temperature during testing shall be greater than 70°F.

4. Add clause to FIELD TRIAL BATCH ACCEPTANCE that clumping is to be avoided. We suggest adding an additional bullet item:
 - There shall be no clumping of portland cement, SCM, or internal curing agents observed during discharge.
 -
5. A Tollway Approved List of Superabsorbent Polymer (SAP) is recommended for SAP products as shown on the following pages. We recommend that AquaSmart SAP products are included in the Approved List although they were not included in all aspects of lab and field testing in this project. The AquaSmart SAP is delivered as a layer bonded to sand, thus

introducing unique aspects of mixing and dispersion. For dosage calculation, it is important to know that the AquaSmart SAP product is 92% sand and 8% SAP by mass. AquaSmart SAP products are recommended on the basis of experience and test results reported by CTLGroup Report # 057226:



Client: AquaSmart Enterprises, LLC
 Project: Concrete Internal Curing R&D
 Contact: Calder Hendrickson
 Date: April 25, 2018

CTLGroup Project No: 057226
 CTLGroup Project Mgr.: J. Vosahlik
 Technician: N/A
 Approved: J. Pacheco

ASTM C192 Mixture Summary

		Mixture ID: NA9-Control NA9-6 NA9-12 NA9-24				
		Date Fabricated:	2/27/2018	2/27/2018	2/27/2018	2/27/2018
Material		SG	lbs/yard ³			
Cement	ASTM C150 Type I	3.15	372	375	378	382
Fly Ash	ASTM C618 - Class C	2.75	93	94	94	95
Coarse Aggregate	CM-11 Crushed Limestone	2.72	1749	1765	1775	1796
SAP-coated Fine Aggregate	AquaSmart #8	2.50	--	6	12	25
Fine Aggregate	ASTM C33 Fine Aggregate	2.63	1525	1494	1467	1416
Water	Potable	1.00	275	277	279	282
Total Cementitious Content			465	469	472	477
w/cm (not including water in admixtures)			0.59	0.59	0.59	0.59
SAP concentration, % by mass of cementitious			--	0.10	0.21	0.42
Paste Content Volume (including air), %			27.4%	27.6%	27.9%	28.3%
Chemical Admixtures			fl. oz./cwt			
Water Reducer/Set Retarder	BASF Pozzolith 80		3.5	3.5	3.5	3.4
High Range Water Reducer	BASF Glenium 7511		--	--	4.8	9.6
Target Properties			Design Values			
Target Slump			6 to 8 in.			
Design Air Content			2.0%			
Fresh Concrete Properties			Measured Values			
Slump, in.	ASTM C143		6.50	4.50	5.00	7.25
Air Content, %	ASTM C231		1.9	2.4	2.6	3.7
Temperature, °F	ASTM C1064		74.1	73.4	73.4	73.0
Fresh Density, lb/ft ³	ASTM C138		151.1	149.7	147.9	147.3
Test	Test Method	Curing	Age, days		Test Results	
Initial Set, mins.	ASTM C403	--	--	315	325	360
Final Set, mins.	ASTM C403	--	--	405	410	460
Compressive Strength, psi	ASMT C39	73°F/Mold	1	1,860	1,850	1,680
		73°F/Limewater	3	3,580	3,580	3,320
		73°F/Limewater	7	4,280	4,250	4,000
		73°F/Limewater	14	4,990	5,050	4,640
		73°F/Limewater	21	5,320	5,250	5,190
		73°F/Limewater	28	5,530	5,490	5,370
		73°F/Limewater	56	6,230	6,100	5,640
Length Change, %	ASTM C157	73°F/Limewater, 7d	--	-0.045@49d	-0.047@49d	-0.046@49d
Total Void Content ⁵⁾ , %	ASTM C457	--	--	1.8	2.2	4.1
Voids Created by SAP Particles, %	ASTM C457	--	--	0.0	0.7	1.3
Air Content, %	ASTM C457	--	--	1.8	1.5	2.8
Spacing Factor, in.	ASTM C457	--	--	0.035	0.018	0.017
Specific Surface, 1/in.	ASTM C457	--	--	205	382	303

Notes:

- 1) This report may not be reproduced except in its entirety
- 2) All test specimens fabricated by CTLGroup with proportions approved by others.
- 3) Specific gravity value of Aquasmart sand was assumed.
- 4) Dry Aquasmart sand was added to the mixture at the end of the batching sequence, i.e. after addition of all other materials. No additional water was added.
- 5) The total air content is a sum of entrapped air voids and voids created by SAP particles.

Corporate Office: 5400 Old Orchard Road, Skokie, Illinois 60077-1030

Page 1 of 1

Illinois Tollway
APPROVED LIST OF SUPERABSORBENT POLYMER (SAP)

August 28, 2021

Performance-Related Special Provision for
High Performance Concrete Mix Designs for
Concrete Superstructure (Tollway)

Powdered SAP

BASF Admixtures, Inc.
23700 Chagrin Blvd.
Cleveland, OH 44122-5554
Phone: 216-839-7500
Attention: Mr. Mark Piechuta
IDOT Producer/Supplier No. 4179-04
www.basf-admixtures.com
“BASF SAP”

M² Polymer Technologies Inc
17N580 Adams Dr
West Dundee, IL
Phone: 847-836-1393
Attention: Martin Matushek
martin@m2polymer.com
“Waste Lock PAM/ 63micron”
“WL 770” (Sodium neutralized acrylic homo-polymer)
“WL PAM/Type S” (Potassium neutralized acrylic-acrylamide co-polymer)

Evolution Paving Resources LLC DBA Evolution Pervious
3322 Belvedere
Salem, OR 97304
Phone: 503.932.0157
Toll-Free: 800.357.8217
Attention: Scott Erickson, Principal
scott@evolutionpervious.com
www.evolutionpervious.com
“Hydromax”

Sand with SAP coating

AquaSmart Enterprises LLC
5760 40th Street, Unit C,
Lubbock, Texas 79407
Phone: 806-993-5031
Attention: Oliver K. Mulamba, PhD, Director of Technology
oliver@aquasmartenterprises.com
www.aquasmartglobal.com
“Hydromesh 100 mesh sand” (sodium polyacrylate)
“Hydromesh 20-30 sand” (sodium polyacrylate)

A. Scope

Before a commercial Superabsorbent Polymer (SAP) product is used for an Illinois Tollway project, it must be tested and approved. The following guidelines are provided to clarify the submittal requirements and expedite the testing process for SAP products:

B. Procedure

Contact the Illinois Tollway with your desire to have a product considered for SAP approval.

The Tollway contact is:

Daniel J. Gancarz Illinois Tollway Materials Department 2700 Ogden Avenue
Downers Grove, Illinois 60515-1703

The Tollway will provide a product application form for the initial submittal of your product for use in Tollway projects. The material requirements are provided in the Tollway's HPC special provision.

The SAP shall be evaluated in accordance with the Teabag test per the procedure given in the Appendix of Weiss et al.⁴. The Teabag test must be conducted using a simulated pore solution⁵. To make simulated pore solution, add the following chemicals to 1.0 liter of water, mix well and maintain at 20±2°C temperature:

Chemicals	NaOH	K ₂ SO ₄	KOH	Ca (OH) ₂
Weight (g)	16	7	18	0.08

If you have any questions regarding the testing and approval process, contact Dan Gancarz at 630-241-6800, ext. 3961.

The Illinois Tollway shall be notified of any changes in material or contact information. Failure to do so may result in removal of product from the approved list.

If you have any questions regarding the testing and approval process, contact Dan Gancarz at 630-241-6800, ext. 3961.

⁴ Weiss, W.J.; Montanari, L. Guide Specification for Internally Curing Concrete (InTrans Project No. 13-482); Iowa Department of Transportation: Ames, IA, USA, 2017

⁵ Mechtcherine V, Reinhardt HW, editors. Application of super absorbent polymers (SAP) in concrete construction: state-of-the-art report prepared by Technical committee 225-SAP. Springer Science & Business Media; 2012 Jan 3.